



**Understanding the relationship between PV degradation and its key
electrical characteristics**

Chujun Yan

H00236598

Supervisor: Dr. Mehreen Gul

Submitted for the MEng degree of Architectural Engineering

Heriot-Watt University

School of Energy, Geoscience, Infrastructure and Society

April 2019

The copyright in this thesis is owned by the author. Any quotation from the thesis or use of any of the information contained in it must acknowledge this thesis as the source of the quotation or information.

DECLARATION STATEMENT

IChujun Yan....., confirm that this work submitted for assessment is my own and is expressed in my own words. Any uses made within it of the works of other authors in any form (e.g. ideas, equations, figures, text, tables, programmes) are properly acknowledged at the point of their use. A full list of the references employed has been included.

Signed:

Date:05/04/19.....

ABSTRACT

Under the pressure of environmental pollution and rapidly growing energy consumption, renewable technologies started to play an important role in energy generation. Photovoltaic panel (PV) is one of the widespread options with good energy generation performance and relatively cheaper price. When PV exposed to the unpredictable environmental conditions, its energy output will most likely to be affected. Therefore, it is important to find out how PV performance is affected under real conditions.

This study is to understand the significance of key electrical characteristics regard to PV degradation. All key findings are based on the analysis of a set of data obtained from a one-year period test carried out Obing, Germany, which include four types of solar panel: CIS, mono-Si, μ c-Si and CdTe.

Analysis showed that the most affected solar panel is CIS panel with a degradation of 1.343%, then Sharp - μ c-Si panel with a degradation of 0.212%. The least affected solar panel is Solar World - mono-Si panel with an improvement of 4.239%, then First - CdTe panel with an improvement of 0.216%. Furthermore, the analysis also showed the most dominant factors that affected the PV performance are the Series Resistance, Shunt Resistance and Reverse Saturation Current.

ACKNOWLEDGMENT

I would like to take this chance to express my gratitude to my supervisor Dr. Mehreen Gul, for introducing me into such an inspiring field of study, for the continuous support and for the incredible patience she showed when I faced difficulties throughout this dissertation.

I would also want to give lots of thanks to Dr. Faisal Ghani, researcher from Engineering and Physical Sciences School of Heriot-Watt University, for all the time and help he has given since the dissertation started.

Also, many thanks to all the technicians from the mechanical workshop and electrical workshop, who installed the test site -Shed 5 on campus which was originally going to be used for this dissertation.

A special thanks to my boyfriend Daniel. Bee, for the incredible amount of help he offered me in writing the analysis programme in Python and for all the mental support he offered during this stressful time.

A heartfelt thanks to my parents for all the support and love they showed during this stressful time.

Finally, I would like to thank my counselor Kenny Boyle for his continuous support and all my close friends in university who encouraged each other from the very beginning to the end.

GLOSSARY

Abbreviation	Meaning
a-Si	amorphous silicon
c-Si	crystalline silicon
CdTe	cadmium telluride
CIS	copper indium gallium selenide
I-V	current-voltage
I_{SC}	short-circuit current
I_0	reverse saturation current
I_{PH}	photogenerated current
IEA	International Energy Agency
IRENA	International Renewable Energy Agency
IQR	interquartile range
Mono-Si	monocrystalline silicon
n	ideality factor
Poly-Si	polycrystalline silicon
PV	photovoltaic
P-V	power-voltage
P_{MPP}	maximum power point
R_{SH}	shunt resistance
R_S	series resistance
STC	standard test conditions
T_{amb}	ambient temperature
T_{mod}	module temperature
V_{oc}	open-circuit voltage
μ c-Si	micro-morphous silicon

Table of Contents

1. Introduction	1
1.1 Background	1
1.2 Rationale for this Research	3
1.3 Research aim, objectives and hypothesis	5
1.4 Dissertation Structure.....	5
2. Literature Review	7
2.1 Photovoltaics (PV)	7

2.1.1 PV installation status.....	7
2.1.2 PV application.....	9
2.1.3 PV cell.....	11
2.1.4 PV panel technology	12
2.2 PV cell characteristics	15
2.2.1 I-V characteristics	15
2.2.2 Electrical Characteristics.....	18
2.3 Impacts on PV performance.....	21
2.3.1 Key factors affecting the PV performance.....	21
2.3.2 Summary	23
3. Methodology	26
3.1 <i>Edinburgh Data (original plan)</i>	26
3.1.1 Site background.....	26
3.1.2 Experiment procedure	26
3.1.3 Limitations	27
3.2 <i>Germany Data (Alternative Plan)</i>	27
3.2.1 Site background.....	27
3.2.2 Data collection	28
3.2.3 Data analysis	28
4. Results and Discussion.....	31
4.1 Würth Solar – CIS solar panel	31
4.1.1 I-V curve and P-V curve	31
4.1.2 Electrical Characteristics and Environment Factors	32
4.1.3 Electrical Characteristics and Degradation	36
4.2 Solar World – mono-Si solar panel.....	41
4.2.1 I-V curve and P-V curve	41
4.2.2 Electrical Characteristics and Environment Factors	42
4.2.3 Electrical Characteristics and Degradation	46
4.3 Sharp – μ c-Si solar panel	51
4.3.1 I-V curve and P-V curve	51
4.3.2 Electrical Characteristics and Environment Factors	52
4.3.3 Electrical Characteristics and Degradation	56
4.4 First Solar – CdTe solar panel.....	61
4.4.1 I-V curve and P-V curve	61
4.4.2 Electrical Characteristics and Environment Factors	62
4.4.3 Electrical Characteristics and Degradation	66
4.5 Comparisons among CIS, mono-Si, μ c-Si and CdTe panels	71
4.5.1 Level of degradation	71
4.5.2 Change in key electrical characteristics	73

Dissertation	Heriot-Watt University	H00236598
4.5.3 PV performance under STC and under real conditions	75	
5. Conclusion	76	
5.1 Key findings	76	
5.2 Limitations	79	
5.3 Recommendations for future study	80	
6. References	81	

1. Introduction

1.1 Background

The demand for energy is growing day by day due to the effects brought by economy and population growth. Meanwhile, the global warming, climate change and environmental pollution have developed to the major concerns nowadays. These concerns are highly related to the growth of the energy consumption. In order to reduce the effects of these concerns, the concept of renewable energy has been proposed in the past few decades. Traditionally, electricity is generated by burning fossil fuels, including coals and oil, whereas renewable energy is energy generated from renewable sources, such as, wind, solar, wave, biomass energy, geothermal etc. (Marques,A. *et al.*,2018). According to the data published by the International Energy Agency (IEA, 2018), in OECD countries, the electricity production (1974-2017, provisional) by renewables has a tendency to keep growing, on the other hand, the general trend of the electricity production by fossil fuels is declining. Hence, the renewable energy is becoming an essential part of the overall electricity generation due to the fact that it stands a better chance to react to the climate change as one of the main mitigation options.

Solar photovoltaic panels (PV panels) is one of the most popular options among all the renewable technologies. For the worldwide, IEA (2018) has stated the electricity generation by different technologies from 2000 to 2017, as well as the prediction for the future until 2040 in the latest World Energy Outlook (WEO), as seen in Figure 1.1 below.

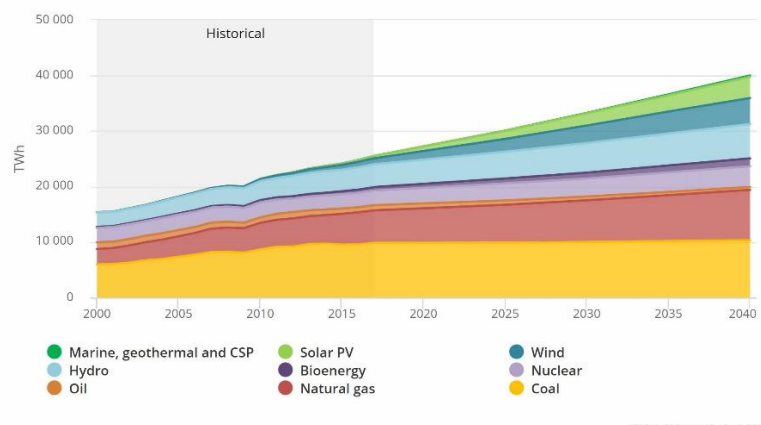


Figure 1.1 Historical and predicted data of electricity generation by different technologies (Source: IEA, World Energy Outlook, 2018)

1.1 Background

The figure clearly shows the growing trend of all the renewable technologies and it is obvious that Solar PV has the highest increasing rate in terms of electricity generation both historically and in the future. For the UK, Centre of Economics and Business Research (Cebr) (2014) has reported to the Solar Trade Association that in 2012 and 2013, compare to the other renewable sectors, Solar PV has supported twice the number of companies per £1 million of investment, as seen in Figure 1.2 below. The fast development of photovoltaics technology does not only contribute to the electricity generation, but also has a relatively high business value.

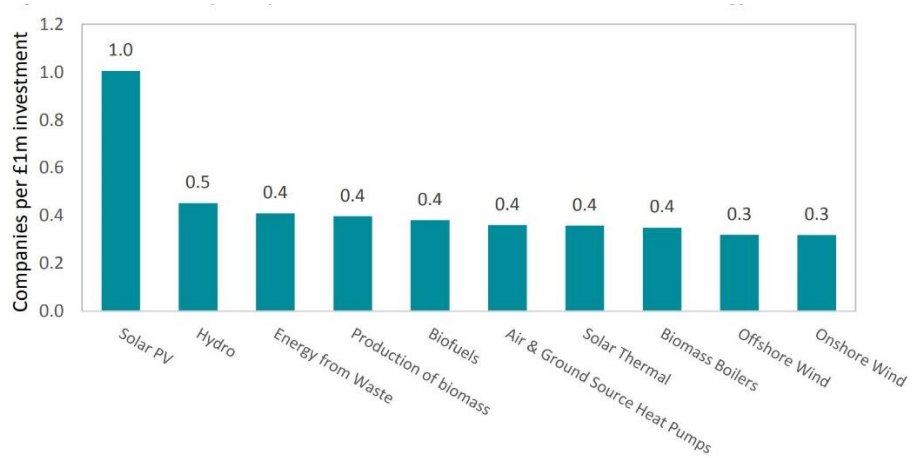


Figure 1.2 Numbers of companies per £1million investment supported by different renewable technologies (Source: Cebr, 2014)

In fact, there are 936,478 sites in the UK that generating electricity from Solar PV in 2017 (BEIS, 2018), which is the highest among all the available renewable sources. At the same time, the installed capacity of sites generating electricity from Solar PV is 12,775.7 MWe (BEIS, 2018), which is the second highest. According to the data, it is clear that PV panels is one of the most important renewable sources for generating electricity. Compare to the other renewable technologies, PV panels are relatively affordable, as well as the installation and maintenance. According to British Research Establishment (BRE) (2016), there is no need for planning permissions for most of the domestic-scale PV systems. For individual dwellings, PV output goes to the dwellings concerned, whereas for buildings with multiple dwellings, PV output either goes to the matching individual dwellings or apply to households' supply as a whole. For large, centralised commercial-scale installations, certain planning permissions are required. BRE (2015) stated that planning permissions are needed for ground mounted solar PV projects that are more than 50kWp. Environmental Impact Assessment (EIA) and

Planning Performance Agreement (PPA) must be carried out before applying any planning permissions. The considerations of the application include development in relation to current land use, assessment of the impact upon agricultural land, ground maintenance, construction compound, access, security, orientation, visual impact, ecology, historic environment, glare, airport safety, drainage, flooding etc.

The cost trend of PV installation in these three leading countries of PV installations mentioned above, clearly represented that the initial cost of mounting a PV system has been decreasing and it is considered that the continuing growth of PV deployment is led by the falling price. In the USA, to install an average domestic-scale PV system costs about \$40,000 in 2010, but \$18,000 in 2019, the price of PV installation has dropped dramatically in the last decade, over 70% (SEIA,2019). In Germany, the cost of installing a rooftop PV system costs around €14/Wp (up to 10kWp) in 1990 and it only costs less than €2/Wp in 2018 (ISE,2019). In the UK, Green Business Watch (no date) summarised that in 2017, the installation cost for a 4kW PV system has dropped 67% since 2010. It costs about £20,000 to mount a 4kW PV system in 2010, but £6,668 for the same system in 2017. Furthermore, the Feed-In Tariff (FIT) scheme launched in 2010 in the UK also contributed to the rapid growth of PV installations. The tariff for stand-alone PV with capacity ranged up to 5000kW is 37.42p/kWh for the first year when FIT was first launched, and it was adjusted to 0.05p/kWh in January 2019 (Ofgem,2019). With the wide spread of PV installations, it is reasonable to see a drop in the tariff rate after it has been carried out for 9 years. The continuing falling price of PV installation with the return rate paid by the FIT scheme, PV is still the best choice among all the renewable technologies.

1.2 Rationale for this Research

The electrical characteristics of all the PV products provided by the manufacturers are results obtained by measuring the devices under standard test conditions (STC). It is a controlled indoor environment with fixed temperature at 25°C, fixed solar irradiance at 1000W/m² and atmospheric air mass value at 1.5. Values collected under STC are advantageous for benchmarks, however, these values cannot be used for calculating the actual energy output. Under real conditions, the non-linear electrical behaviour (Ghani,F. *et al.*, 2014) and the exposure to the unpredictable environmental conditions will affect the energy output. The energy output under real conditions depends on many factors, such as the installation, the local climate, the weather conditions, types of PV

1.2 Rationale for this Research

and its manufacturer. Hence, a gap has been developed between the information manufacturers provided and the actual performance under real conditions. Table 1.1 below gives the average of efficiency data provided by manufacturers for five common PV technologies (Gul,M. *et al.*,2016) and the tested efficiency under real conditions (Cañete,C. *et al.*,2014), (Balaska.A. *et al.*, 2017) and (Sharma,V. *et al.*,2013). It is obvious that in general, the efficiency of a PV system under real conditions is lower than the provided value from manufacturers.

Types of PV	Monocrystalline	Polycrystalline	a-Si	CdTe	CIS
Efficiency (Manufacture)	18.45%	15.45%	7.45%	15.5%	12.9%
Efficiency (Real Conditions)	14.63%	13.83%	7.23%	9.3%	11.41%

Table 1.1 Comparison between manufacturers' data and real condition data

Therefore, it is important to understand what factors make what kind of impacts on the PV performance, in order to find out the better ways to enhance the PV performance and reduce the degree of PV performance degradation. Apart from external environment factors mentioned above, the change of electrical characteristics of PV cells can also affect PV performance to a significant level. Hence, analyse the variation in electrical characteristics is significant for understanding PV performance and its degradation.

This research is based on a data set of four different PV panels obtained in Obing, Germany from 31st August 2009 to 30th September 2010. It will be focusing on learning the PV electrical characteristics and understanding the significance of the key electrical characteristics in terms of performance degradation of all four PV panels.

1.3 Research aim, objectives and hypothesis

Research Aim: Investigating electrical characteristics and the performance of PV panels. Understand the significance of electrical characteristics regarding the performance degradation.

Research hypothesis: There is a strong correlation between key electrical characteristics and the PV performance.

Based on the research aim and hypothesis, the objectives of this study are as follows:

1. To understand PV panels' basic theories and electrical characteristics
2. To identify which key electrical characteristics are significant in relation to PV performance.
3. To understand the relationship between the key electrical characteristics and PV performance.
4. To analyse the relationship between the key electrical characteristics and PV performance/degradation under real conditions.

1.4 Dissertation Structure

- Chapter1 – Introduction: This Chapter provides a general overview of PV technology and states the research gap, research hypothesis, research aims and objectives.
- Chapter2 – Literature Review: This Chapter provides a literature review that covers PV installation status, PV technology, PV characteristics and PV performance. Furthermore, it emphasises the corresponding findings in the previous literature that are relevant to this research.
- Chapter3 – Methodology: This Chapter provides the methodology of the whole research, includes the data set background, the details of the Python programme written for data analysis. Furthermore, it outlines the analysis procedure.
- Chapter4 – Results and Discussion: This Chapter provides the results (mainly graphs and tables) and discussion based on the data analysis from the Python programme for four different PV panels individually. Moreover, a cross comparison of four different panels is also covered at the end.
- Chapter5 – Conclusion: This Chapter provides the conclusion of all findings in this research, a discussion of the limitations for this research and followed by a list of recommendations for future relevant research.
- References: List of references.

1.4 Dissertation Structure

- Appendices: Information sheet from manufacturers and the Python programme GitHub link.

2. Literature Review

Although the growth of energy demand is decelerating, it has been predicted to expand by 30% between now and 2040 (IEA, 2017). IEA also pointed out that electricity is gradually becoming “the rising force among worldwide end-uses of energy” (IEA, 2017a) due to the increasing amounts of electric cars and smart electrical appliances. In order to reduce the impacts of climate change and react to the shortage of fossil fuels, the world is at a decisive moment in the transition from traditional sources to renewable sources. Therefore, renewable sources like solar became increasingly important and it is crucial to research into this field of study.

2.1 Photovoltaics (PV)

2.1.1 PV installation status

- Worldwide

The global solar PV cumulative installed capacity achieved around 398 GW in 2017. It is expected to increase by 580GW gradually from now to 2023, which means in 2023, the capacity will be almost 2.5 times more than 2017 (IEA, 2018). According to IEA, the global average annual net capacity additions of Solar PV between 2010 and 2016 is 39GW. It is expected to reach 74GW between 2017 and 2040, which will account for almost the half of all the renewable capacity addition by that time (IEA, 2017b).

- Europe

Installation status of solar PV are considerably different from country to country due to different climate conditions and energy policies. Looking at the countries in Europe as a whole, the total installed capacity of solar PV in 2017 is about 109GW, which is around 27% of the global installation capacity (IRENA, 2018). Although it appears to be successful, it was indicated in the PV Status Report that “the Europe’s share is not only declining in relation to a growing market worldwide, but also in actual installation figures.” (European Commission, 2017). The European Union (EU) has proposed a target in the 2030 climate and energy framework: At least 27% share for renewable energy of EU energy consumption (European Commission, 2013). It is clear that the target will be difficult to meet if the solar PV installation is at this rate, therefore, new policies and strategies are necessary at this stage.

- Germany

2.1 Photovoltaics (PV)

Germany is moving towards a none fossil-nuclear age and it is believed that PV technology will play a critical role in the future. According to Wirth,H. summarised in the Recent Facts about Photovoltaics in Germany (2018), the Federal Network Agency in Germany has reported that there were 1.75 GW new PV capacity installed in Germany in 2017, which contributed 2% of new installation in the world. In order to meet the renewable energy generation target, Germany has to install approximately 5GW new PV annually until 2050 with around 7GW new PV replacement every year. Wirth,H. also mentioned in the report that, electricity generated by PV has covered 7.2% of Germany's net electricity consumption including grid loss in 2017.

- UK

By the end of 2017, the solar PV installed capacity in the UK has reached 12.78GW and it increased to 12.95 GW in September 2018 (BEIS, 2018c). It is likely that there are two main reasons behind the gradual growth of solar PV installation. Firstly, the cost of installing solar PV has been dropped from year to year. The UK government has indicated that the average cost for 0-4kW installations in 2017/2018 was 1.4% lower than in 2016/2017 (BEIS, 2018d). Secondly, the government incentive: Feed-In Tariff (FIT) scheme has been encouraged the installation of small-scale renewable technologies.

- Scotland

At a smaller scale, in Scotland, there were no solar PV installation before 2010. However, it started to grow rapidly from 2010 and reached 0.323GW by the end of 2017, growing trend shown in Figure2.1 (BEIS,2018e). There has been a small decline between 2016 and 2017, the reason behind it could be the FIT's rate keeps decreasing every year since it was executed. In order to support the expansion of solar energy applications, it was mentioned in the Scottish Energy Strategy document that the Scottish Government will: "consider the on-going role for solar (and other renewable technologies) as part of a further review of energy standards within building regulations; and ensure that Good Practice guidance for shared ownership developments fully recognises the opportunities for solar." (Scottish Government, 2017).

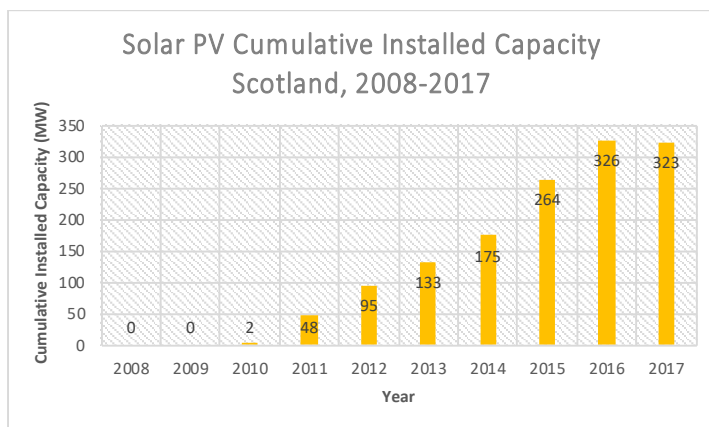


Figure2.1 Solar PV Cumulative Installed Capacity in Scotland (illustration by author, source: BEIS, 2018, Renewable electricity capacity and generation (ET6.1) table 6.1c)

2.1.2 PV application

As a modular technology, PV can be manufactured in large production lines, which leads to economies of scale. Furthermore, PV are qualified for a wide range of application due to the diversification of its deployment. They can be installed in a small system like a calculator, a stand-alone system or a solar farm (IEA, 2018a).

- Stand-alone system

Stand-alone systems are also known as off-grid systems. The most common type of this system is called a solar home system (SHS), it is particularly popular among dwellings and suitable for most of the residential electrical appliances (Salas,V, 2016). In this system, PV modules are connected to a charge controller, batteries and an inverter. (shown in Figure2.2) Batteries are used for storing the generated DC power and it will be converted to AC power by the inverter to supply the AC load required in the households. However, the energy loss at the storage stage is one of the unavoidable circumstances when generating power from solar PV. Take a three bedrooms house in the UK as an example, a 3-4kW installation will cost around £5520-£6040 (*Solar Guide*, 2018).

- Grid-connected system

A Grid-connected system generates electricity and feeds the generated energy back into the national electricity grid (Wu,L. *et.al*, 2017). There are two different types of solar systems under this application: building integrated PV systems and terrestrial PV systems, which includes plants in desert etc. (Mahela,O. and Shaik,A. 2016). A typical grid-connected system includes PV panels, a DC-DC converter, an inverter, a filter and a distribution panel which is

2.1 Photovoltaics (PV)

connected to the local loads and the grid (shown in Figure 2.2). The cost of building a grid-connected system is similar to a stand-alone system, however, with the closure of FITs in 2019 in the UK, there will be no payback from installing any solar PV systems in households until the next incentive support being published (BEIS, 2018f).

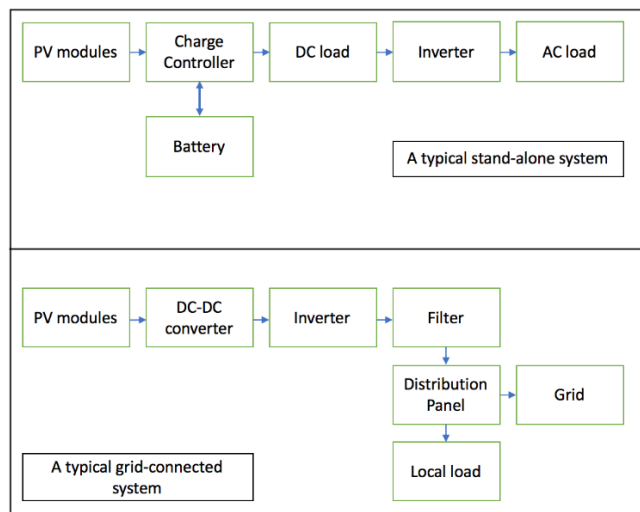


Figure 2.2 A simple illustration of stand-alone and grid-connected PV system (illustration by author)

- Solar power station

Apart from the two relatively small systems reviewed above, another type of application of solar PV has caught the attention nowadays: solar power stations, it is also known as utility-scale PV systems, solar farms or solar parks. A solar power station contains a large number of solar panels that are connected together and generate bulk power to feed into the electricity grid (Wolfe, P.R., 2011).

The article (Financial Express, 2017) reported that the Longyangxia Dam Solar Park in China contains 4 million solar panels with a total area over 25 square kilometres which made it the world largest solar park in 2017. The park can generate about 220 GWh of electricity every year, which means it has the ability to power up to 200,000 homes. The building cost is equivalent to £721.3 million. Although a solar farm's performance seems to be considerable, to plan and build a solar farm requires strict site selection, complicated regulation permit, sufficient funding and mature technologies (Wolfe, P.R., 2011a).

- Summary

In general, installing solar PV systems can reduce electricity bills and most of the small-scale systems only require frequent cleaning as maintenance. However, the performance of solar PV systems is depending on the

environmental conditions (Fouad,M.M.*et.al.*, 2017) and the initial cost of setting up a solar PV system is relatively expensive. Solar PV system can also take up a lot of space and energy loss during the distribution is inevitable. In order to show the differences among the three systems discussed, a table was made to show the comparison. (Table2.1)

System types	Scale	Costs	Benefits	Problems
Stand-alone system	Small-medium	Relatively expensive	<ul style="list-style-type: none"> • Saving on energy bills • Renewable energy, less carbon emission 	<ul style="list-style-type: none"> • Energy loss at storage
Grid-connected system	Small-medium	Relatively expensive	<ul style="list-style-type: none"> • Saving on energy bills • Payback from FITs scheme • Renewable energy, less carbon emission 	<ul style="list-style-type: none"> • Closure of FITs in the UK (31st March 2019) • Energy loss during distribution
Solar power station	Large	Exceedingly expensive	<ul style="list-style-type: none"> • Considerably performance • Enough to power large numbers of households 	<ul style="list-style-type: none"> • Sufficient funding is a must have • Difficulties on site selection • Energy loss during distribution • Maintenance is demanding

Table2.1 Comparison among three different types of solar PV applications (Summarised by author)

2.1.3 PV cell

A photovoltaic cell is commonly known as a solar cell. Solar cells are devices that convert the light energy into electricity through photovoltaic effect (Fonash, R.T. *et.al.* no date). In 1839, photovoltaic effect was first introduced by French physicist Alexandre-Edmund Becquerel who observed that some specific materials can produce small amounts of electric current when exposed to light (Knier,G.,2008). According to Nocito,C. and Koncar,V. (2016) “The photovoltaic effect can be defined as being the appearance of a potential difference (voltage) between two layers of semiconductor slice in which the conductivities are opposite, or between a semiconductor and a metal, under the effect of a light stream.” Solar cells are mostly made of two layers of semiconductor materials, such as silicon. The top layer is known as n-type layer, contains free electrons which is negatively charged, whereas the bottom layer is known as p-type layer contains free holes which is positively charged. The area where n-type layer and p-type layer joined is called p-n junction, where an electric field is formed (Figure2.3). When the solar cell is exposed to solar radiation, the photons of the sunlight will free the electrons in the electric field, then these electrons will be pushed out of the junction by the electric field, which will cause electricity flow (Dhar,M.,2017). The p-n junction is sitting close to

2.1 Photovoltaics (PV)

the top to maximise the collection of photogenerated charge carriers (Rahman,M.Z. and Khan, S.I.,2012).

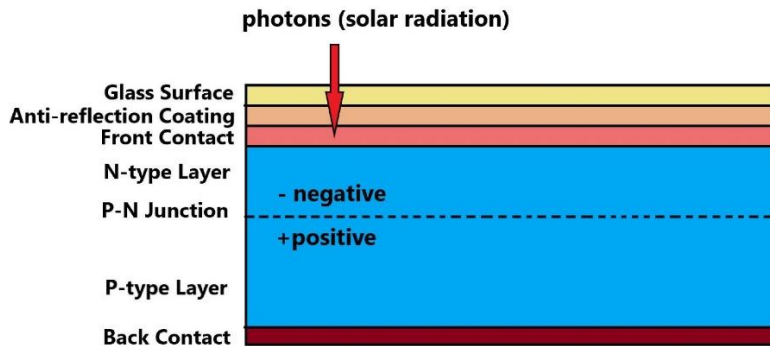


Figure2.3 A simple diagram of the cross-section of a solar cell (illustration by author)

According to Oazi,S. (2016,pp.31-82), in general, the voltage output of a single PV cell is in the range of 0.5V to 0.6V and the current output is the range of 2A to 5A, depends on

the efficiency and the size of the PV cell. However, the output voltage from a single PV cell is limited, it can hardly meet the requirements for any large-scale applications. Therefore, PV cells are often connected in series or in parallel in order to increase the voltage output, setup like this is called a PV module. Furthermore, if larger voltage output is needed, a PV array will be made by connecting several individual PV modules (Figure2.4).

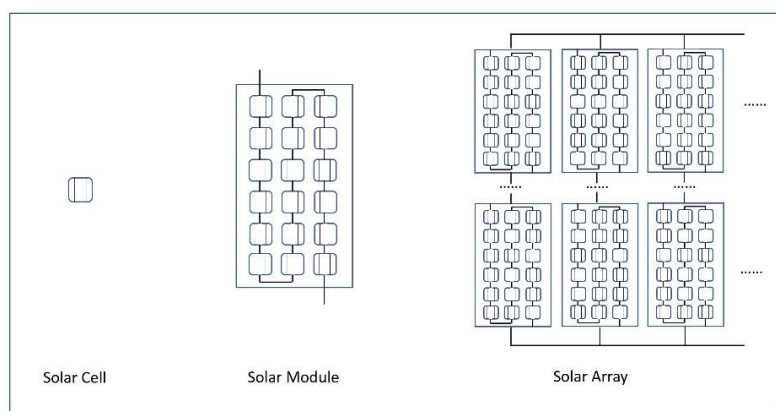


Figure2.4 A simple diagram of solar cell's physical configuration (illustration by author)

2.1.4 PV panel technology

PV cells on the market can be categorised into three generations:

- First generation: wafer-based crystalline PV cells
monocrystalline PV cells (mono-Si), polycrystalline PV cells (poly-Si) etc.
- Second generation: thin-film PV cells (TFSC)
amorphous silicon PV cells (a-Si), micro-amorphous silicon (a-Si/ μ c-Si) etc.
- Third generation: biohybrid PV cells, concentrated PV cells (CVP) etc.

(Bagher, A.M. *et.al*, 2015) and (IEA,2010)

Cheshire (2012) mentioned in CIBSE guide F, monocrystalline, polycrystalline and amorphous PV cells are the most common types of PV applied in buildings.

Monocrystalline is made of a slice from a single crystal, it is the most efficient, but also the most expensive cell (CIBSE TM25, no date, p.1). Polycrystalline is made from molten silicon, cast in a mould and it is relatively cheaper compare to monocrystalline (Niclas, 2012). Thin film amorphous silicon is deposited as a thin layer, only about 1 micrometre thick, therefore it is a flexible material for solar panels. It has lower efficiency, but it is the cheapest compare to the other two mentioned above (Richardson, L. 2018). In order to show the differences among the three solar cells clearly, a table was made to show the comparison. (Table2.2)

Table2.2 Comparison among three different types of solar cells (Summarised by author) source:

Solar cell types	Monocrystalline	Polycrystalline	Thin film amorphous
Appearance	Blue/ Black Individual modules	Blue Multifaceted	Grey/Brown/Black Matt
Cost (£/m²)	450	375	160
Cell efficiency (%)	13-17	12-15	5-10
Module efficiency (%)	12-15	11-14	4-7.5
Advantages	Most efficient	Cheaper than monocrystalline	Cheapest
Disadvantages	Expensive	Slightly less than monocrystalline	Least efficient Requires bigger space

CIBSE TM25 (no date, p.1 a) & CIBSE KS15 (no date, p.41)

However, the efficiency noted above are not fixed. The solar cell technology is developing continually. IEA noted that the monocrystalline commercial module efficiency is 21% between 2010-2015, it is predicated to increase to 23% before 2020 and targeted to reach 25% between 2020-2030/2050. For polycrystalline, the commercial module efficiency is 17% between 2010-2015, it is expected to increase to 19% by 2020 and 21% in the longer term. For thin film silicon, the commercial module efficiency is 10% between 2010-2015, it is targeted to raise up to 12% by 2020 and 15% by 2030 (IEA, 2010a).

Apart from the most common types of PV panels (monocrystalline, polycrystalline and thin film amorphous) that mentioned above, a few other types of PV panels have started to be installed more frequent.

2.1.4.(a) CdTe (Cadmium Telluride)

CdTe is a type of thin-film chalcogenide PV cells. It has a proper bandgap value that can absorb sunlight like Silicon (Li,C. *et al.*, 2017), the cost for production is relatively low with a relatively high efficiency, which is 21.4% with a 0.4% variation tested under lab environment (Green, M,A., *et al.*, 2017).

2.1 Photovoltaics (PV)

2.1.4.(b) CIS (Copper Indium Gallium Selenide)

CIS is also a type of thin-film chalcogenide PV cells. It has a relatively higher absorption coefficient and shows a high conversion efficiency, the simpler composition process makes it suitable for mass production (Hsiang,H. *et al.*, 2016).

2.1.4.(c) HCPV (High Concentration Photovoltaic)

HCPV contains optical devices to increase the light received on the module surface by multiple reflection (Fernández,F. *et al.*, 2013). HCPV has shown a growing efficiency under a standard test condition (STC), from 33.2% in 2013 to 34.9% in 2014, with the development of the junction cells, it is expected to reach more than 40% (Ghosal,K. *et al.*, 2015).

2.1.4.(d) Bifacial

Unlike monofacial PV cells, bifacial PV cells collect photons on both the front and backside (Guerrero-Lemus,R. *et al.*, 2016), based on the experiment carried out by Cuevas,A. *et al.* (1981), bifacial PV panels can potentially generate 42 -63% more power than monofacial panels.

Furthermore, tests on different types of single junction PV cells have been carried out in multiple third parties' test centres under the STC, which were under a standard test conditions: solar irradiance 1000W/m^2 , air mass 1.5 and cell temperature 25°C . The results of five types of single junction solar cell mentioned above have been sorted in Table2.3 below.

	Mono-Si	Poly-Si	Amorphous	CdTe	CIS
Efficiency (%)	26.7 ± 0.5	22.3 ± 0.4	10.2 ± 0.3	21.0 ± 0.4	21.7 ± 0.5
Area (cm^2)	79	3.923	1.001	1.0623	1.044
Voc (V)	0.738	0.6742	0.896	0.8759	0.718
FF (%)	84.9	80.5	69.8	79.4	74.3
Manufacturer	Kaneka	FhG-ISE	AIST	First Solar	Solar Frontier

Table2.3 Five different solar cells' performance test results under STC (Sorted by author)

source: Green,M.A. *et al.* (2017a)

In order to take a closer look of different PV cells' performance, eight different types of solar cells mentioned previously were chosen from eight different manufacturers and their electrical configurations are summarised in Table2.4 below.

Manufacturers	PV Types	I _{sc} (A)	V _{oc} (V)	I _{MP} (A)	V _{MP} (V)	P _{MPP} (W)	FF (%)	Efficiency (%)	Area (m ²)
SUNPOWER	Mono-Si	6.55	75.3	6.05	64.5	390	79.07	22.1	1.77
Trinasolar	Poly-Si	9.15	45.5	8.63	37.1	320	76.86	16.5	1.94
Amerisolar	Amorphous	1.27	115.8	1.06	94.4	100	68.00	/	1.56
Polysolar	Micromorph	1.33	170	1.22	131	160	70.77	/	1.54
First Solar	CdTe	2.54	218.5	2.33	180.4	420	75.68	17	2.48
Flisom	CIS	1.82	47	1.54	35	55	64.30	/	0.66
bsq solar	HCPV	4.3	78	4	70	280	83.48	28	1.01
YINGLI SOLAR	Bifacial*	10.91	46.7	10.36	38	390	76.55	19.9	1.96

Table2.4 Configurations of eight different types of solar cell (*mono-Si bifacial panel)

(Summarised by author) Source: from eight manufacturers that listed in the first column

The electrical parameters in the Table2.3 and 2.4 will be reviewed in the next section:

2.2 PV cell characteristics

2.2.1 I-V characteristics

- Current-Voltage curve

Also known as I-V characteristics curve, often seen as I-V curve. The curve represents the relationship between current and voltage output of a solar cell and the shape of the curve represents the performance of the solar cell. Figure2.5 (A) below shows a typical I-V curve.

According to Ma,T. *et al.* (2014) there are three critical points on the curve: the open-circuit voltage (V_{oc}), short-circuit current (I_{sc}) and maximum power point (P_{MPP}), which were discussed in the following points.

2.2 PV cell characteristics

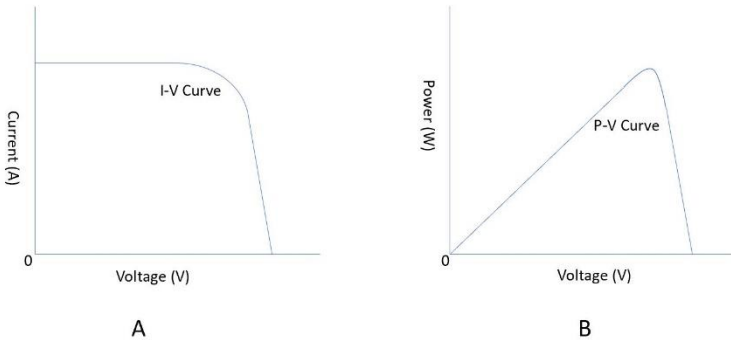


Figure 2.5 A typical I-V curve (A) and a typical P-V curve (B) of a solar cell (illustration by author)

- Power-Voltage curve

Often seen as P-V curve, it represents the relationship between power output and voltage output of a solar cell as well as the performance of the solar cell.

Figure 2.5 (B) above shows a typical P-V curve.

The formula of calculating the power can be stated as

$$P = V \times I$$

where P is Power with unit W

V is Voltage, measured in V

I is Current, measured in A

(Georgia State University, no date)

- Short circuit current (I_{SC})

A short circuit is a faulty situation in electrical circuits that causes excessive current flows in the opposite direction. When under a short circuit condition, a maximum current will be provided by the solar cell, which is known as short circuit current (I_{SC}) while no voltage will be provided. I_{SC} has a higher value than any other current under the day- to- day operating situation (Alternative Energy Tutorials, no date).

On an I-V curve, I_{SC} is the point where voltage is 0 and current is at its maximum (seen as the starting point of the I-V curve).

- Open circuit voltage (V_{OC})

An open circuit is a situation that the electrical circuit is not complete, which means no current flows in the circuit. Horowitz,P. and Hill,W. (2015) stated that the difference between an open circuit and a short circuit is “an open circuit has nothing connected to it, whereas a short circuit is a piece of wire bridging the output.” When under an open circuit condition, the solar cell is not connected to

any loads, a maximum voltage will be provided by the solar cell, which is known as open circuit voltage (V_{OC}) while no current will be provided. V_{OC} has a higher value than any other voltage under the usual operating situation (Alternative Energy Tutorials, no date, a).

On an I-V curve, V_{OC} is the point where voltage is at its maximum and current is 0 (seen as the end point of the I-V curve).

- **Maximum power point (P_{MPP})**

Solar cells under the situation mentioned above (short circuit and open circuit) do not generate any power, but power will be generated when the circuit is under the normal operating conditions. The power will reach to its maximum value at some point under a normal operating circumstance, this point is known as maximum power point (P_{MPP}). The value of P_{MPP} is the product of maximum power voltage (V_{MP}) and maximum power current (I_{MP}).

$$P_{MPP} = V_{MP} \times I_{MP}$$

On an I-V curve, P_{MPP} is the point where both voltage and current at their maximum value (under normal operating conditions), which is located at somewhere on the bending part of the curve. The optimal operation of a solar cell is designated to be at the P_{MPP} (Alternative Energy Tutorials, no date, b).

- **Fill factor (FF)**

Fill factor (FF) represents the quality of the solar cells. The definition of FF is the ratio of the value of P_{MPP} and the product of V_{OC} and I_{SC} , which can be written in the equation:

$$FF = \frac{P_{MPP}}{I_{SC} \times V_{OC}} = \frac{I_{MP} \times V_{MP}}{I_{SC} \times V_{OC}}$$

(Azli,N.A. *et al*, 2008)

Ideally, the value of FF is expected to be as close to 1 as possible, however, in real life, FF ranged between 0.52 and 0.82 (National Instruments, 2012).

- **Efficiency (η)**

The efficiency (η) of the solar cell is the ratio of the electrical power output (P_{OUT}) produced by the solar cell and the solar power input (P_{IN}) to the solar cell. P_{IN} is the product of the solar irradiance measured in W/m^2 with the solar cells' surface area measured in m^2 .

The equation of η is:

$$\eta = \frac{P_{OUT}}{P_{IN}}$$

2.2 PV cell characteristics

(National Instruments, 2012, a)

- Summary of I-V characteristics

Figure 2.6 below is a summary on a typical I-V curve, includes all the I-V characteristics mentioned above. It is noticeable that FF is the ratio of the area enclosed by the orange dash lines and the area enclosed by the green dash lines.

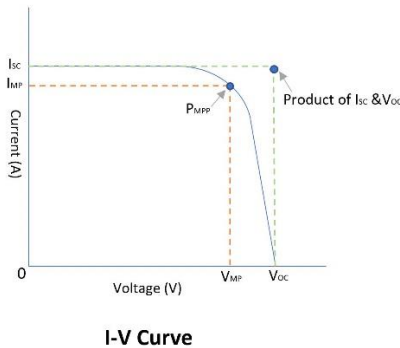


Figure 2.6 A typical I-V curve includes all the important points (illustration by author)

2.2.2 Electrical Characteristics

- Shunt resistance (R_{SH})

Shunt resistance (R_{SH}) is sometimes called parallel shunt resistance. According to Ghani,F. *et al* (2013), the value of the shunt resistance (R_{SH}) is defined as “any parallel high-conductivity paths across the solar cell p-n junction”.

According to Ramalingam,K. and Indulkar,C. (2017) when the R_{SH} decreased, the P_{MPP} will decrease and potentially if R_{SH} is decreased to a certain level, V_{OC} will also decrease. Furthermore, R_{SH} cannot be measured precisely but can be calculated from the tangent of the I-V curve that intersects with the point of I_{SC} , as seen in Figure 2.7 (A) below. The reduction in R_{SH} has a huge impact on P_{MPP} and FF, which means it will lead to a noticeable degradation of the PV performance, therefore it cannot be neglected. According to Meyer,E.L. and Ernest van Dyk,E. (2005), a maximum 63% of power loss can occur with a low R_{SH} . R_{SH} is affected by shading within a-Si and CIS panels (Meyer,E.L and Ernest van Dyk,E., 2005a) and also strongly affected by the cell temperature within crystalline panels (Ghani,F. *et al.*,2015).

- Series resistance (R_s)

Series resistance (R_s) is defined as “a lumped parameter value which represents the summation of several loss mechanisms in a solar cell” (Ghani,F. *et al.*, 2013). According to Ramalingam,K. and Indulkar,C. (2017,a) when the R_s increased, the P_{MPP} will decrease and potentially if R_s is increased to a certain

level, I_{sc} will also decrease. R_s cannot be measured precisely as current or voltage, but it can be calculated from the tangent of the I-V curve that intersects with the point of V_{oc} , as seen in Figure 2.7 (B) below.

The increase of R_s also has a huge impact on P_{MPP} and FF, hence, leads to the impact on the PV performance. Study carried out by Ernest van Dyk,E. and Meyer, E.L.(2004) shows that when R_s increased from 0.36Ω to 1.80Ω , an approximately 25% loss in P_{MPP} and FF has occurred. Likewise, P_{MPP} and FF have dropped almost 50% when R_s increased from 0.36Ω to 3.60Ω . R_s is rather sensitive to the cell temperature within crystalline panels (Ghani,F. *et al.*,2015a).

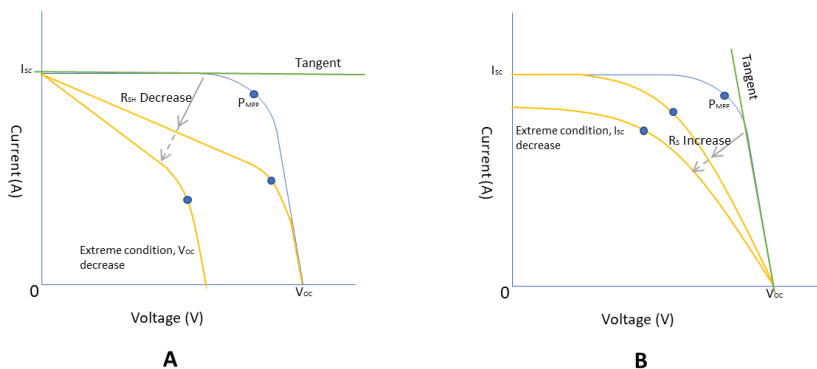


Figure 2.7 Shunt resistance (A) and Series resistance (B) on I-V curve (illustration by author)

- Ideality factor (n)

Ideality factor (n) is also commonly seen as diode factor. Singh,N.S.*et al.*,(2009) states that n is a real quality factor that demonstrates the level of which a p-n junction solar cell's performance is close to the ideal diode model. The literature (Bayhan,H. and Bayhan,M., 2011) mentioned n is a crucial parameter that is sensitive to temperature and solar irradiance. Furthermore, Amaral da Luz,C.M., *et al.* (2018)'s study also shows that there are clear evidences to prove that n is mainly influenced by the change in R_{sh} and R_s .

- Reverse saturation current (I_0)

The reverse saturation current (I_0) is sometimes called dark saturation current, it is defined as “the leakage or recombination of minority carriers across the p-n junction in reverse bias” by Ghani,F. *et al.*(2015a), the literature also stated that it is one of the main factors can affect the V_{oc} . Furthermore, Boyle stad,R. and Nashelsky,L. (1998) mentioned that in germanium based solar cell, the increase of I_0 is proportional to the increase of temperature, every 10°C increase in temperature results in a double of the value of I_0 , whereas it is not as

2.2 PV cell characteristics

obvious in a silicon based solar cell, this is also one of the reasons silicon based solar cell has a higher efficiency.

- Photo-generated current (I_{PH})

The photo-generated current (I_{PH}) is sometimes seen as light-generated current or photovoltaic current. It is generated when the photons are absorbed by the solar cell. Villalva,M.G., *et al.*(2009) stated that I_{PH} is relatively hard to be evaluated, which means when model a PV cell, the assumption of $I_{PH} = I_{SC}$ is usually made. In the literature (Chenni,R. *et al.*,2007), it has been proved that I_{PH} is sensitive to both solar irradiance and temperature. Therefore, the following equation (Villalva,M.G., *et al.*, 2009a) gives the linear relationship between I_{PH} , temperature and solar irradiance.

$$I_{PH} = (I_{PH,n} + K_I \times \Delta T) \times \frac{G}{G_n}$$

where $I_{PH,n}$ is the photo-generated current under nominal condition (with temperature 25°C and solar irradiance 1000W/m²), G is the solar irradiance on the cell surface and G_n is the nominal irradiance.

I_{PH} is one of the five parameters when modelling a single-diode model, the equivalent circuit of a single-diode model is shown in Figure2.8 below, the following equation shows the relationship between each parameters of a single-diode model:

$$I = I_{PH} - I_0 [\exp(\frac{V + R_S \times I}{V_t \times n}) - 1] - \frac{V + R_S \times I}{R_{SH}}$$

where V_t is the junction thermal voltage.

(Sera,D. *et al.*, 2007)

It is obvious that all these parameters can have an impact on the generation of the current, therefore they are all dominant factors that can have impacts on PV performance.

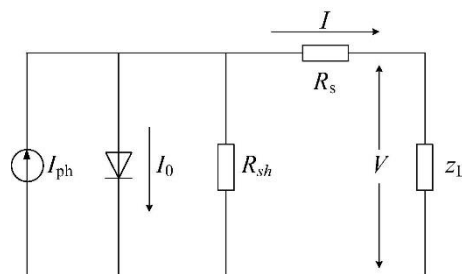


Figure2.8 An equivalent circuit of a single-diode model (Zhang,Y.,*et al.*, 2017)

2.3 Impacts on PV performance

Although PV panels have benefited the society for a long time, there are still limitations of the technology. One of the significant limitations is the efficiency of the PV cells.

According to Kabir,E., *et al.*(2018), most of the solar panels for domestic use have an efficiency between 10%-20%, the costs increases with the efficiency. Furthermore, the efficiency of the solar panels is rather sensitive to the environmental factors, solar panels exposed in an outdoor environment are most likely to suffer from degradation.

2.3.1 Key factors affecting the PV performance

Degradation will start to appear as soon as the PV panel is in use and it is expected to have a degradation rate around 0.71% annually in average (Ueda,Y. *et al.*, 2013).

- Time

Time is one of the biggest impacts on PV performance. Most of the manufacturers provide a warranty 20-25 years for PV products. Therefore, it is common to expect PV panels to work for up to 25 years. Some experiments were carried out in the past, in order to find out the degradation rate during a long period of time. Alshushan,M.A.S. and Saleh,I.M. (2013) found that a crystalline silicon PV panel that have been working in a desert in Libya for 31 years showed an average 13.86% degradation. Another experiment carried out by Cassini,D.A. *et al.*, (2017) showed that after 15 years exposed in an outdoor environment in Brazil, three of the four tested modules have a degradation rate at 2.3%, 3.7% and 2.97% respectively, which are much higher than the 1% annually degradation rate from the manufacturers' warranty.

- Cell Temperature

Based on the previous literature (Thongpao,K.*et al.*,2010), the 3- year period outdoor experiment on amorphous cells and polycrystalline cells has proved that V_{OC} is linearly proportional to the cell temperature. It decreases with an increasing in cell temperature. Whereas, I_{SC} showed a small positive relationship with cell temperature, but not enough to be a linear relationship.

As mentioned above, changes in V_{OC} and I_{SC} can lead to the shift of P_{MPP} , which means the performance will be affected. Ibrahim,H. and Anani,N. (2017) have proved that the voltage generated from PV panels decreased when the cell temperature increased. In conclusion, when cell temperature increases, there is a possibility that degradation will happen.

- Solar Irradiance

2.3 Impacts on PV performance

Thongpao,K. *et al.*(2010a) also investigated the relationship between solar irradiance and the solar performance. V_{OC} and I_{SC} are both found have a linear relationship with the solar irradiance. When solar irradiance increases, both V_{OC} and I_{SC} increase. However, solar irradiance does not have a significant impact on V_{OC} . Ibrahim,H. and Anani,N. (2017a) have also proved that current generated by the solar panels increased when the solar irradiance increased. Therefore, when solar irradiance increase, the performance of the solar panel will improve.

- Ambient Temperature

Ambient temperature is also an environmental parameter can potentially affect the PV performance. The results from the test carried out in Morocco by Maftah,A. and Maaroufi,M. (2019) showed that in a two-month period time, amorphous PV cells and monocrystalline PV cells are both affected by the change of ambient temperature. Dhoke,A. and Mengede,A. (2017) stated that when ambient temperature increases, R_S will usually increase due to the absorption of long wavelength photons. As mentioned previously in section 2.2.2, when R_S increases, I_{SC} decreases, which will lead to degradation.

- Shading

When install PV panels, shading is one of the most important factors that need to be considered carefully (Ramli,M.Z. and Salam,Z., 2019). High-rise buildings, trees and anything that might cover the panel surface are considered to be shading. Sundareswaran,K. *et al.* (2015) stated that approximately 50% of power loss occurs with 9% shading. Shading also has a big impact on R_{SH} , Meyer,E.L. and Ernest van Dyk,E. (2005b)'s study showed that there is a strong correlation between R_{SH} and the slope of a shaded cell's reverse I-V curve, which means there is a negative relationship between R_{SH} and shading, shading leads to a decreasing in R_{SH} . As mentioned previously in Section 2.2.2, a reduction in R_{SH} will cause the reduction in V_{OC} . Therefore, shading also contributes to the degradation. The same study also mentioned that shading 50% of a PV cell can result in 38% reduction in power generation.

- Soiling Effects

Similar to shading, the coverage on the panel surface created by dirt, sand, soil, dust, snow etc. are considered to be a factor that affect the PV performance. In fact, leaving dust on the surface for a long time will develop a dust accumulation, which, eventually, will intensify the soiling effect (Maghami,M.R. *et al.*, 2016). In the same study, it is proved that coverage of

part of the module by individual soil patches, such as leaves have a critical effect on the PV performance. In Mekhilef,S. *et al.* (2012)'s research, it is evidenced that dust, air velocity (wind speed) and humidity in the air all have impacts on PV performance, while influencing each other. The results showed that the efficiency dropped when there was more dust accumulation. Furthermore, humidity caused more dust settlement and the impact on efficiency is fluctuated with significant drop occasionally. However, the efficiency can be improved based on the wind speed and whether it clears the dust settlement or brings more dust, along with the change of humidity level. Schill,C. *et al.* (2015) reports in the literature that heavy soiling accumulated on the glass surface of solar panels resulted in about 20% temporary efficiency reduction, where the efficiency was completely recovered after cleaning the surface. A more comprehensive study included monocrystalline, polycrystalline and amorphous panels done in Cyprus (Kalogirou,S.A. *et al.*, 2013) shows that the reduction of PV panels' performance caused by soiling effect can increase up to 43%.

- Ground Albedo

Ground albedo is the ratio between the radiation reflected from a surface and the radiation incident on the surface. A study done recently by Revesz,M. *et al.* (2018) shows that the energy yield of PV increased by increasing the ground albedo, the literature also mentioned that the PV yield can be raised by 20% potentially with a highly reflective surface.

- Mismatch

The production of PV cells cannot guarantee all the cells are 100% same, therefore, sometimes the cells that are connected in series or parallel do not produce the same amount of electricity which causes energy loss (Maghami,M.R. *et al.*, 2016a).

2.3.2 Summary

As mentioned previously, literatures have already covered many relationships between PV's electrical characteristics, environmental factors and PV degradation. It is worth mentioning that among all the PV's electrical characteristics, R_s , R_{sh} , I_0 , I_{ph} and n are the most significant factors that affect the PV performance. However, there are external factors that affect these electrical characteristics, hence, cause degradation in the solar

2.3 Impacts on PV performance

cells. Furthermore, P_{MPP} , FF and η could be used as indicators to detect degradation.

Table 2.5 below summarises the findings from literatures, note that

Electrical Characteristics	PV types	Environmental Factor	Notes
R_{SH}	Crystalline Silicon	Cell temperature and shading	R_{SH} decreases, V_{OC} decreases, FF& P_{MPP} decrease
	CIS	Shading	
R_s	Crystalline Silicon	Ambient and cell temperature	R_s increases, I_{SC} decreases, FF& P_{MPP} decrease R_s increases by 10 times, FF& P_{MPP} decrease by 50%
	CIS	Shading	
n	CIS	Temperature and solar irradiance	Also changes when R_s and R_{SH} changes
I_0	Germanium	Temperature	Germanium: Every 10°C increases in temperature, I_0 doubles I_0 increases, FF& P_{MPP} decreases
	Crystalline Silicon	*Impacts on Crystalline Silicon are not as strong as germanium	
I_{PH}	CIS	Temperature and solar irradiance	Solar irradiance decreases, I_{PH} decreases, FF& P_{MPP} decreases
	Mono-Si		
	Multi-Si		

Table 2.5 Relationships between electrical characteristics, environmental factors and degradation

(Summarised by author)

3.1 Edinburgh Data (original plan)

3. Methodology

3.1 Edinburgh Data (original plan)

3.1.1 Site background

In order to achieve the aim of this study, first-hand data will be collected from a new-build experiment site (Figure 3.1). The site is located in Heriot-Watt University Edinburgh Campus. A shed has been built over the summer in 2018 with polycrystalline solar panels, a computer, a source measure unit (SMU) and a power supply unit installed.



Figure 3.1 Experiment site (photo taken by author)

3.1.2 Experiment procedure

1. Control

One polycrystalline panel will be cleaned regularly, 2-3 times per week. The other polycrystalline panel will be left without any cleaning process.

2. Electrical performance measurement

Current (I) and voltage (V) from both polycrystalline panels will be measured and recorded simultaneously by the SMU. The SMU data logger APP will be set up to record the data every 10 seconds, recording data at 10 seconds interval could lead to the shortage of the device's storage capacity. In order to avoid the problems of collecting useless data (night time) and save storage space, the SMU will be set up to only collect data from 06:00 to 20:00 every day. Data will

be recorded and downloaded to LabView, this process will take about two weeks. It will then be repeated for two times in two different months.

3. Analyse the data

Current-Voltage (I-V) curve and Power-Voltage (P-V) curve will be traced.

Both of the curves represent the values of the PV panel's electrical characteristics, including the open circuit voltage, short circuit current, maximum power output, voltage at maximum power and current at maximum power. Therefore, the impact of dust accumulation on PV performance will be presented in I-V curves and P-V curves.

Furthermore, the impact on each individual electrical characteristic will be analysed and compared the impact level among each other.

3.1.3 Limitations

The experiment was postponed due to the delay in site installation and delivery of key equipment (SMU, source measuring unit). Later when started to collect data, it was discovered that the SMU delivered is a faulty product. Till this point, the experiment was postponed again and due to the time limit of the dissertation, an alternative plan is needed.

3.2 Germany Data (Alternative Plan)

3.2.1 Site background

The data set was given by the supervisor. The data were obtained in Obing, Germany. The collection period is between 31st August 2009 and 30th September 2010. Obing is located in south Germany, the local climate has been identified as oceanic climate, also known as marine climate. Typically, it has a mild winter and mild summer period, with a certain level of humidity, relatively high precipitation, hence lack of dry seasons. The average temperature and precipitation in Obing has been calculated based on the data from Meteoblue (no date) and summarised in Table 3.1 below. Data from Meteoblue are based on hourly weather model simulations over 30 years.

	Average	Maximum	Minimum
Temperature (°C)	8.4	22	-4
Precipitation (mm)	92.2	124	68

Table 3.1 Average climate data in Obing (summarised by the author)

3.2 Germany Data (Alternative Plan)

3.2.2 Data collection

Four different types of panels have been installed and tested on site:

- Copper Indium Selenium (CIS) panel (model: WSG0036E080) manufactured by WURTH SOLAR
- Monocrystalline silicon (mc-Si) panel (model: SW175mono) manufactured by SOLAR WORLD
- Micro-amorphous (μ c-Si) panel (model: NA-851WQ) manufactured by SHARP
- Cadmium Telluride (CdTe) panel (model: FS Series2) manufactured by First Solar

Configurations of four panels are attached to Appendix1. to Appendix4.

Data were collected on a minute by minute basis and they can be categorized into two parts:

- Environment data: horizontal solar irradiance (W/m^2 measured by pyranometer), tilted solar irradiance on the panel surface (W/m^2 , measured by pyranometer), wind direction (North azimuth degrees), wind speed (m/s), atmospheric pressure (hPa), ambient temperature ($^\circ\text{C}$), cell temperature ($^\circ\text{C}$), humidity (%), rain duration (s) and rain intensity (mm/h)
- I-V data: A MATLAB programme has been developed by the Researcher Dr.Faisal Ghani from the School of EPS, Heriot-Watt University. The programme is designed to be able to determine all I-V characteristics: open circuit voltage (V_{oc}), short circuit current (I_{sc}), value of maximum power point (P_{MPP}), fill factor (FF) and efficiency (η), based on the I-V data collected from the solar panels. Moreover, the programme is also designed to be able to calculate all five electric characteristics: shunt resistance (R_{sh}), series resistance (R_s), reverse saturation current (I_0), photogenerated current (I_{ph}) and ideality factor (n).
- The raw data were already sorted by Dr. Faisal Ghani based on three different levels of tilted solar irradiance: 500W/m^2 , 750W/m^2 and 1000W/m^2 for the ease of analysis.

3.2.3 Data analysis

In order to analyse the data in a more comprehensive way, another programme has been written in Python (attached in Appendix5).

The analysis procedure has been divided into five parts: The analysis of WURTH SOLAR: CIS solar panel, the analysis of SOLAR WORLD: mono-Si solar panel, the analysis of SHARP: μc-Si solar panel, the analysis of First Solar: CdTe solar panel and a cross comparison of the four panels together.

According to the literature reviewed (Chapter2), the key electrical characteristics are related to the PV performance degradation and they are affected by temperature, time and solar irradiance, therefore, it is worth looking into which one is the most dominant factor that causes the electrical characteristics degradation. Then, which electrical characteristic is responsible for the performance degradation. Furthermore, what is the degradation difference among four panels and whether if it is the same factor that caused the performance degradation.

Therefore, an organised analyse order is required:

1. Analyse the I-V curve and P-V curve of September 2009 and September 2010 at three solar irradiance level: 500W/m², 750W/m² and 1000W/m².
*in Python, the average I-V data of September 2009 and September 2010 will be calculated in order to plot the I-V and P-V curves. The reason choosing September 2009 as the first month instead of August 2009 is because the test started on August 31st, 2009, there are no enough data to calculate accurate averaged values.
2. Find out the relationship of the key electrical characteristics and the cell temperature, the ambient temperature, solar irradiance.
*in Python, graphs will be plotted to show the moving pattern of the key electrical characteristics regard to the ambient temperature, module temperature and solar irradiance. (Outliers will be removed by doing interquartile calculation, in general, outliers are defined as 1.5 x IQR, however, this definition is too narrow that might move away non-outliers. Therefore, for the data analysis in this study, the outliers are defined as 9 x IQR).
3. Use P_{MPP} as the indicator, to determine which key electrical characteristic has the strongest impact on the PV performance in the solar panel.
*in Python, covariance will be calculated in order to find the correlation between P_{MPP} and the key electrical characteristics. Covariance is the measure of the variability of two random variables. 95% confidence and predict limits will be plotted on the correlation graphs only for better presentation of the correlation line.

3.2 Germany Data (Alternative Plan)

4. Compare the four panels.

- Determine the differences degradation level.
- Determine the differences of changing in key electrical characteristics.
- Determine the differences of efficiency under STC and real conditions.

*in Python, all averaged electrical parameters of each month will be calculated, then these values will be recorded in Excel to make tables for further comparisons.

Note that in Python, Würth is easier typed as Wuerth and °C is easier typed as C, on all the graphs that contain Würth and °C, it will be presented as Wuerth and C.

4. Results and Discussion

4.1 Würth Solar – CIS solar panel

4.1.1 I-V curve and P-V curve

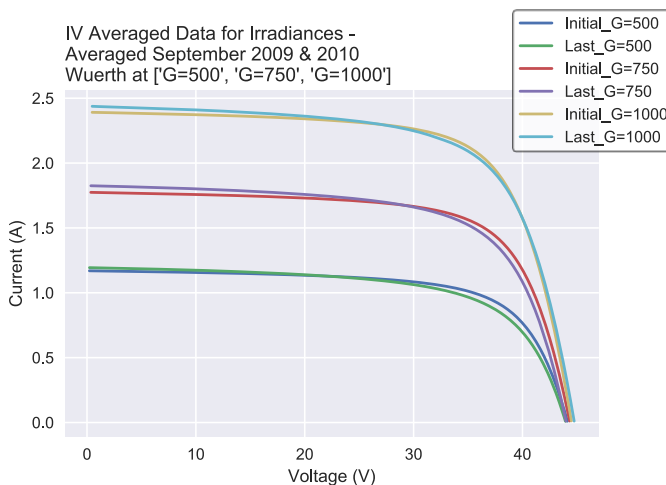


Figure 4.1.1 (a) I-V curve of the averaged September 2009 and 2010 at three irradiance level

on all of the September 2009 curves are higher than the September 2010 curves, which clearly shows that there was a reduction in P_{MPP} during the test.

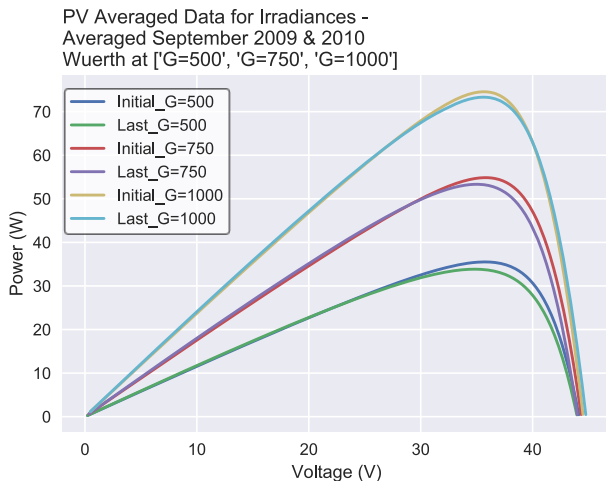


Figure 4.1.1 (b) P-V curve of the averaged September 2009 and 2010 at three irradiance level

Figure 4.1.1 (a) shows that the I-V curves have a same trend at three irradiance level. At all the solar irradiance levels, the V_{OC} have been very stable during the test and the averaged I_{SC} in September 2010 were all higher than September 2009. All curves of in September 2010 started to shift downwards when the voltage passed around 25V. Furthermore, the turning points

Figure 4.1.1 (b) shows that the curve of the last 30 days at 500W/m^2 started to shift downwards when the voltage passed around 25V, whereas at 750 and 1000W/m^2 , the curves in September 2010 started to shift downwards when the voltage passed 30V. The amount of the power loss at 1000W/m^2 is slightly less than its at 500 and 750W/m^2 .

The analysis of both figures above shows that the power output increases with growing solar irradiation. Moreover, they have proved that **there was a degradation in the PV performance within the CIS panel based on the analysis of samples in September 2009 and September 2010**. Small amount of degradation is expected annually (Ueda,Y. et al.,2013) as mentioned in the literature review in Section 2.3.1.

4.1 Würth Solar – CIS solar panel

4.1.2 Electrical Characteristics and Environment Factors

Rs with ambient temperature, module temperature and solar irradiance

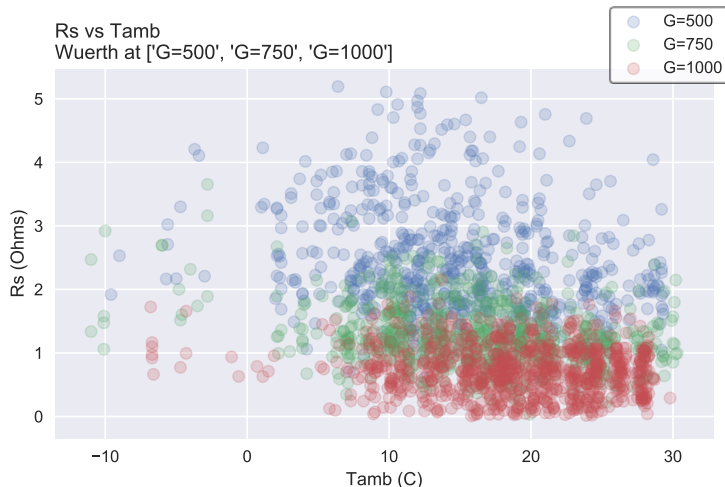


Figure 4.1.2 (a) Scattered plot to show the relationship between R_s and ambient temperature

Figure 4.1.2 (a) shows that at 500W/m^2 and 750W/m^2 , R_s varies randomly with the increase of ambient temperature, a slight drop in R_s has shown when the ambient temperature increased from 15°C to 30°C , but it behaved non-linearly. At 1000W/m^2 , R_s varies in a steadier way with the increase of ambient temperature but did not show any obvious variation.

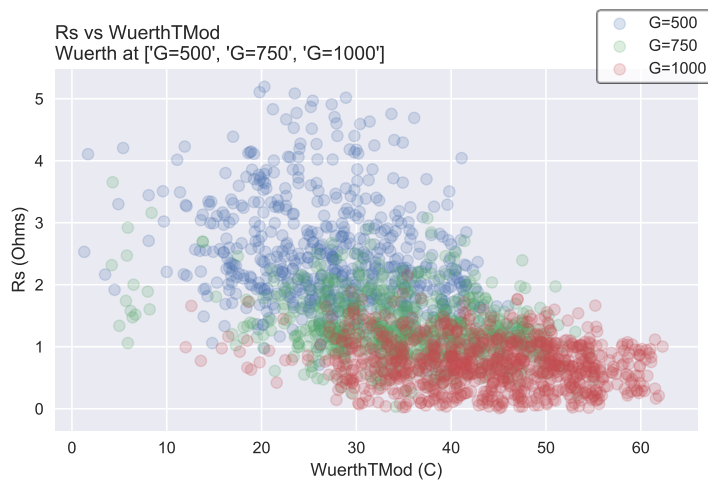


Figure 4.1.2 (b) Scattered plot to show the relationship between R_s and module temperature

Figure 4.1.2 (b) shows that R_s varies randomly with the increase of the module temperature, especially at 500W/m^2 . At 750W/m^2 and 1000W/m^2 , R_s varies in a fixed range, but did not behave linearly.

It is clear to see that the range of R_s increases when solar irradiance decreases from the two figures above. Hence, it is reasonable to consider that **Rs is inversely proportional to the solar irradiance for CIS panel**. This has been proved by the previous literature that R_s in CIS panel is sensitive to shading, where low solar irradiance could be caused by shading. The **Rs's behaviour for CIS panel did not show any particular relevance regard to ambient temperature and module temperature**, which is a key finding that has not been mentioned in any of the literature covered in Chapter2, see Table 2.5.

R_{SH} with ambient temperature, module temperature and solar irradiance

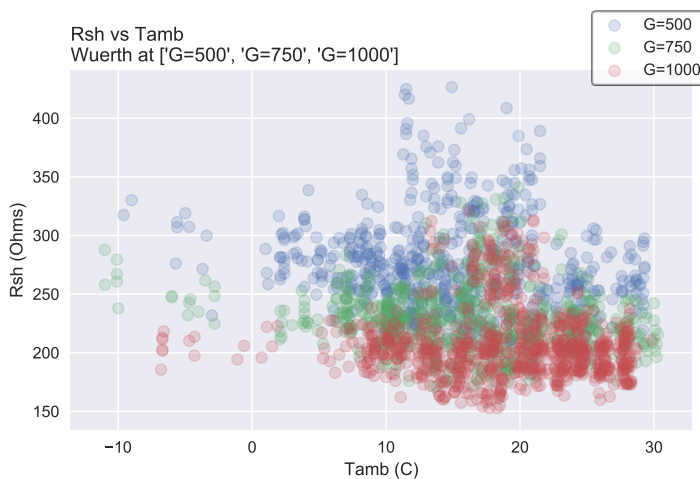


Figure 4.1.2(c) shows that R_{SH} varies randomly with the increase of ambient temperature at all three of the irradiance levels. A small peak appeared in R_{SH} when the ambient temperature reached between 15°C to 20°C, it behaved non-linearly.

Figure 4.1.2 (c) Scattered plot to show the relationship between R_{SH} and ambient temperature

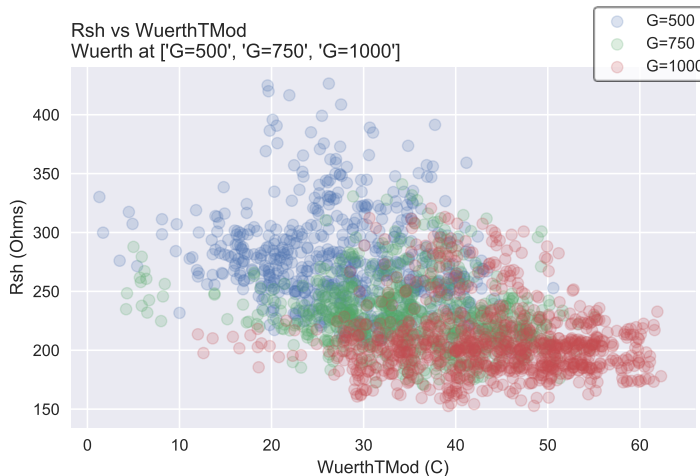


Figure 4.1.2 (d) shows that R_{SH} varies randomly with the increase of module temperature, at all three of the irradiance levels, but compare to R_s , R_{SH} varies less randomly.

Figure 4.1.2 (d) Scattered plot to show the relationship between R_{SH} and module temperature

It is observed from both of the figures that R_{SH} decreases when solar irradiance increases, therefore, same as R_s , it is considered that **R_{SH} is inversely proportional to the solar irradiance for CIS panel**. This has also been proved in the previously mentioned literature, which can be related to that R_{SH} in CIS panel is sensitive to shading.

The **R_{SH}'s behaviour for CIS panel did not show any particular relevance regard to ambient temperature and module temperature**, which is another key finding that has not been mentioned in any of the literature covered in Chapter2, see Table 2.5.

4.1 Würth Solar – CIS solar panel

n with ambient temperature, module temperature and solar irradiance

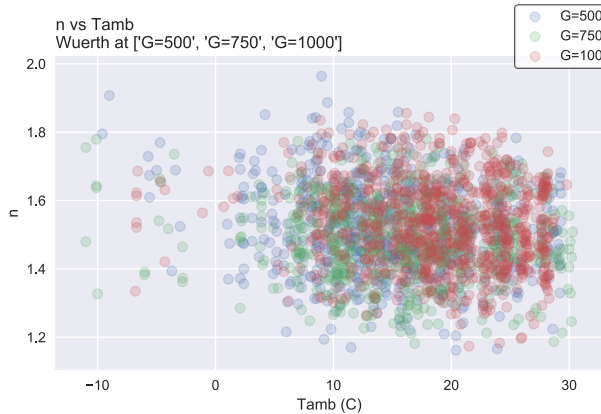


Figure 4.1.2 (e) Scattered plot to show the relationship between n and ambient temperature

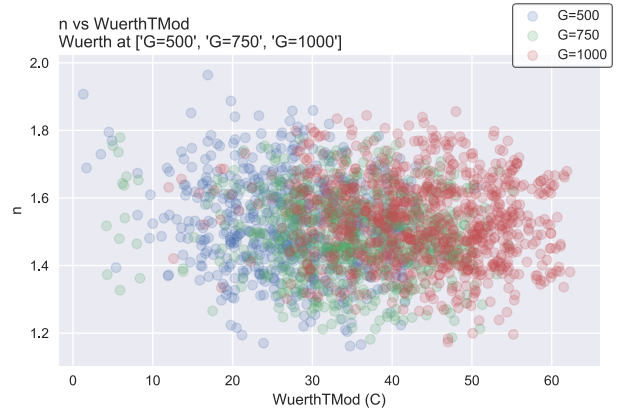


Figure 4.1.2 (f) Scattered plot to show the relationship between n and module temperature

Two figures above clearly show that n varies randomly without any patterns regard to ambient temperature, module temperature and solar irradiance. Therefore, it is reasonable to conclude that based on this data set, **n is not sensitive to ambient temperature, module temperature and solar irradiance for CIS panel**. However, these results are completely different from the literature covered in Chapter2 (see Table 2.5), according to Bayhan,H. and Bayhan,M. (2011), n is sensitive to the temperature and solar irradiance for CIS panel. One of the possible reasons caused this difference is: the variance of temperature and solar irradiance are too small for n to show any relevant changes.

I₀ with ambient temperature, module temperature and solar irradiance

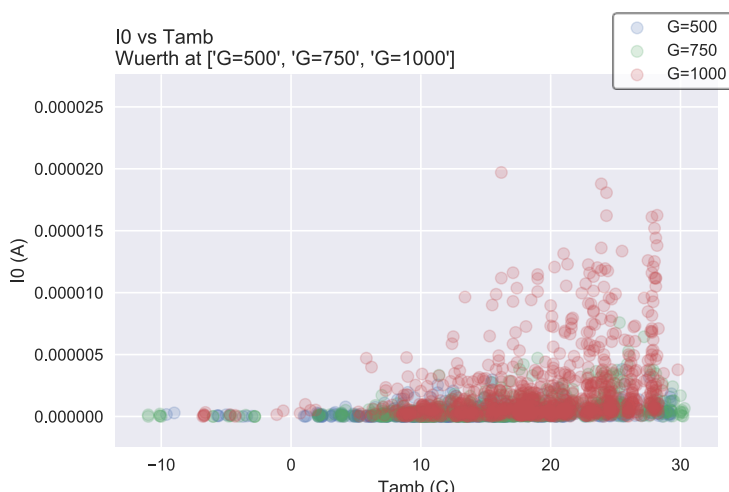


Figure 4.1.2 (g) Scattered plot to show the relationship between I_0 and ambient temperature

On the Figure 4.1.2 (g), at 500W/m^2 , I_0 did not respond to the changes in ambient temperature. At 750W/m^2 , I_0 varies between 0A to 0.000005A . At 1000W/m^2 , I_0 varies up to 0.00002A , with the increasing ambient temperature.

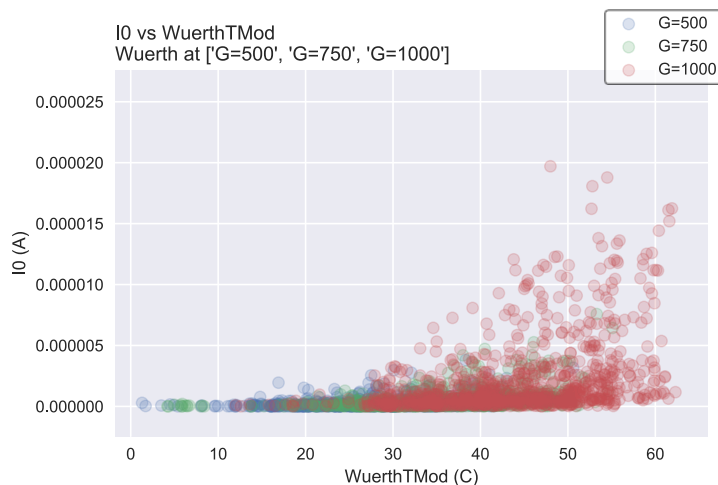


Figure 4.1.2 (h) Scattered plot to show the relationship between I_0 and module temperature

For the relationship between I_0 and the module temperature shows in Figure 4.1.2 (h), I_0 varies in a bigger range with the growing module temperature at 1000W/m^2 , between 0A and varied up to 0.00002A. However, most of the points landed in the range of 0A and 0.000005A.

Two figures above show that I_0 varies in a relatively bigger range with increasing temperature when the solar irradiance is higher. However, they are no evidences to show that there is a direct connection between I_0 and the temperature. Therefore, it is reasonable to conclude that, **I_0 is only sensitive to ambient temperature and module temperature at a higher solar irradiance for CIS panel**. This finding has not been mentioned in any of the literature covered in Chapter2, see Table 2.5.

I_{PH} with ambient temperature, module temperature and solar irradiance

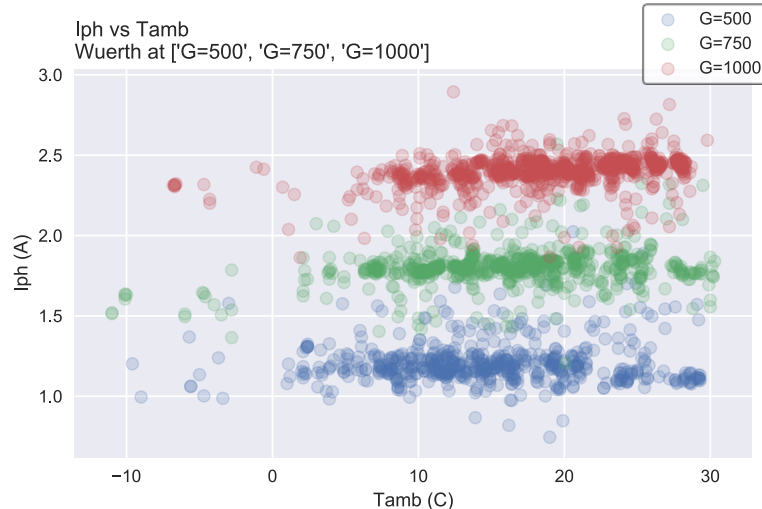


Figure 4.1.2 (i) Scattered plot to show the relationship between I_{PH} and ambient temperature

Figure 4.1.2 (i) shows that I_{PH} remains at the same level when the ambient temperature increases. At 500W/m^2 , the majority of I_{PH} is between 1A and 1.5A. At 750W/m^2 , the majority of I_{PH} is between 1.5A and 2A. At 1000W/m^2 , the majority of I_{PH} is between 2A and 2.5A.

4.1 Würth Solar – CIS solar panel

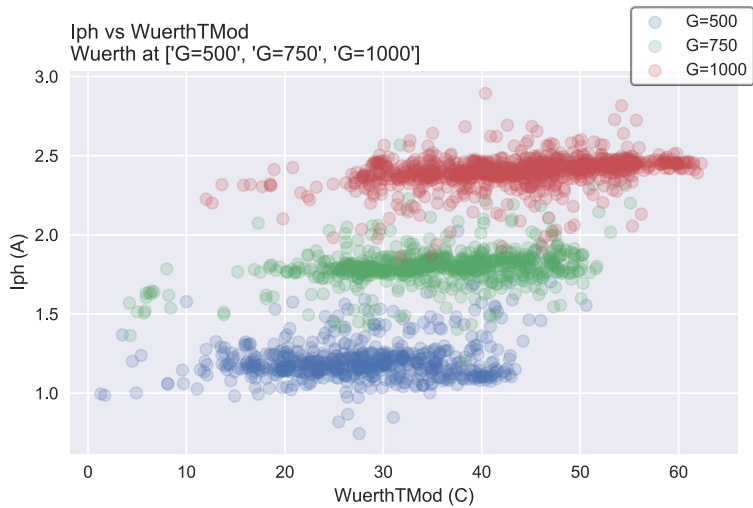


Figure 4.1.2 (j) Scattered plot to show the relationship between I_{PH} and module temperature

temperature at 750W/m^2 and 1000W/m^2 .

Both Figure 4.1.2 (i) and Figure 4.1.2 (j) show that I_{PH} varies with the change of solar irradiance. They clearly present that **I_{PH} increases while solar irradiance increases for CIS panel**. Furthermore, I_{PH} shows a small increasing trend with the growing module temperature at 750W/m^2 and 1000W/m^2 . **I_{PH} shows a very slight increase with the growth of module temperature at higher solar irradiance for CIS panel**. These have also been proved in the previously mentioned literature for the CIS panel in Chapter2, see Table2.5.

4.1.3 Electrical Characteristics and Degradation P_{MPP} and R_s

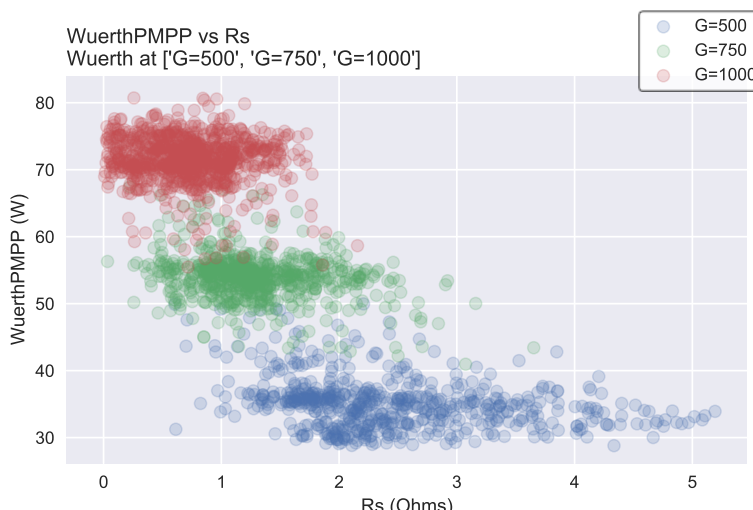


Figure 4.1.3 (a) Scattered plot to show the relationship between P_{MPP} and R_s at three irradiance level

Figure 4.1.2 (j) also shows that I_{PH} remains in the same range when the module temperature increases at each irradiance level. Note that module temperature increases when the solar irradiance increases. A slight increasing of I_{PH} can be seen with the growth of the module

Figure 4.1.3 (a) shows that at each solar irradiance level, R_s did not show any obvious changes within the growth of R_s . In order to investigate the relationship between P_{MPP} and R_s precisely, the results at 1000W/m^2 have been used for

calculating the correlation, 95% confidence and predication limits, as seen in Figure 4.1.3 (b).

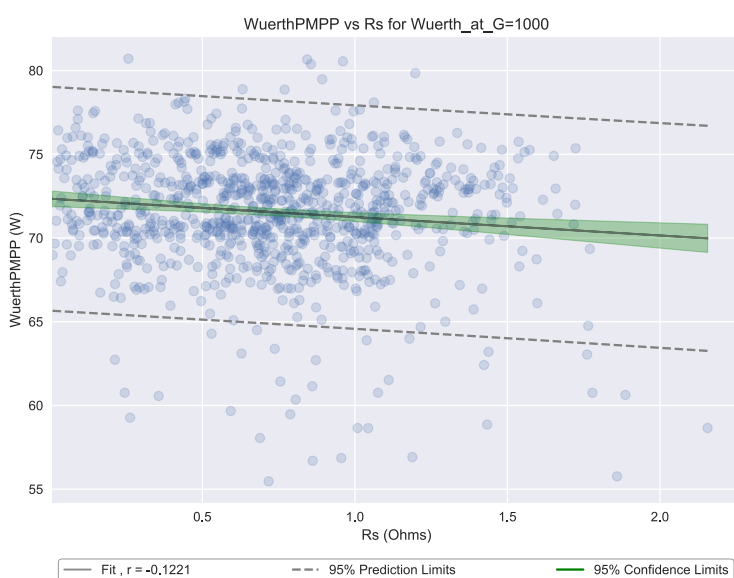


Figure 4.1.3 (b) Graph to show the correlation of P_{MPP} and R_s at $1000W/m^2$

R_s increases, P_{MPP} decreases, which was covered in the literature in Chapter2, see Table 2.5.

The correlation of R_s and P_{MPP} is -0.1221 which is almost equal to 0. Therefore, it is considered that R_s and P_{MPP} are not linearly related. The change of R_s has no impacts on the performance degradation in CIS panel.

However, the negative value of the correlation has proved the general trend of

P_{MPP} and R_{SH}

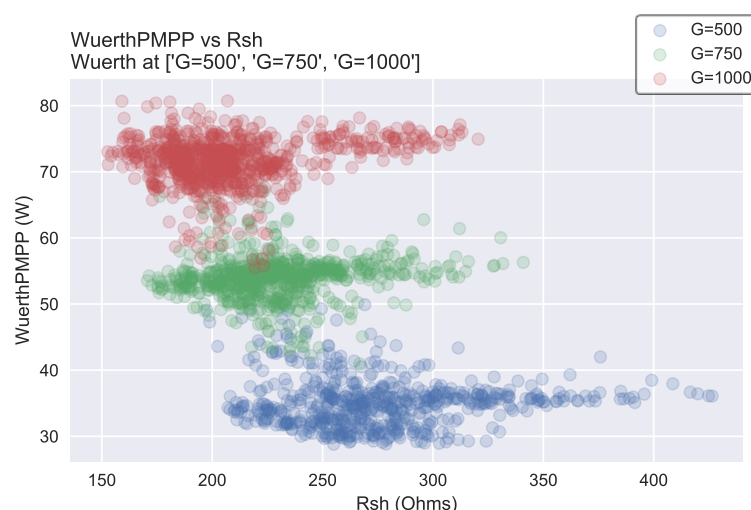


Figure 4.1.3 (c) Scattered plot to show the relationship between P_{MPP} and R_{SH} at three irradiance level

confidence limits and 95% predication limits, as seen in Figure 4.1.3 (d).

Figure 4.1.3 (c) shows that at each solar irradiance level, the P_{MPP} showed a slight increasing trend while R_{SH} increasing. In order to investigate the relationship between P_{MPP} and R_{SH} precisely, the results at $1000W/m^2$ have been chosen to calculate the correlation, 95%

4.1 Würth Solar – CIS solar panel



Figure 4.1.3 (d) Graph to show the correlation of P_{MPP} and R_{SH} at $1000W/m^2$

no impacts on the performance degradation in CIS panel. However, the positive value of the correlation has proved the general trend of R_{SH} decreases, P_{MPP} decreases, which was covered in the literature in Chapter2, see Table 2.5.

The correlation of R_{SH} and P_{MPP} is $+0.1840$, which is extremely close to 0. Therefore, it is considered that R_{SH} and P_{MPP} are not linearly related. However, the value of the correlation of R_{SH} is bigger than R_s , which means in this case, R_{SH} has slightly more impact on P_{MPP} than R_s .

The change of R_{SH} has

P_{MPP} and n

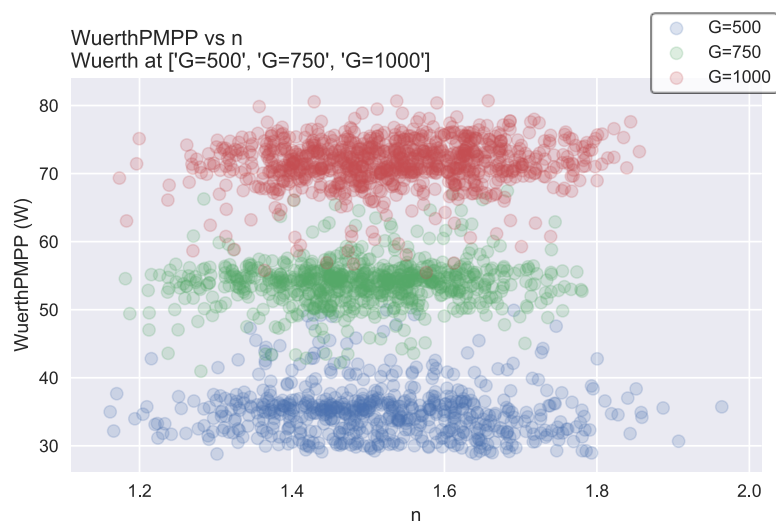


Figure 4.1.3 (e) Scattered plot to show the relationship between P_{MPP} and n at three irradiance level

Figure 4.1.3 (e) shows that n at three irradiance level are evenly distributed, between 1.2 and 1.8. Same as R_s and R_{SH} , the correlation, 95% confidence and predication limits are calculated, see Figure 4.1.3.(f), the

correlation of n and P_{MPP} is $+0.1181$, which is extremely close to 0. Therefore, it is considered that n and P_{MPP} are not linearly related.

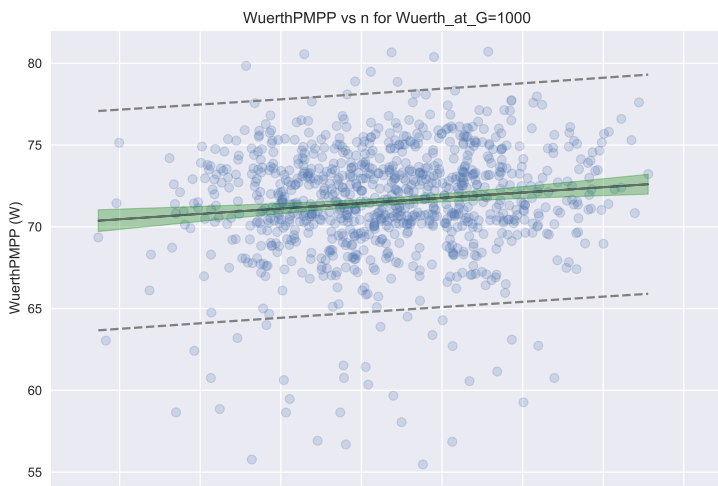


Figure 4.1.3 (f) Graph to show the correlation of P_{MPP} and n at $1000W/m^2$

P_{MPP} and I_0

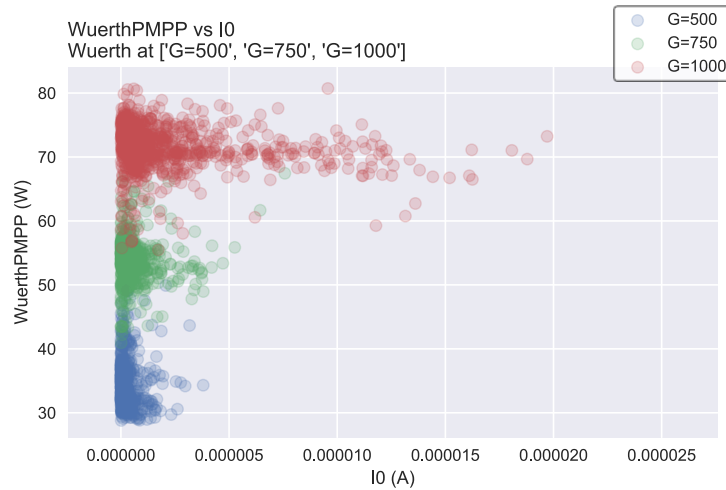


Figure 4.1.3 (g) Scattered plot to show the relationship between P_{MPP} and I_0 at three irradiance level

from varying in a certain range to the average value of the range while I_0 increasing at all three levels of the solar irradiance.

Therefore, it is reasonable to determine **that P_{MPP} converges from varying in a broader range to an averaged value of the range when I_0 increases in CIS panel, which is dynamic**. This finding has not been mentioned in any of the literature covered in Chapter2, see Table 2.5.

The change of n has no impacts on the performance degradation in CIS panel. This finding has not been mentioned in any of the literature covered in Chapter2, see Table 2.5.

Figure 4.1.3 (g) shows that there is obviously no linear relationship between I_0 and P_{MPP} at any of the irradiance level. The range of I_0 at $500W/m^2$ and $750W/m^2$ are the same. However, the range became bigger at $1000W/m^2$, up to $0.00002A$. In general, P_{MPP} shows a small converging trend

4.1 Würth Solar – CIS solar panel

P_{MPP} and I_{PH}

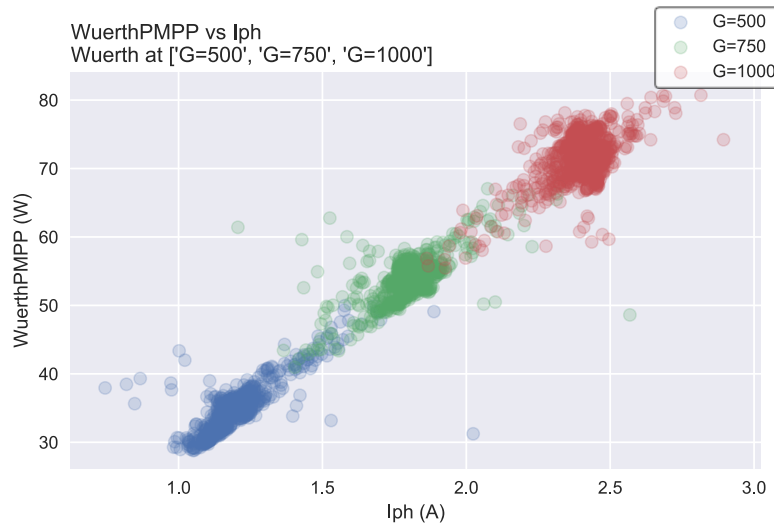


Figure 4.1.3 (h) Scattered plot to show the relationship between P_{MPP} and I_{PH} at three irradiance level

calculate the correlation, 95% confidence and predication limits, seen in Figure 4.1.3 (i).

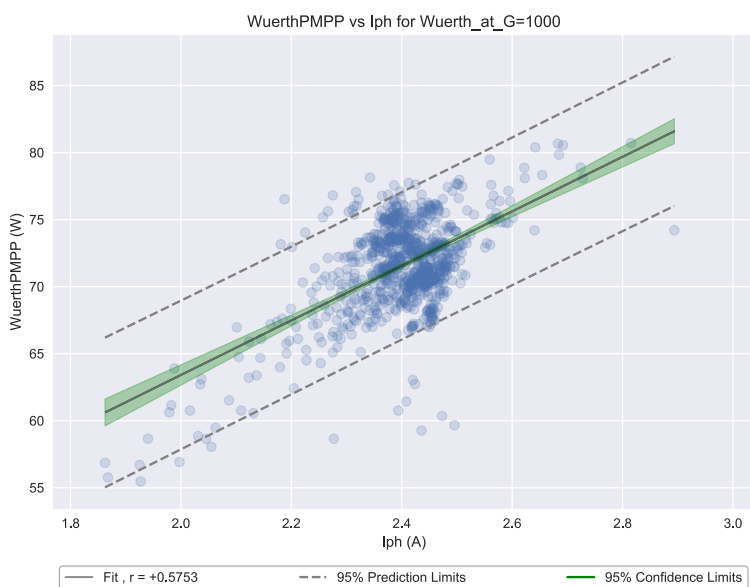


Figure 4.1.3 (i) Graph to show the correlation of P_{MPP} and I_{PH} at $1000W/m^2$

Figure 4.1.3(h) clearly shows that when I_{PH} increases, P_{MPP} increases, it is easy to observe a linear relationship between the two variables. In order to investigate the relationship between P_{MPP} and I_{PH} precisely, the results at $1000W/m^2$ have been chosen to

The correlation of I_{PH} and P_{MPP} is $+0.5753$, which is between 0 and 1. Therefore, it is reasonable to argue that **there is a positive linear relationship between I_{PH} and P_{MPP} in CIS panel**, which is expected based on the literature covered in Chapter2 (Table2.5).

In summary, the correlation of R_s , R_{SH} , n and I_{PH} and P_{MPP} are -0.1221 , $+0.1840$, $+0.1181$ and $+0.5753$ respectively. Therefore, the order of the impact strength on degradation of CIS panel is: $I_{PH} > R_{SH} > R_s > n$, the last three almost have no obvious impact on degradation in this case. Furthermore, I_0 has a dynamic impact on the PV performance, that shows a converging trend when I_0 increases.

4.2 Solar World – mono-Si solar panel

4.2.1 I-V curve and P-V curve

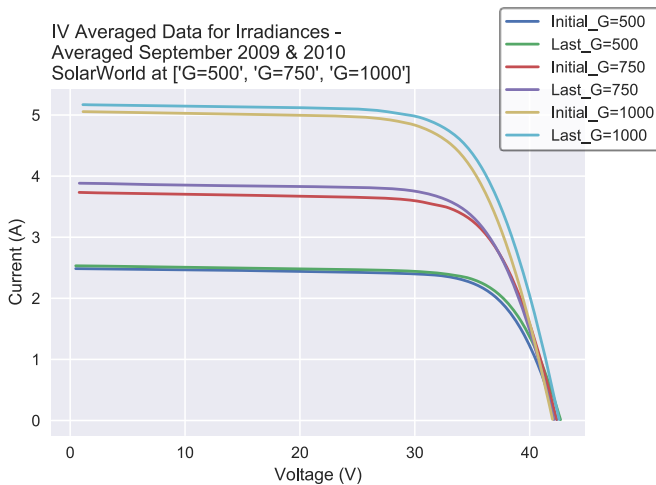


Figure 4.2.1 (a) I-V curve of the averaged September 2009 and 2010 at three irradiance level

in September 2010 was improved compare to it in September 2009.

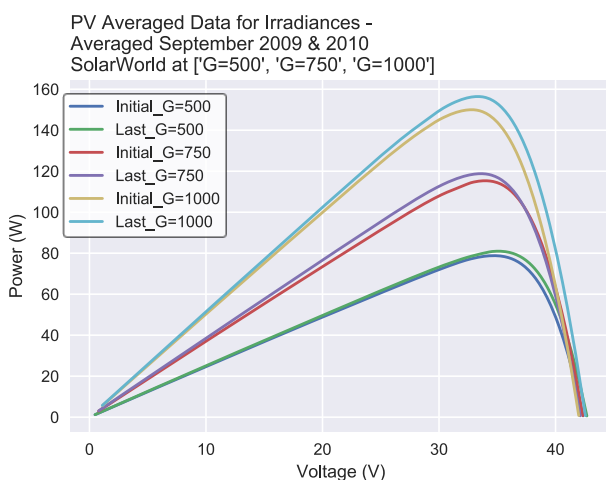


Figure 4.2.1 (b) P-V curve of the averaged September 2009 and 2010 at three irradiance level

Figure 4.2.1 (a) shows that the I-V curves have a same trend at three irradiance level. At all the solar irradiance levels, the V_{oc} have been very stable during the test and the averaged I_{sc} in September 2010 were all higher than September 2009. All curves in September 2010 are higher than curves in 2009, which means there was no reduction in P_{MPP} during the test, in fact, P_{MPP}

Figure 4.2.1 (b) shows all curves in September 2010 are higher than curves in 2009, which proved again that there was an improvement on P_{MPP} instead of a degradation between September 2009 and 2010. The power improvement at 1000W/m^2 is the highest and the improvement at 500W/m^2 is the lowest.

The analysis of both figures above shows that the power output increases with growing solar irradiation. Moreover, they have proved that **there was no degradation in the PV performance within the mono-Si panel based on the analysis of samples in September 2009 and September 2010**. Although small amount of degradation is expected annually (Ueda,Y. *et al.*,2013) as mentioned in the literature review in Section 2.3.1, it is not impossible to see improvement in the performance, since the performance of solar PV is highly depend on the surrounding environment.

4.2 Solar World – mono-Si solar panel

4.2.2 Electrical Characteristics and Environment Factors

Rs with ambient temperature, module temperature and solar irradiance

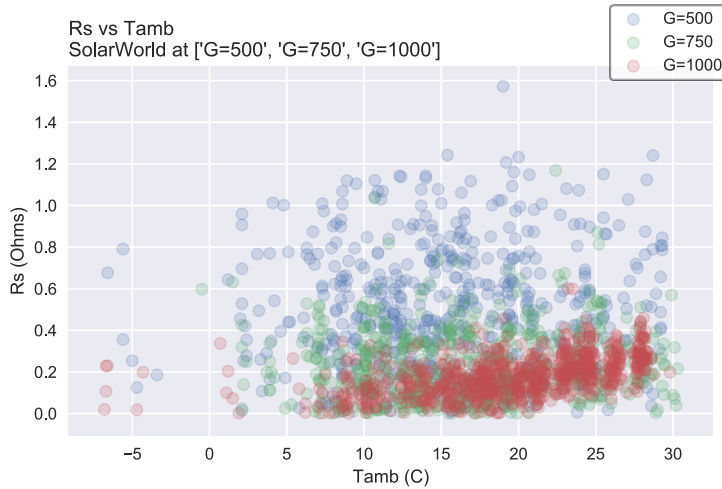


Figure 4.2.2 (a) Scattered plot to show the relationship between R_s and ambient temperature

Figure 4.2.2 (a) shows that at 500W/m^2 , R_s varies very randomly with the increase of ambient temperature. At 750W/m^2 , R_s varies in a steadier way. At 1000W/m^2 , R_s shows an obvious increasing trend with the increase of ambient temperature.



Figure 4.2.2 (b) Scattered plot to show the relationship between R_s and module temperature

Figure 4.2.2 (b) shows that R_s varies randomly with the increase of the module temperature at 500W/m^2 and 700W/m^2 . At 1000W/m^2 , same as above, R_s shows a positive linear relationship with the module temperature.

It is clear to see that the range of R_s decreases when solar irradiance increases from the two figures above. Hence, it is reasonable to consider that **Rs is inversely proportional to the solar irradiance for mono-Si panel**. This has been proved by the previous literature that R_s in mono-Si panel is sensitive to shading, where low solar irradiance could be caused by shading. The R_s 's behaviour for mono-Si panel showed that **at higher irradiance level, R_s increases when ambient temperature and module temperature increases**, which is also proved in the literature covered in Chapter2, see Table 2.5.

R_{SH} with ambient temperature, module temperature and solar irradiance

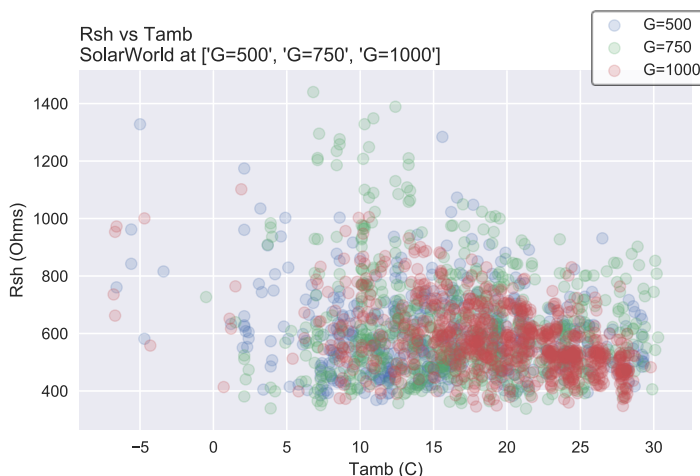


Figure 4.2.2 (c) Scattered plot to show the relationship between R_{SH} and ambient temperature

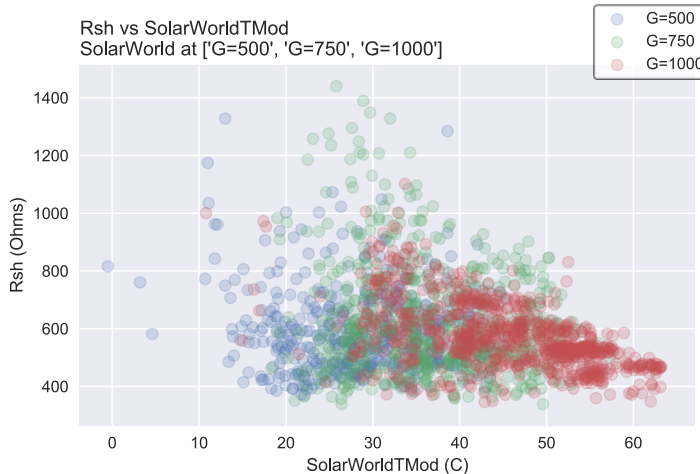


Figure 4.2.2 (d) Scattered plot to show the relationship between R_{SH} and module temperature

Unlike R_S , R_{SH} did not show any sensitivities to the change of solar irradiance. Hence, it is reasonable to consider that **change in solar irradiance does not have any impacts on R_{SH} for mono-Si panel**. The literature (Ghani,F. *et al.*,2015) covered in Chapter2 stated that R_{SH} in mono-Si panel is sensitive to shading, see Table2.5. However, lower solar irradiance does not necessarily mean it is caused by shading. The R_{SH} 's behaviour for mono-Si panel showed that **at higher irradiance level, R_{SH} decreases when module temperature increases**, which is proved in the same literature covered in Chapter2, see Table 2.5.

Figure 4.2.2(c) shows that R_{SH} varies very randomly at $500W/m^2$ and $750W/m^2$. At $1000W/m^2$, R_{SH} showed a slight decreasing trend against the increase of the ambient temperature, between $15^\circ C$ to $30^\circ C$.

Figure 4.2.2 (d) also shows that R_{SH} varies randomly with the increase of module temperature at $500W/m^2$ and $750W/m^2$. R_{SH} showed a rather clear negative trend against the increase of the module temperature, between $30^\circ C$ to $65^\circ C$.

4.2 Solar World – mono-Si solar panel

n with ambient temperature, module temperature and solar irradiance

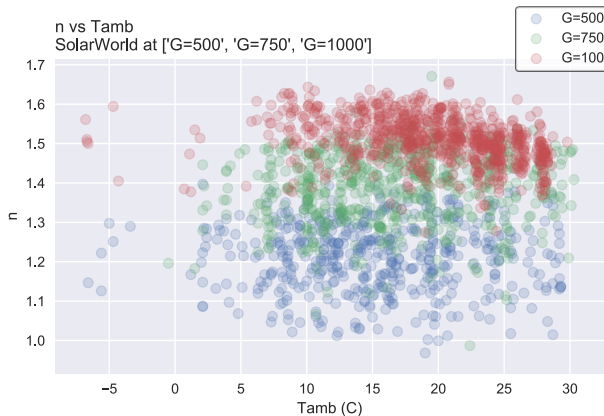


Figure 4.2.2 (e) Scattered plot to show the relationship between n and ambient temperature

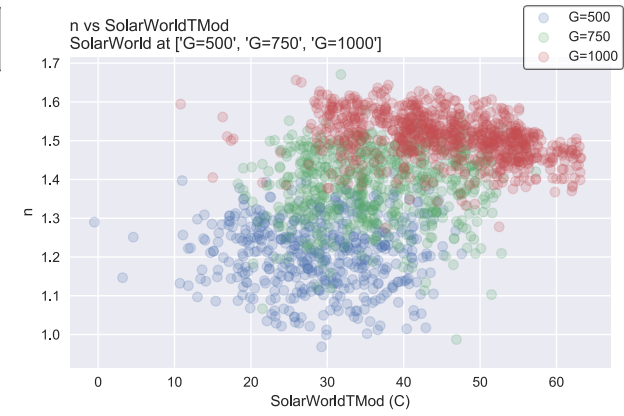


Figure 4.2.2 (f) Scattered plot to show the relationship between n and module temperature

Two figures above clearly show that n varies randomly in the range between 1.0 and 1.5 at 500W/m^2 and 750W/m^2 with the growth of both ambient and module temperature. At 1000W/m^2 , n decreases when ambient and cell temperature increases. It is also obvious to see that the range of n increases when solar irradiance increases. Hence, it is reasonable to conclude that **n is proportional to the solar irradiance for mono-Si panel**. Furthermore, it is reasonable to conclude that based on this data set, **at higher irradiance level, n decreases when ambient and module temperature increases in mono-Si panel**. This finding has not been mentioned in any of the literature covered in Chapter2, see Table 2.5.

I₀ with ambient temperature, module temperature and solar irradiance

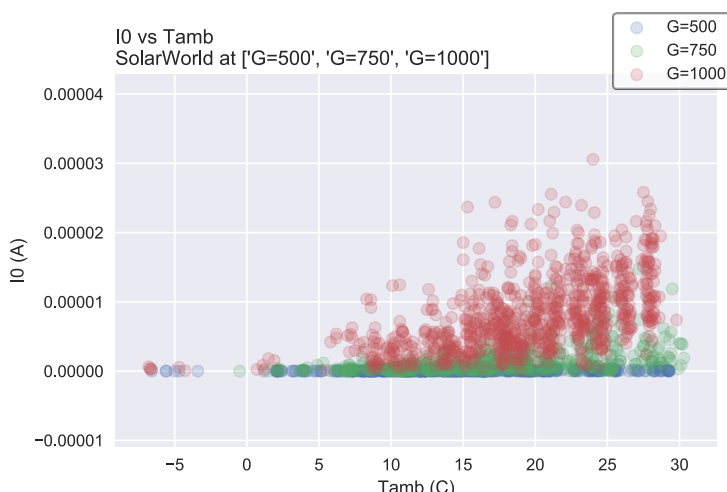


Figure 4.2.2 (g) Scattered plot to show the relationship between I_0 and ambient temperature

On the Figure 4.2.2 (g), at 500W/m^2 , I_0 did not respond to the changes in ambient temperature. At 750W/m^2 , I_0 varies between 0A to 0.00001A . At 1000W/m^2 , I_0 increases gradually from 0A to 0.00003A , with the increase of the ambient temperature.

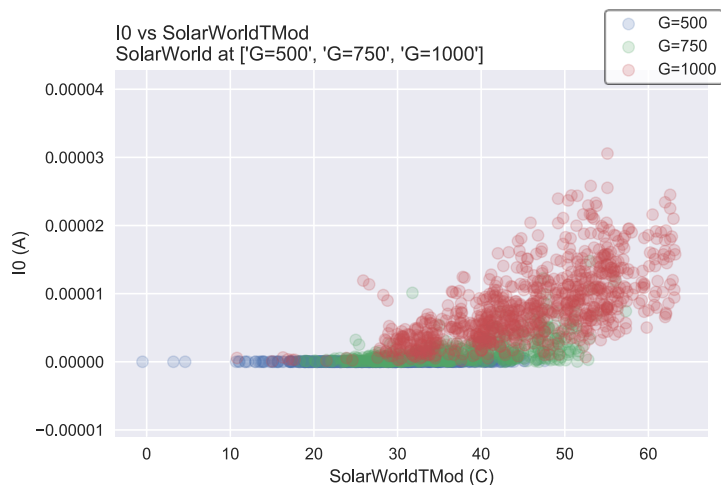


Figure 4.2.2 (h) Scattered plot to show the relationship between I_0 and module temperature

Figure 4.2.2 (h) shows the relationship between I_0 and the module temperature. I_0 at 500W/m² and 750W/m² did not show any obvious change within the growth of module temperature. However, at 1000W/m², I_0 increases gradually when module temperature increases from 30°C to 65°C.

Two figures above show that I_0 increases gradually with the increasing temperature when the solar irradiance is higher. Therefore, it is reasonable to conclude that, **I₀ increases gradually when ambient temperature and module temperature increases at a higher solar irradiance for mono-Si panel**. This has been proved in the literature covered in Chapter2, see Table 2.5.

I_{PH} with ambient temperature, module temperature and solar irradiance

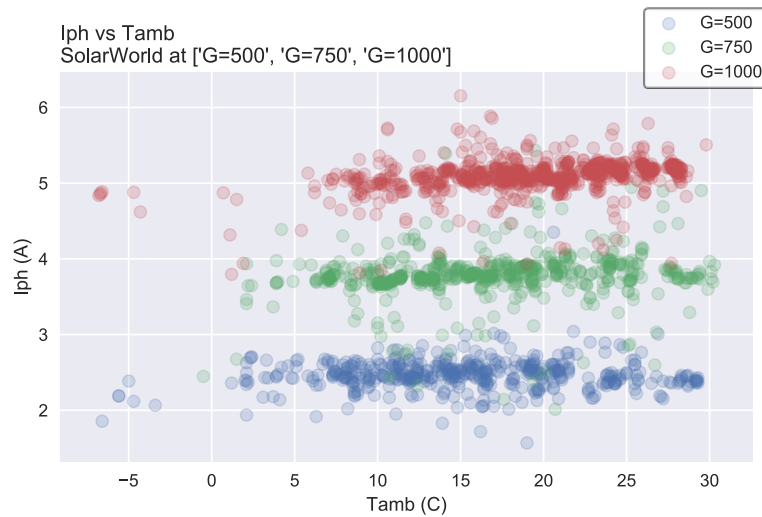


Figure 4.2.2 (i) Scattered plot to show the relationship between I_{PH} and ambient temperature

Figure 4.2.2 (i) shows that I_{PH} remains at the same level when the ambient temperature increases. At 500W/m², the majority of I_{PH} is between 2A and 3A. At 750W/m², the majority of I_{PH} is between 3A and 4A. At 1000 W/m², the majority of I_{PH} is between 5A and 6A.

4.2 Solar World – mono-Si solar panel

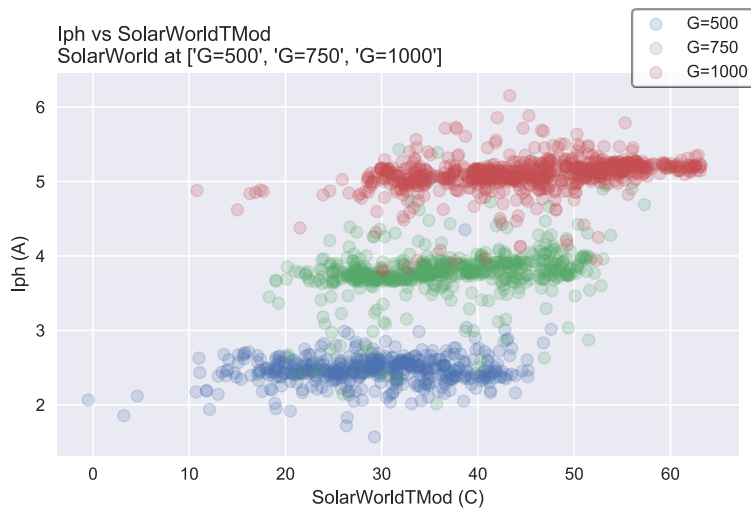


Figure 4.2.2 (j) Scattered plot to show the relationship between I_{PH} and module temperature

temperature at 750W/m^2 and 1000W/m^2 .

Both Figures above show that I_{PH} varies with the change of solar irradiance. They clearly present that **I_{PH} increases when solar irradiance increases for mono-Si panel**. Furthermore, I_{PH} shows a small increasing trend with the growing module temperature at 750W/m^2 and 1000W/m^2 . **I_{PH} shows a very slight increase with the growth of module temperature at higher solar irradiance for mono-Si panel**. These have also been proved in the literature covered in Chapter2, see Table2.5.

4.2.3 Electrical Characteristics and Degradation P_{MPP} and R_S

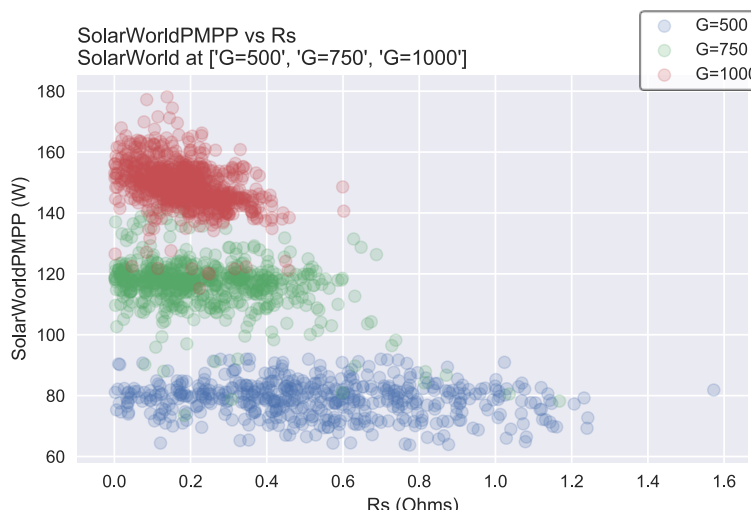


Figure 4.2.3 (a) Scattered plot to show the relationship between P_{MPP} and R_S at three irradiance level

Figure 4.2.2 (j) also shows that I_{PH} remains in the same range when the module temperature increases at each irradiance level. Note that module temperature increases when the solar irradiance increases. A slight increasing of I_{PH} can be seen with the growth of the module

Figure 4.2.3 (a) shows that at 500W/m^2 and 750W/m^2 , R_S did not show any obvious changes within the growth of R_S . However, at 1000W/m^2 , P_{MPP} decreases steeply when R_S increases.

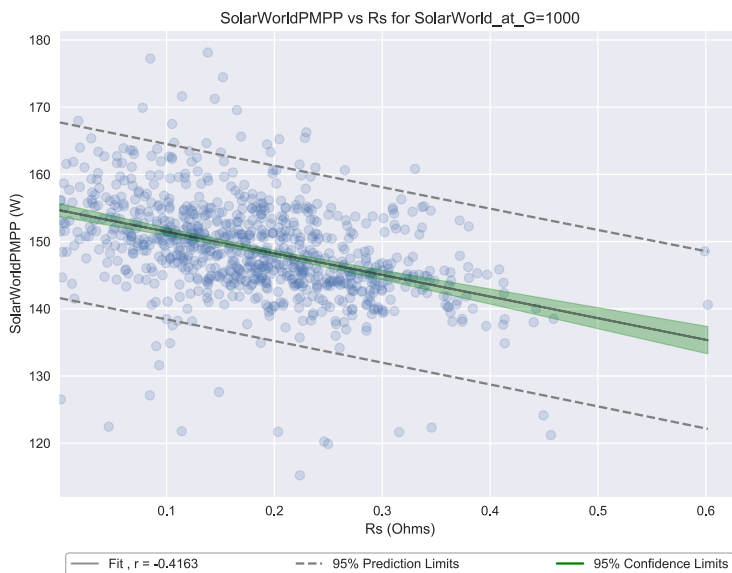


Figure 4.2.3 (b) Graph to show the correlation of P_{MPP} and R_s at $1000W/m^2$

panel.

The increasing R_s can cause reduction in P_{MPP} in mono-Si panel, which was also proved in the literature covered in Chapter2, see Table 2.5.

P_{MPP} and R_{SH}

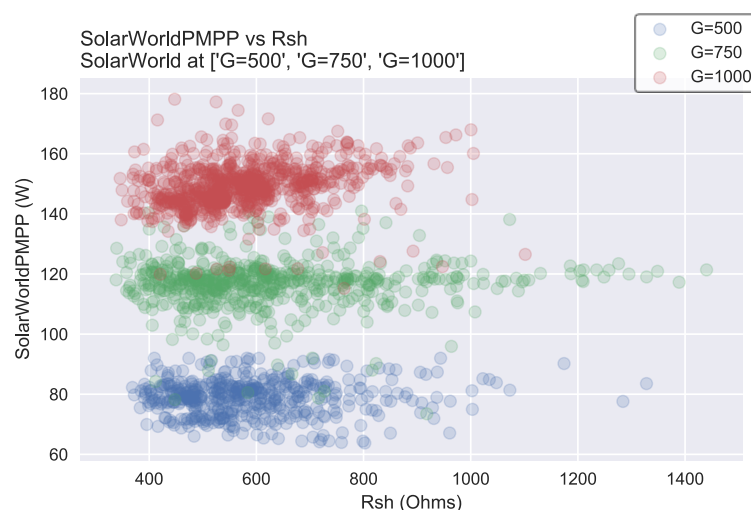


Figure 4.2.3 (c) Scattered plot to show the relationship between P_{MPP} and R_{SH} at three irradiance level

Figure 4.2.3 (d) shows the correlation, 95% confidence and predication limits of the values at $1000W/m^2$.

Figure 4.2.3 (b) shows the correlation, 95% confidence and predication limits of the values at $1000W/m^2$. **The correlation of R_s and P_{MPP} is -0.4163** which is between 0 and 1. Therefore, it is reasonable to argue that **there is a negative linear relationship between R_s and P_{MPP} in mono-Si panel.**

Figure 4.2.3 (c) shows that at $500W/m^2$ and $750W/m^2$, R_s did not show any obvious changes within the growth of R_{SH} . While, at $1000W/m^2$, P_{MPP} showed a gradual increasing trend when R_{SH} increases. Inversely speaking, P_{MPP} decreases when R_{SH} decreases.

4.2 Solar World – mono-Si solar panel

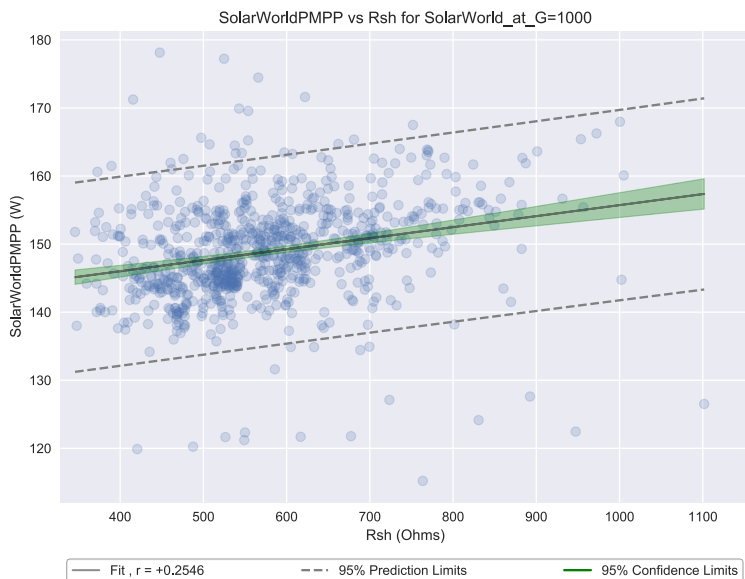


Figure 4.1.3 (d) Graph to show the correlation of P_{MPP} and R_{SH} at $1000W/m^2$

in this case. **The change of R_{SH} has minimum impacts on the performance degradation in mono-Si panel.** However, the positive value of the correlation has proved the general trend of R_{SH} decreases, P_{MPP} decreases, which was covered in the literature in Chapter2, see Table 2.5.

The correlation of R_{SH} and P_{MPP} is +0.2546, which is close to 0. There is no sufficient statistical proof to show a linear relationship. Thus, it is considered that R_{SH} and P_{MPP} are not linearly related. The value of the correlation of R_{SH} is smaller than R_s , which means R_s has more impact on P_{MPP} than R_{SH}

P_{MPP} and n

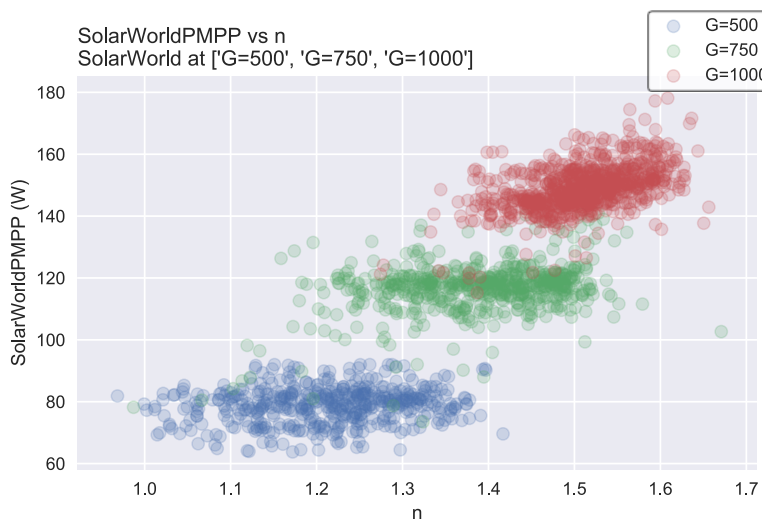


Figure 4.2.3 (e) Scattered plot to show the relationship between P_{MPP} and n at three irradiance level

Figure 4.2.3 (e) shows that at $500W/m^2$ and $750W/m^2$, the values are evenly distributed, between 1 and 1.4, 1.2 and 1.6 respectively. At $1000W/m^2$, the values are more concentrated, mainly distributed between 1.4 and 1.6. Furthermore, P_{MPP} shows a clear increasing

trend when n increases at $1000W/m^2$.

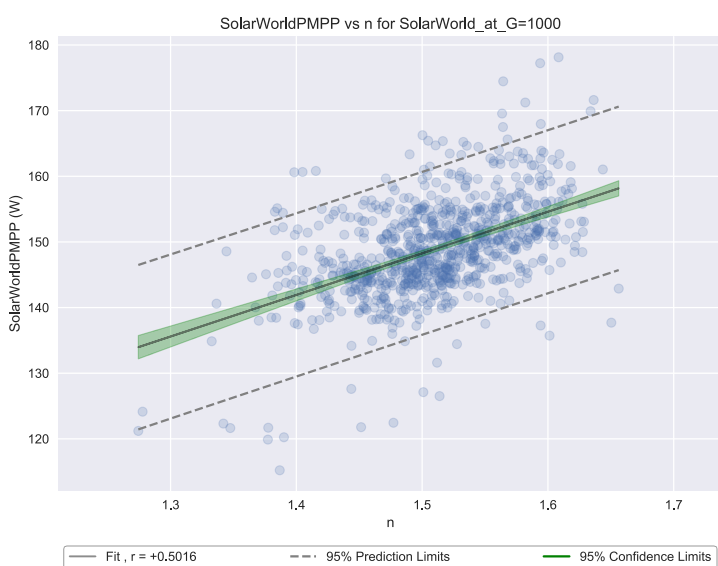


Figure 4.2.3 (f) Graph to show the correlation of P_{MPP} and n at 1000W/m^2

P_{MPP} in mono-Si panel, this finding has not been mentioned in any of the literature covered in Chapter2, see Table 2.5.

Figure 4.2.3 (f) shows the correlation, 95% confidence and predication limits of the values at 1000W/m^2 . The correlation of n and P_{MPP} is $+0.5016$, which is between 0 and 1. Therefore, it is reasonable to argue that **there is a positive linear relationship between n and P_{MPP} in mono-Si panel.**

The reduction in n can cause the reduction in

P_{MPP} and I_0

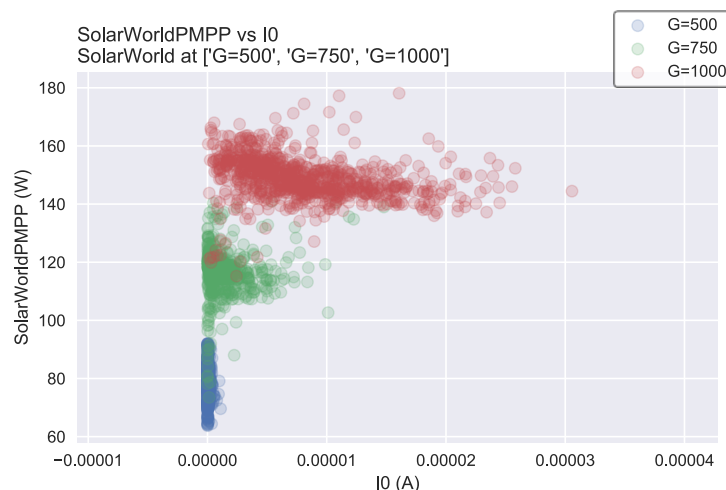


Figure 4.2.3 (g) Scattered plot to show the relationship between P_{MPP} and I_0 at three irradiance level

Figure 4.2.3 (g) shows that at 500W/m^2 , the values varied between 60W and 100W when I_0 is 0A. At 750W/m^2 , P_{MPP} shows a converging trend from varying between 100W and 140W to around 110W while I_0 increasing. At 1000W/m^2 , P_{MPP} shows a decreasing trend while I_0 increasing.

increasing. Therefore, it is reasonable to determine that **the relationship between P_{MPP} and I_0 varies depends on different solar irradiance in mono-Si panel**. This finding has not been mentioned in any of the literature covered in Chapter2, see Table 2.5.

4.2 Solar World – mono-Si solar panel

P_{MPP} and I_{PH}

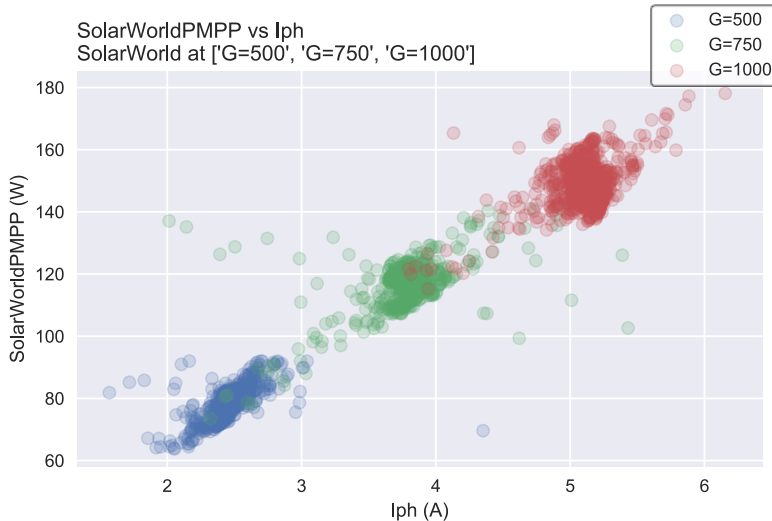


Figure 4.2.3 (h) Scattered plot to show the relationship between P_{MPP} and I_{PH} at three irradiance level

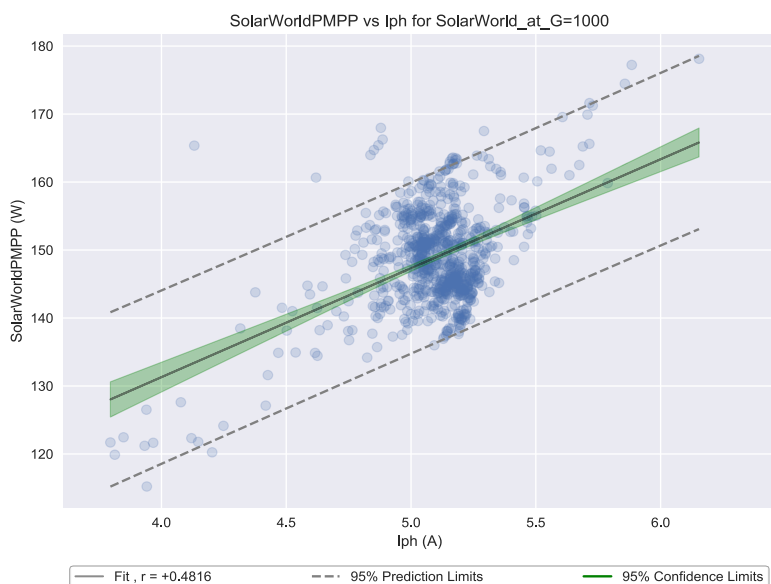


Figure 4.2.3 (i) Graph to show the correlation of P_{MPP} and I_{PH} at $1000\text{W}/\text{m}^2$

in mono-Si panel, which is expected based on the literature covered in Chapter2 (Table2.5).

In summary, the correlation of R_s , R_{SH} , n and I_{PH} and P_{MPP} are **-0.4163**, **+0.2546**, **+0.5016** and **+0.4816** respectively. Therefore, the order of the impact strength on degradation of mono-Si panel is: $n > I_{PH} > R_s > R_{SH}$, the last one only has minimum impact on P_{MPP} in this case. Furthermore, the relationship between P_{MPP} and I_0 varies depends on different solar irradiance in this case.

Figure 4.2.3(h) clearly shows that when I_{PH} increases, P_{MPP} increases, it is easy to observe a linear relationship between the two variables.

Figure 4.2.3 (i) shows the correlation, 95% confidence and predication limits of the values at $1000\text{W}/\text{m}^2$. The correlation of I_{PH} and P_{MPP} is $+0.4816$, which is between 0 and 1. Therefore, it is reasonable to argue that **there is a positive linear relationship between I_{PH} and P_{MPP}**

4.3 Sharp – μc-Si solar panel

4.3.1 I-V curve and P-V curve

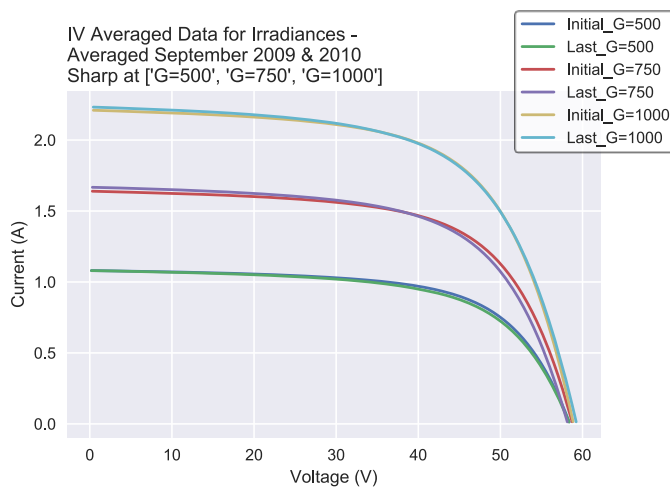


Figure 4.3.1 (a) I-V curve of the averaged September 2009 and 2010 at three irradiance level

curves, except curves at 1000W/m² where two curves coincided. It shows that there was a small reduction in P_{MPP} during the test.

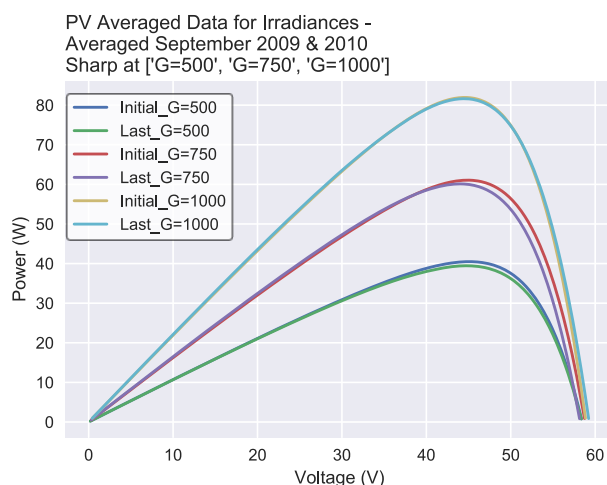


Figure 4.3.1 (b) P-V curve of the averaged September 2009 and 2010 at three irradiance level

The analysis of both figures above shows that the power output increases with growing solar irradiation. Moreover, they have proved that **there was a small degradation in the PV performance within the μc-Si panel based on the analysis of samples in September 2009 and September 2010**. Small amount of degradation is expected annually (Ueda, Y. et al., 2013) as mentioned in the literature review in Section 2.3.1.

Figure 4.3.1 (a) shows that the I-V curves have a same trend at all the irradiance levels. The Voc have been very stable during the test and the Isc in September 2010 were only slightly higher than September 2009. The Last curves started to shift downwards when the voltage passed around 30V, the turning points on all of the Initial curves are higher than them on the Last

Figure 4.3.1 (b) shows that the Last curves at 500W/m² and 750W/m² started to shift downwards when the voltage passed around 30V, whereas at 1000W/m², the curves are coincided. The amount of the power loss at 750W/m² is slightly higher than its at 500W/m² and almost no power loss at 1000W/m².

4.3 Sharp – μ c-Si solar panel

4.3.2 Electrical Characteristics and Environment Factors

Rs with ambient temperature, module temperature and solar irradiance

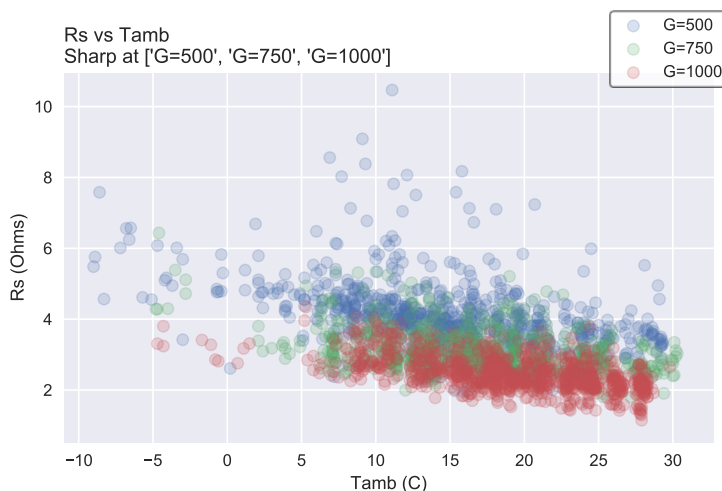


Figure 4.3.2 (a) Scattered plot to show the relationship between R_s and ambient temperature

Figure 4.3.2 (a) shows that at 500W/m^2 , R_s varies randomly in a bigger range with the increase of ambient temperature. R_s decreases gradually at all the irradiance levels when the ambient temperature increases. Therefore, it is reasonable to argue that there is a negative linear relationship between R_s and ambient temperature at all irradiance levels.

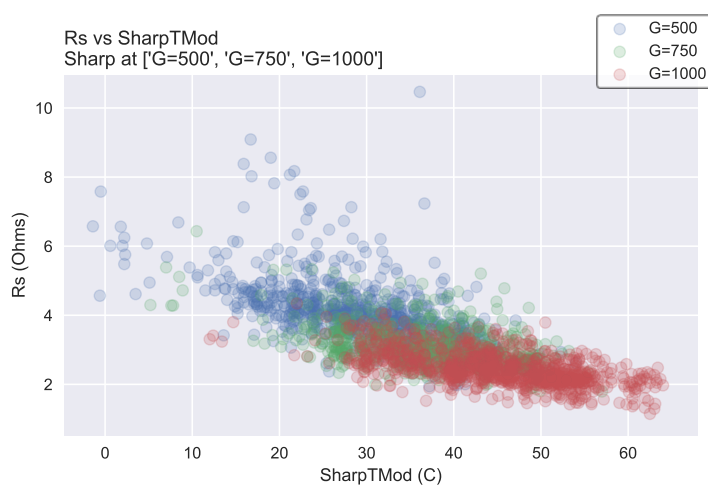


Figure 4.3.2 (b) Scattered plot to show the relationship between R_s and module temperature

Figure 4.3.2 (b) shows that at 500W/m^2 , R_s varies randomly in a relatively bigger range with the increase of the module temperature. The decreasing trend of R_s against the increasing module temperature is steeper than its against ambient temperature.

It is clear to see that the range of R_s increases when solar irradiance decreases from the two figures above. Hence, it is reasonable to consider that **R_s is inversely proportional to the solar irradiance for μ c-Si panel**. The R_s 's behaviour for μ c-Si panel showed that **at all irradiance levels, R_s decreases when ambient temperature and module temperature increases**. These are findings that have not been mentioned in any of the literature covered in Chapter2, see Table 2.5.

R_{SH} with ambient temperature, module temperature and solar irradiance

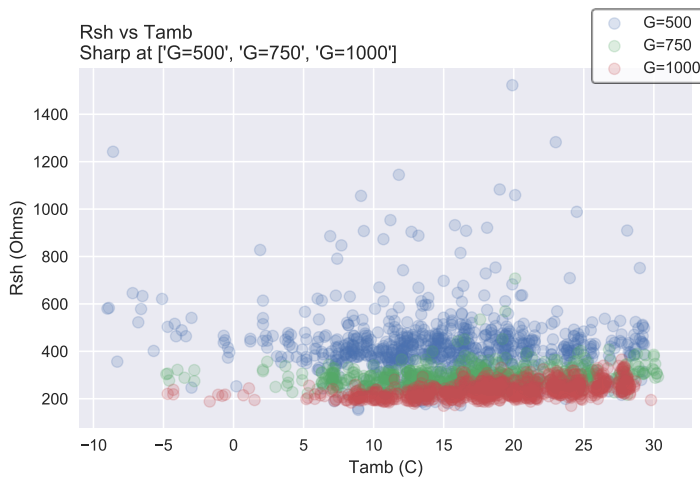


Figure 4.3.2 (c) Scattered plot to show the relationship between R_{SH} and ambient temperature

ambient temperature at higher irradiance levels.

Figure 4.3.2(c) shows that R_{SH} varies in a bigger range with the increase of ambient temperature at 500W/m^2 . It is obvious that at 750W/m^2 and 1000W/m^2 , R_{SH} increases gradually when the ambient temperature increases. Hence, it is reasonable to argue that there is a positive linear relationship between R_{SH} and

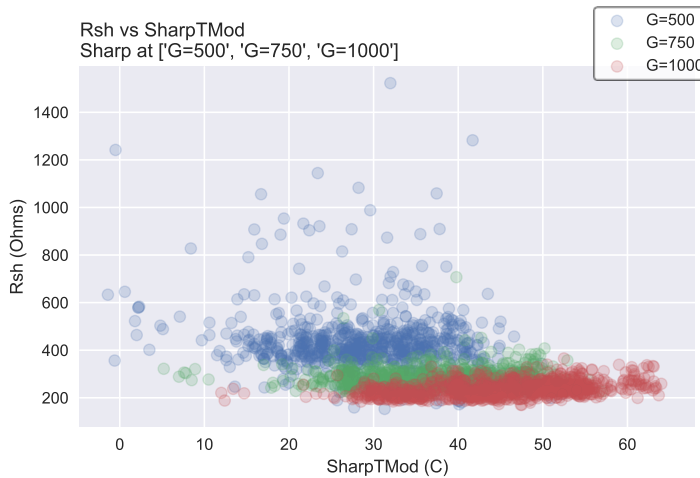


Figure 4.3.2 (d) Scattered plot to show the relationship between R_{SH} and module temperature

Figure 4.3.2 (d) shows that R_{SH} varies in a bigger range with the increase of module temperature at 500W/m^2 . At 1000W/m^2 , R_{SH} increases gradually when the module temperature increases.

It is observed from both of the figures that R_{SH} decreases when solar irradiance increases, therefore, same as R_S , it is considered that **R_{SH} is inversely proportional to the solar irradiance for $\mu\text{c-Si}$ panel**. The R_{SH} 's behaviour for $\mu\text{c-Si}$ panel show that, **R_{SH} increases when ambient and module temperature increases at higher irradiance level**. These are findings that have not been mentioned in any of the literature covered in Chapter2, see Table 2.5.

4.3 Sharp – μ c-Si solar panel

n with ambient temperature, module temperature and solar irradiance

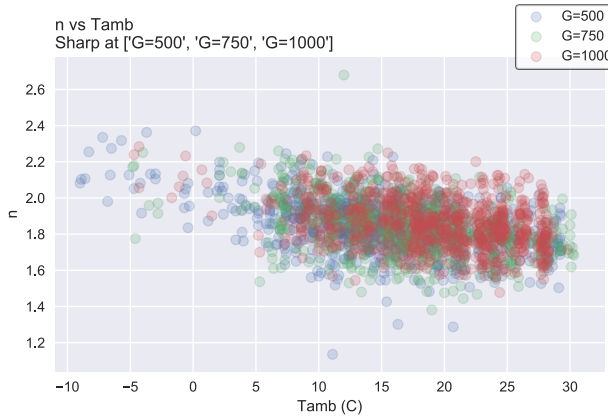


Figure 4.3.2 (e) Scattered plot to show the relationship between n and ambient temperature



Figure 4.3.2 (f) Scattered plot to show the relationship between n and module temperature

Figure 4.3.2(e) clearly shows that n varies randomly in the range between 1.4 and 2.4 without any patterns regard to ambient temperature and solar irradiance. Figure 4.3.2 (f) shows that n varies randomly in a fixed range without any patterns regard to module temperature and solar irradiance. Therefore, it is reasonable to conclude that based on this data set, **n is not sensitive to ambient temperature, module temperature and solar irradiance for μ c-Si panel**. These are findings that have not been mentioned in any of the literature covered in Chapter2, see Table 2.5.

I_0 with ambient temperature, module temperature and solar irradiance

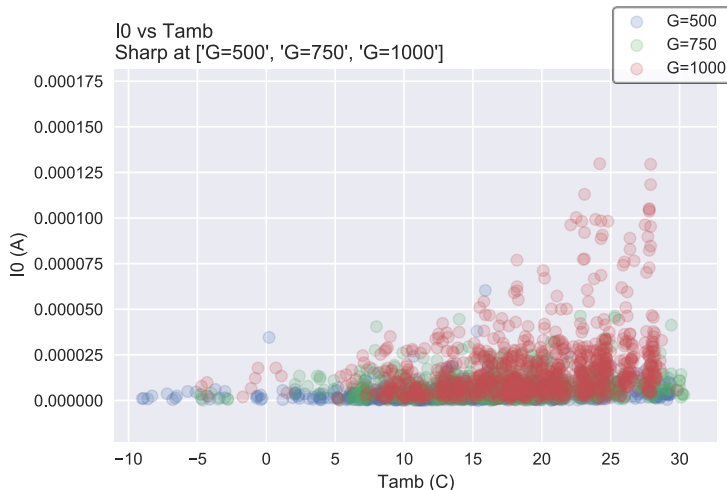


Figure 4.3.2 (g) Scattered plot to show the relationship between I_0 and ambient temperature

On the Figure 4.3.2 (g), at $500W/m^2$ and $750W/m^2$, I_0 did not respond to the changes in ambient temperature. At $1000W/m^2$, I_0 increases gradually from 0A to 0.000125A, with the increase of the ambient temperature.

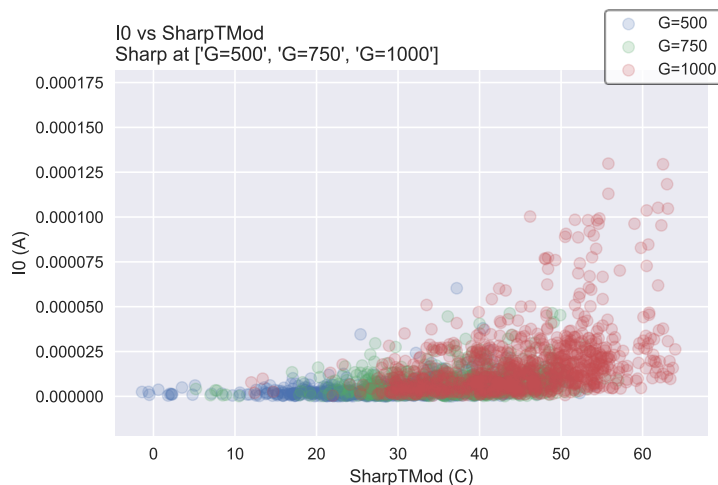


Figure 4.3.2 (h) Scattered plot to show the relationship between I_0 and module temperature

at 1000W/m^2 , I_0 increases gradually when module temperature increases from 30°C to 60°C .

Two figures above show that I_0 increases gradually with the increasing temperature when the solar irradiance is higher. Therefore, it is reasonable to conclude that, **I_0 increases gradually when ambient temperature and module temperature increases at a higher solar irradiance for $\mu\text{-Si}$ panel**. This finding has not been mentioned in any of the literature covered in Chapter2, see Table 2.5.

I_{PH} with ambient temperature, module temperature and solar irradiance

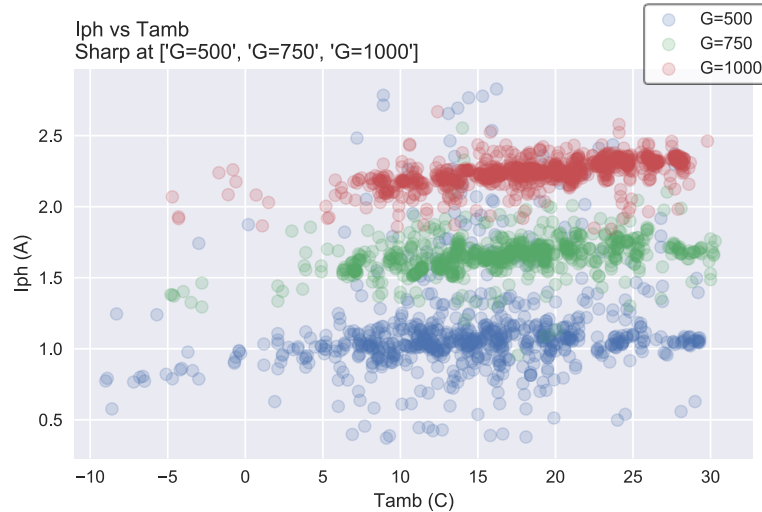


Figure 4.3.2 (i) Scattered plot to show the relationship between I_{PH} and ambient temperature

Figure 4.2.2 (h) shows the relationship between I_0 and the module temperature. I_0 at 500W/m^2 did not show any obvious change within the growth of module temperature. However, at 750W/m^2 I_0 increases gradually when module temperature increases from 20°C to 50°C and at

Figure 4.3.2 (i) shows that I_{PH} remains at the same level when the ambient temperature increases. A slight increasing of I_{PH} can be observed with the growth of ambient temperature at 750W/m^2 and 1000W/m^2 .

4.3 Sharp – μ c-Si solar panel

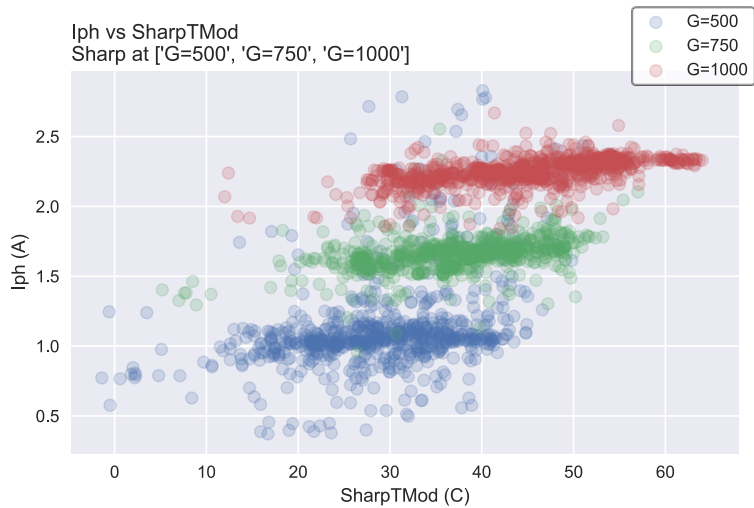


Figure 4.3.2 (j) Scattered plot to show the relationship between I_{PH} and module temperature

temperature at all irradiance levels.

Both figures above show that I_{PH} varies with the change of solar irradiance. They clearly present that **I_{PH} increases while solar irradiance increases for μ c-Si panel**. Furthermore, I_{PH} shows a small increasing trend with the growing module temperature at $750W/m^2$ and $1000W/m^2$. **I_{PH} increase with the growth of ambient and module temperature for μ c-Si panel**. These have also been proved in the previously mentioned literature for the CIS panel in Chapter2, see Table2.5.

4.3.3 Electrical Characteristics and Degradation P_{MPP} and R_S

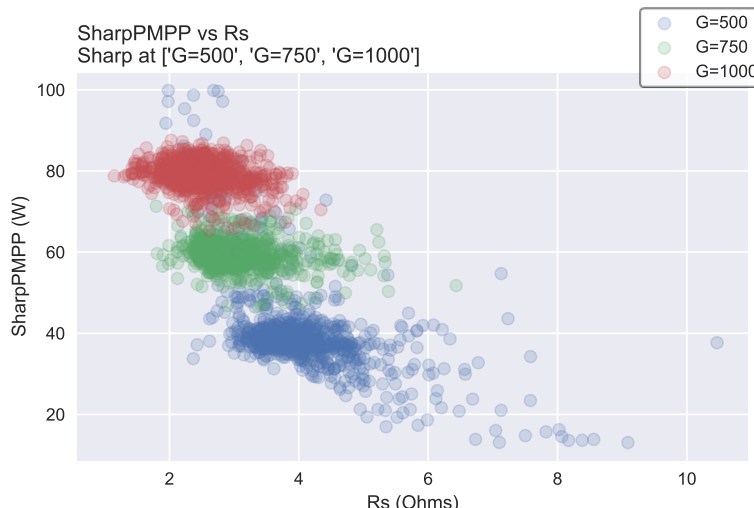


Figure 4.3.3 (a) Scattered plot to show the relationship between P_{MPP} and R_S at three irradiance level

Figure 4.3.2 (j) also shows that I_{PH} remains in the same range when the module temperature increases at each irradiance level. Note that module temperature increases when the solar irradiance increases. A slight increasing of I_{PH} can be seen with the growth of the module

Figure 4.3.3 (a) shows that at each solar irradiance level, P_{MPP} did not show any obvious changes within the growth of R_S . Figure 4.3.3 (b) below shows the correlation, 95% confidence and predication limits of the values at $1000W/m^2$.

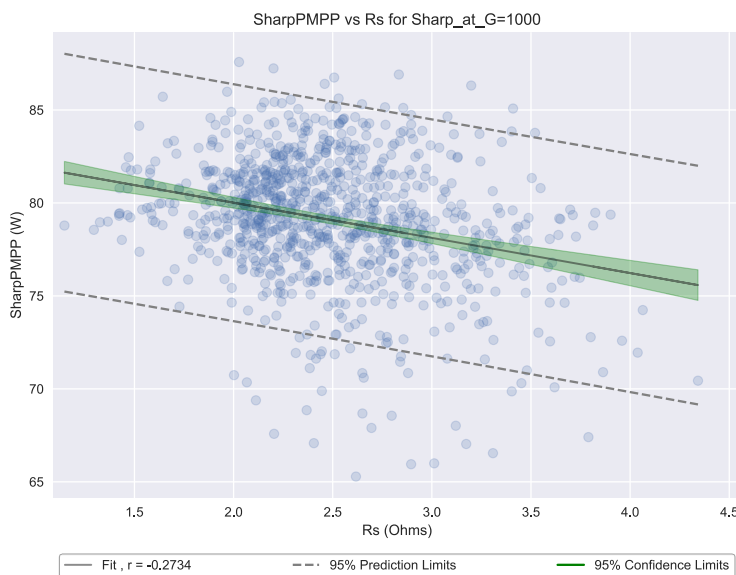


Figure 4.3.3 (b) Graph to show the correlation of P_{MPP} and R_S at $1000W/m^2$

general trend of R_S increases, P_{MPP} decreases, which was covered in the literature in Chapter2, see Table 2.5.

P_{MPP} and R_{SH}

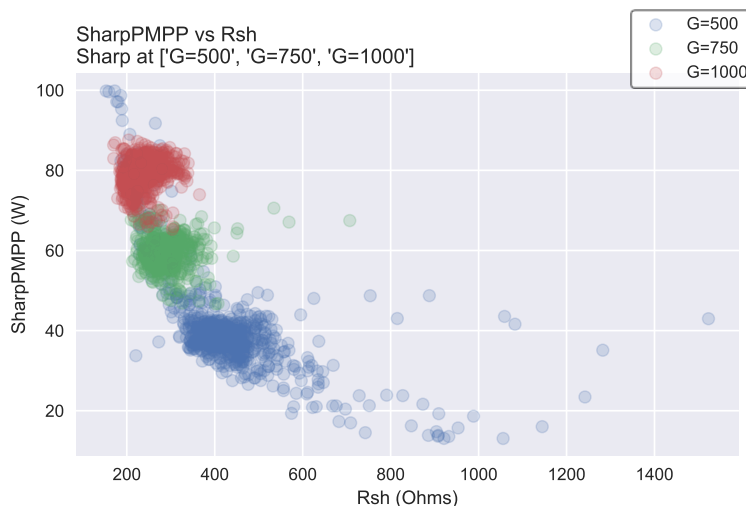


Figure 4.3.3 (c) Scattered plot to show the relationship between P_{MPP} and R_{SH} at three irradiance level

values at $1000W/m^2$.

The correlation of R_S and P_{MPP} is **-0.2734** which is almost very close to 0. Therefore, it is **considered that R_S and P_{MPP} are not linearly related**. The change of R_S has no impacts on the performance degradation in μ c-Si panel. However, the negative value of the correlation has proved the

Figure 4.3.3 (c) shows that at $750W/m^2$ and $1000W/m^2$, the P_{MPP} shows no relevance to the change in R_{SH} . However, at $500W/m^2$, P_{MPP} showed a gradual decreasing trend when R_{SH} increases. 4.3.3 (d) below shows the correlation, 95% confidence and predication limits of the

4.3 Sharp – μ c-Si solar panel

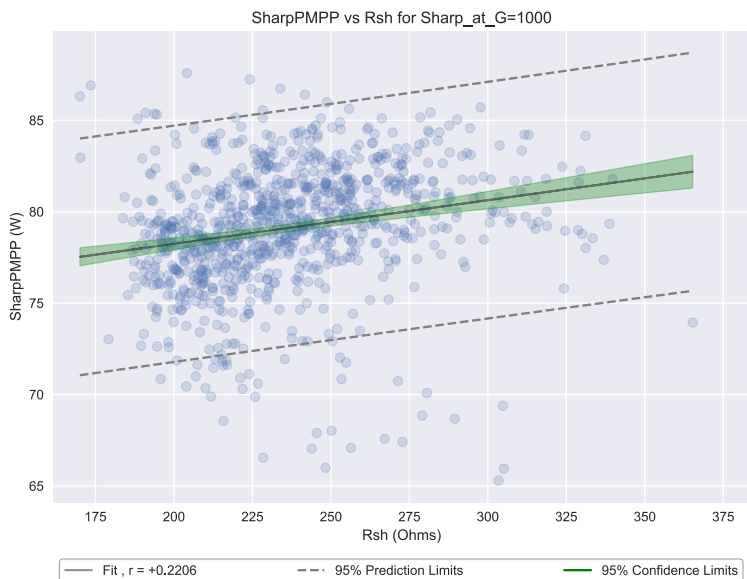


Figure 4.3.3 (d) Graph to show the correlation of P_{MPP} and R_{SH} at 1000W/m^2

The correlation of R_{SH} and P_{MPP} is $+0.2206$, which is very close to 0. Therefore, it is considered that R_{SH} and P_{MPP} are not linearly related. However, the value of the correlation of R_{SH} is smaller than R_s , which means in this case, R_{SH} has slightly less impact on P_{MPP} than R_s .

The change of R_{SH} has

no impacts on the performance degradation in μ c-Si panel. However, the positive value of the correlation has proved the general trend of R_{SH} decreases, P_{MPP} decreases, which was covered in the literature in Chapter2, see Table 2.5.

P_{MPP} and n

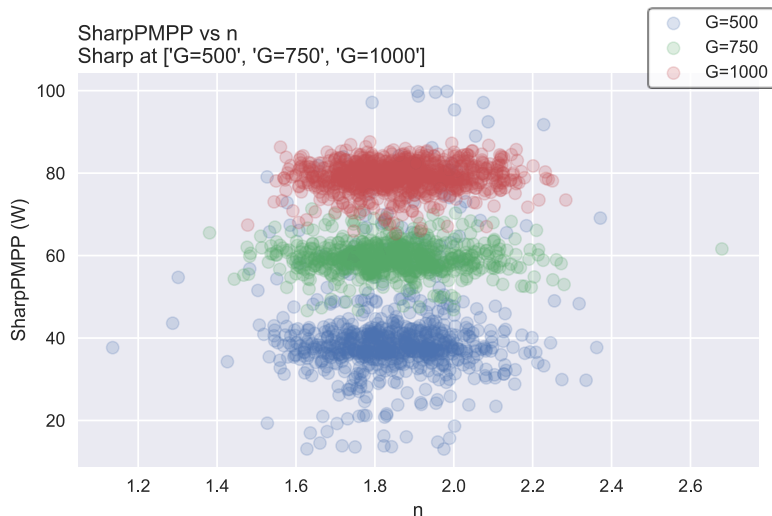


Figure 4.1.3 (e) Scattered plot to show the relationship between P_{MPP} and n at three irradiance level

Figure 4.3.3 (e) shows that n at three irradiance levels are evenly distributed between 1.5 and 2.2. Same as R_s and R_{SH} , the correlation, 95% confidence and prediction limits are calculated, see Figure 4.3.3.(f), the correlation

of n and P_{MPP} is $+0.0572$, which is almost equal to 0. Therefore, it is **considered that n and P_{MPP} are not linearly related.**



Figure 4.3.3 (f) Graph to show the correlation of P_{MPP} and n at $1000\text{W}/\text{m}^2$

P_{MPP} and I_0

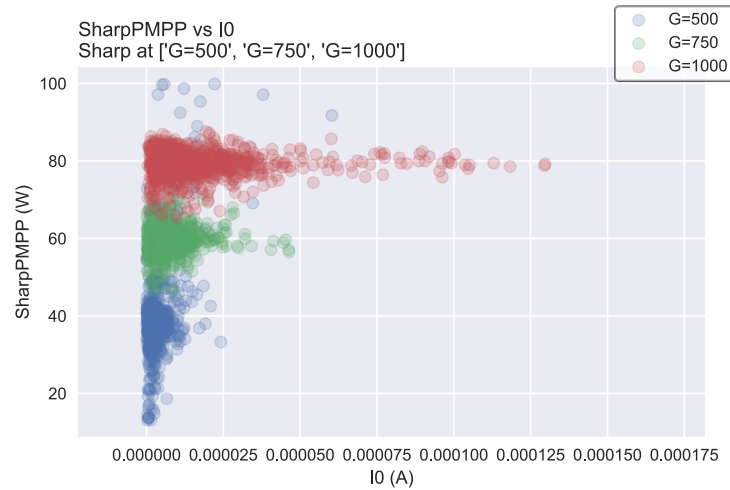


Figure 4.3.3 (g) Scattered plot to show the relationship between P_{MPP} and I_0 at three irradiance level

range while I_0 increasing at all three levels of the solar irradiance.

The change of n has no impacts on the performance degradation in $\mu\text{-Si}$ panel. This finding has not been mentioned in any of the literature covered in Chapter2, see Table 2.5.

Figure 4.3.3 (g) shows that there is obviously no linear relationship between I_0 and P_{MPP} at any of the irradiance level. The range of I_0 becomes bigger when solar irradiance increases. In general, P_{MPP} shows a small converging trend from varying in a certain range to the average value of the range while I_0 increasing at all three levels of the solar irradiance.

Therefore, it is reasonable to determine **that P_{MPP} converges from varying in a broader range to an averaged value of the range when I_0 increases in $\mu\text{-Si}$ panel, which is dynamic.** This finding has not been mentioned in any of the literature covered in Chapter2, see Table 2.5.

4.3 Sharp – μ c-Si solar panel

P_{MPP} and I_{PH}

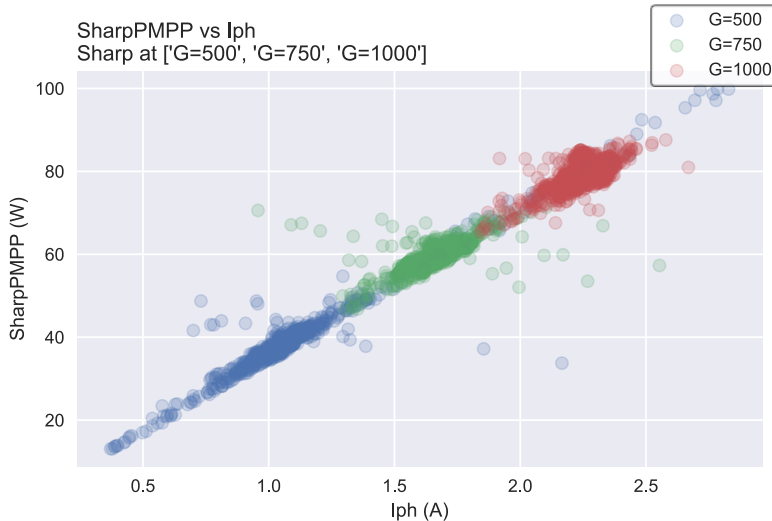


Figure 4.3.3 (h) Scattered plot to show the relationship between P_{MPP} and I_{PH} at three irradiance level

calculate the correlation, 95% confidence and predication limits, seen in Figure 4.3.3 (i).



Figure 4.3.3 (i) Graph to show the correlation of P_{MPP} and I_{PH} at $1000W/m^2$

In summary, the correlation of R_s , R_{SH} , n and I_{PH} and P_{MPP} are -0.2734 , $+0.2206$, $+0.0572$ and $+0.7045$ respectively. Therefore, the order of the impact strength on degradation of μ c-Si panel is: $I_{PH} > R_s > R_{SH} > n$, the last three almost have no obvious impact on degradation in this case. Furthermore, I_0 has a dynamic impact on the PV performance, that shows a converging trend when I_0 increases.

Figure 4.3.3(h) clearly shows that when I_{PH} increases, P_{MPP} increases, it is easy to observe a linear relationship between the two variables. In order to investigate the relationship between P_{MPP} and I_{PH} precisely, the results at $1000W/m^2$ have been chosen to

The correlation of I_{PH} and P_{MPP} is $+0.7045$, which is very close to 1. Therefore, it is reasonable to argue that **there is a positive linear relationship between I_{PH} and P_{MPP} in μ c-Si panel**, which is expected based on the literature covered in Chapter2 (Table2.5).

4.4 First Solar – CdTe solar panel

4.4.1 I-V curve and P-V curve

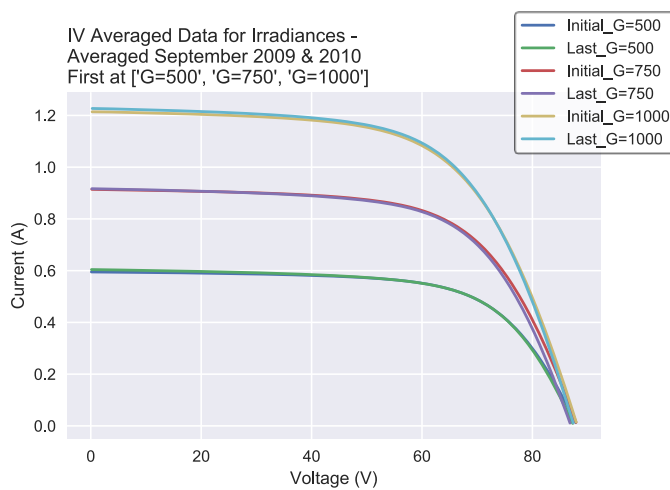


Figure 4.4.1 (a) I-V curve of the averaged September 2009 and 2010 at three irradiance level

Figure 4.4.1 (a) shows that the Voc have been very stable during the test and the Isc in September 2010 were only slightly higher than September 2009. All curves barely shifted and the turning points on Last curves and Initial curves coincided, which means the P_{MPP} barely changed between September 2009 and September 2010. The figure clearly shows

that the PV performance is relatively stable during the test.

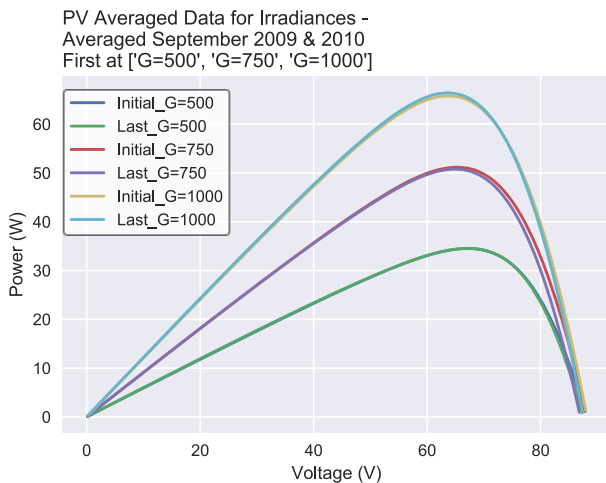


Figure 4.4.1 (b) P-V curve of the averaged September 2009 and 2010 at three irradiance level

Figure 4.4.1 (b) shows that at 500W/m^2 , there is no obvious change in the power output, since the Last curve and the Initial curve are coincided. At 750W/m^2 , there is a slight power loss in September 2010, compare to September 2009. At 1000W/m^2 , there is actually an improvement in September 2010, compare to September 2009.

The analysis of both figures above shows that the power output increases with growing solar irradiation. Furthermore, they have proved that **there was no obvious degradation in the PV performance within the CdTe panel based on the analysis of samples in September 2009 and September 2010**. Although small amount of degradation is expected annually (Ueda,Y. et al.,2013) as mentioned in the literature review in Section 2.3.1, it is possible to detect none performance degradation, since the performance of solar PV is highly depend on the surrounding environment and its material.

4.4 First Solar – CdTe solar panel

4.4.2 Electrical Characteristics and Environment Factors

Rs with ambient temperature, module temperature and solar irradiance

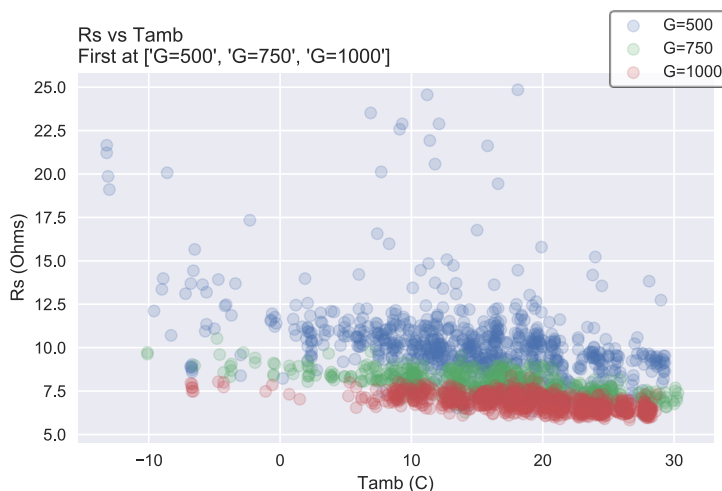


Figure 4.4.2 (a) Scattered plot to show the relationship between R_s and ambient temperature

Figure 4.4.2 (a) shows that at 500W/m^2 varies in a rather bigger range with the increase of ambient temperature. R_s decreases gradually at all the irradiance levels when the ambient temperature increases. Therefore, it is rational to state that there is a negative linear relationship between R_s and ambient temperature at all irradiance levels.

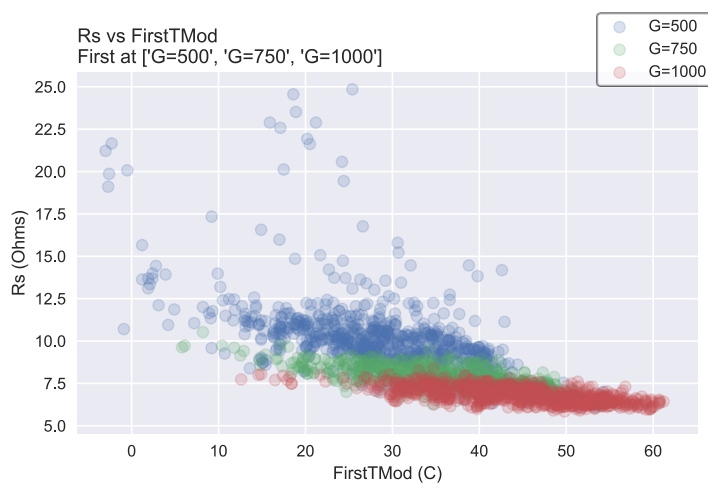


Figure 4.4.2 (b) Scattered plot to show the relationship between R_s and module temperature

Figure 4.4.2 (b) shows that at 500W/m^2 , R_s varies randomly in a relatively bigger range with the increase of the module temperature. At 750W/m^2 and 1000W/m^2 , R_s varies in a smaller range and more concentrate. The decreasing trend of R_s against the growth of

module temperature is relatively steeper.

It is clear to see that the range of R_s increases when solar irradiance decreases from the two figures above. Hence, it is reasonable to consider that **Rs is inversely proportional to the solar irradiance for CdTe panel**. The R_s 's behaviour for CdTe panel showed that **at all irradiance levels, R_s decreases when ambient temperature and module temperature increases**. These are findings that have not been mentioned in any of the literature covered in Chapter2, see Table 2.5.

R_{SH} with ambient temperature, module temperature and solar irradiance

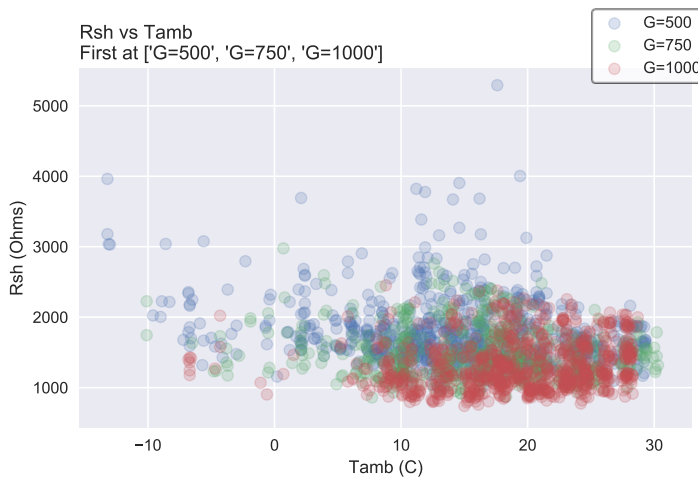


Figure 4.4.2 (c) Scattered plot to show the relationship between R_{SH} and ambient temperature

Figure 4.4.2(c) shows that R_{SH} varies randomly with the increase of ambient temperature at all three of the irradiance levels. There is a slight increasing trend of R_{SH} when ambient temperature increases at 1000W/m^2 . However, it is not sufficient enough to argue that R_{SH} is linearly related to ambient temperature.

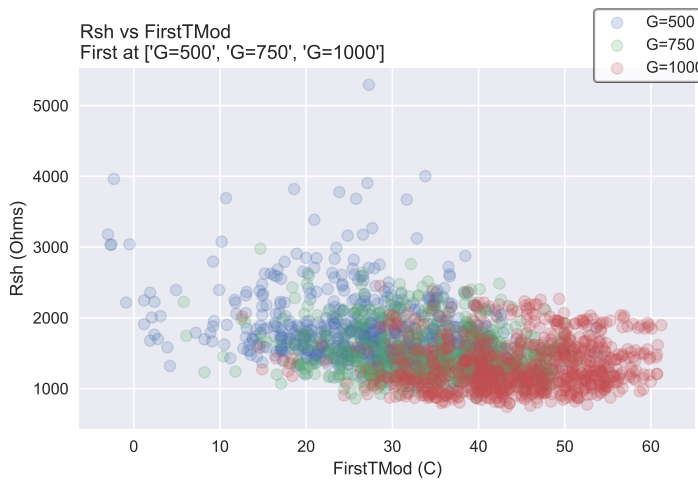


Figure 4.4.2 (d) Scattered plot to show the relationship between R_{SH} and module temperature

Figure 4.4.2 (d) shows that R_{SH} varies randomly with the increase of module temperature, at all three of the irradiance levels. Compare to R_s , R_{SH} varies more randomly.

Both of the figures showed that R_{SH} reduces slightly when solar irradiance increases, therefore, same as R_s , it is considered that **R_{SH} is inversely proportional to the solar irradiance for CdTe panel**. The **R_{SH} 's behaviour for CdTe panel did not show any particular relevance regard to ambient temperature and module temperature**, which is a finding that has not been mentioned in any of the literature covered in Chapter2, see Table 2.5.

4.4 First Solar – CdTe solar panel

n with ambient temperature, module temperature and solar irradiance

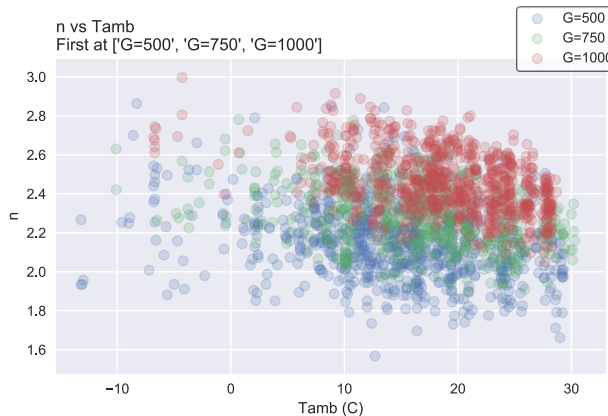


Figure 4.4.2 (e) Scattered plot to show the relationship between n and ambient temperature

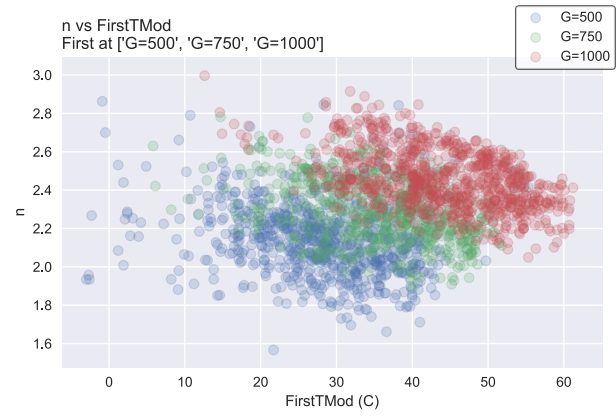


Figure 4.4.2 (f) Scattered plot to show the relationship between n and module temperature

Two figures above clearly show that at all three irradiance levels, n decreases with the growth of both ambient and module temperature. It is obvious to see that the range of n increases when solar irradiance increases. Thus, it is sensible to believe that **n is proportional to the solar irradiance for CdTe panel**. Moreover, it is also reasonable to indicate that **n decreases when ambient and module temperature increases in CdTe panel at all irradiance levels**. This finding has not been mentioned in any of the literature covered in Chapter2, see Table2.5.

I₀ with ambient temperature, module temperature and solar irradiance

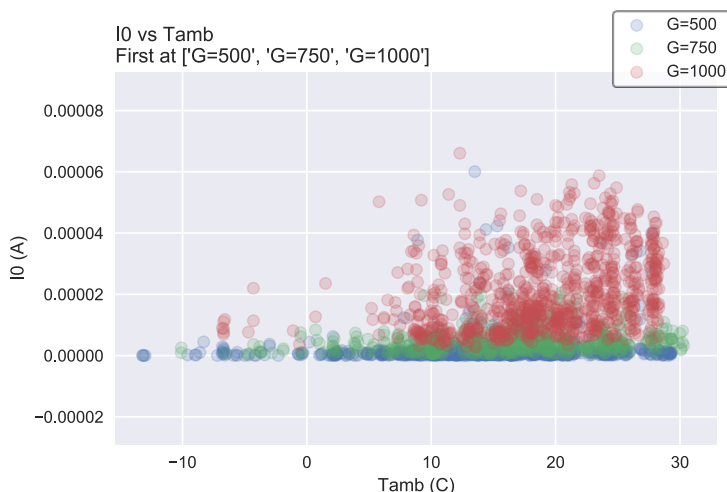


Figure 4.4.2 (g) Scattered plot to show the relationship between I_0 and ambient temperature

On the Figure 4.4.2 (g), at 500W/m^2 , I_0 did not respond to the changes in ambient temperature. At 750W/m^2 , I_0 varies between 0A to 0.00002A . At 1000W/m^2 , I_0 varies up to 0.00006A , with the increasing ambient temperature.

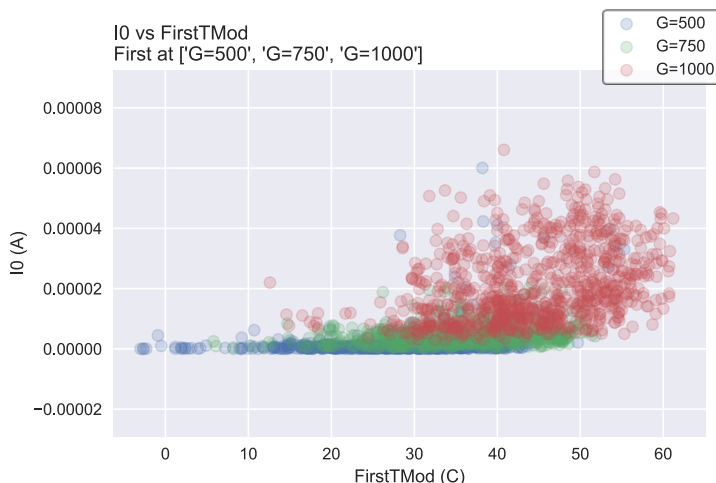


Figure 4.4.2 (h) Scattered plot to show the relationship between I_0 and module temperature

The relationship between I_0 and the module temperature is shown in Figure 4.4.2 (h). I_0 at 500W/m² and 750W/m² did not show any distinct change within the growth of module temperature. At 1000W/m², I_0 increases when module temperature increases from 30°C to 60°C.

Two figures above show

that I_0 increases with the increasing temperature with a higher solar irradiance level. Hence, it is reasonable to indicate that, **at higher solar irradiance, I_0 increases when ambient and module temperature increases for CdTe panel**. This finding has not been mentioned in any of the literature covered in Chapter2, see Table 2.5.

I_{PH} with ambient temperature, module temperature and solar irradiance

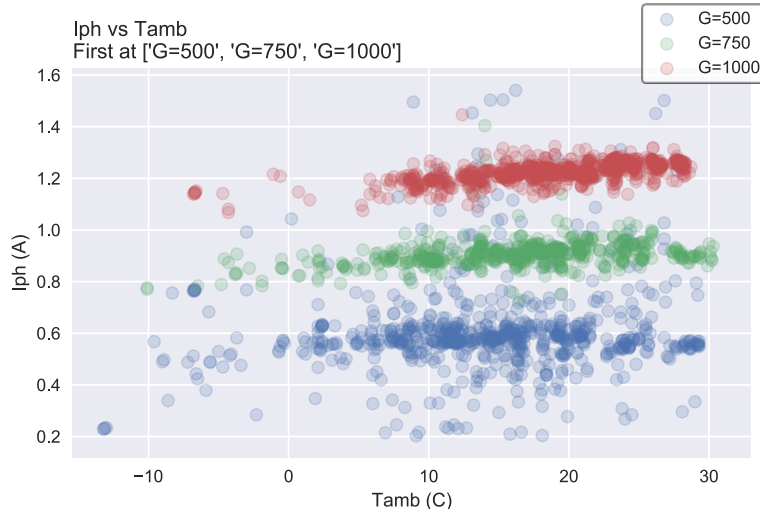


Figure 4.4.2 (i) Scattered plot to show the relationship between I_{PH} and ambient temperature

Figure 4.4.2 (i) shows that I_{PH} remains at the same level when the ambient temperature increases. A slight growing of I_{PH} can be noticed with the growth of ambient temperature at 1000W/m².

4.4 First Solar – CdTe solar panel

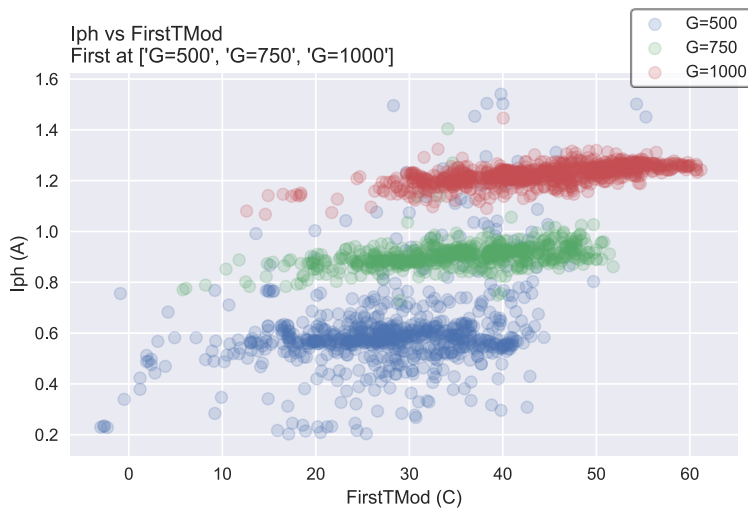


Figure 4.4.2 (j) Scattered plot to show the relationship between I_{PH} and module temperature

temperature at 750W/m^2 and 1000W/m^2 .

Both figures above show that I_{PH} varies with the change of solar irradiance. They clearly show that **I_{PH} increases while solar irradiance increases for CdTe panel**. Moreover, I_{PH} shows a small increasing trend with the growing ambient and module temperature at 750W/m^2 and 1000W/m^2 . **I_{PH} shows a slight increase with the growth of ambient and module temperature at higher solar irradiance for CdTe panel**. This finding has not been mentioned in any of the literature covered in Chapter2, see Table 2.5.

4.4.3 Electrical Characteristics and Degradation

P_{MPP} and R_s

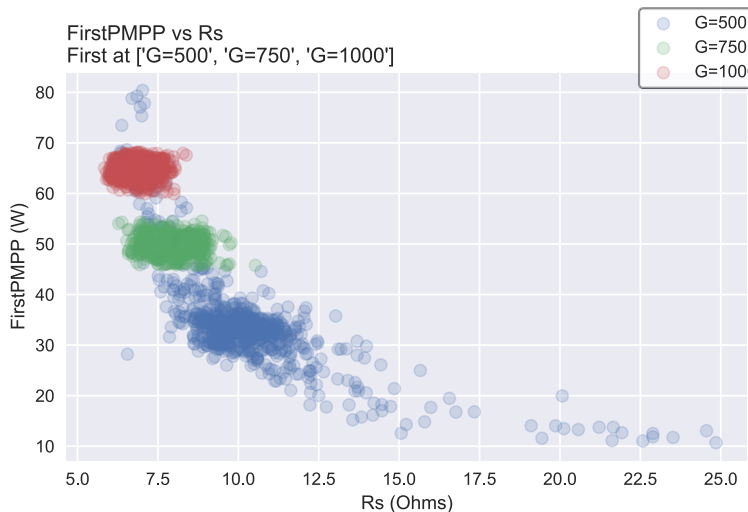


Figure 4.4.3 (a) Scattered plot to show the relationship between P_{MPP} and R_s at three irradiance level

Figure 4.4.2 (j) also shows that I_{PH} remains in the same range when the module temperature increases at each irradiance level. Note that module temperature increases when the solar irradiance increases. A slight increasing of I_{PH} can be seen with the growth of the module

Figure 4.4.3 (a) shows that at each solar irradiance level, P_{MPP} did not show any obvious changes within the growth of R_s . Note that the values varied in a larger range at 500W/m^2 .

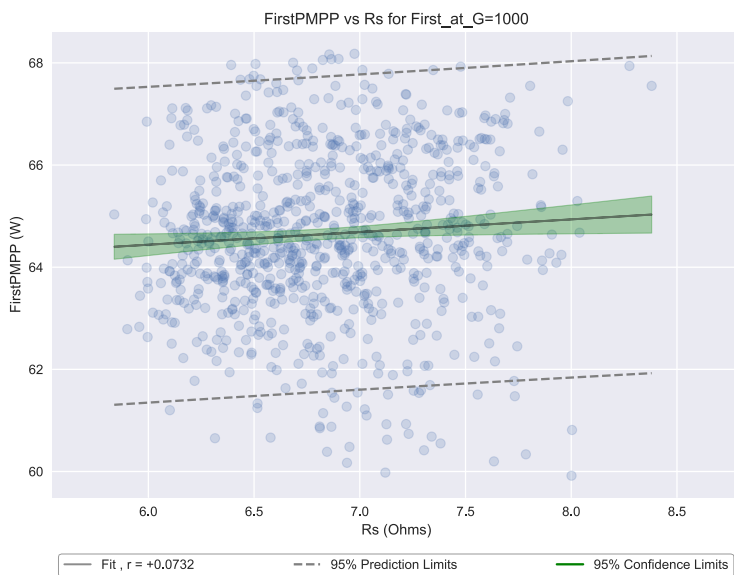


Figure 4.4.3 (b) Graph to show the correlation of P_{MPP} and R_s at $1000W/m^2$

impacts on the performance degradation in CdTe panel. However, the positive value of the correlation has proved the general trend of R_s increases, P_{MPP} increases, which was different from the conclusion in the literature covered in Chapter2, see Table 2.5. The possible reasons caused the difference could be that for CdTe panel, R_s behaves differently, or technical problems occurred when recording the R_s data for CdTe panel.

Figure 4.4.3(b) shows the correlation, 95% confidence and predication limits of the values at $1000W/m^2$.

The correlation of R_s and P_{MPP} is $+0.0732$ which is almost equal to 0. Therefore, it is **considered that R_s and P_{MPP} are not linearly related.** The change of R_s has no

P_{MPP} and R_{SH}

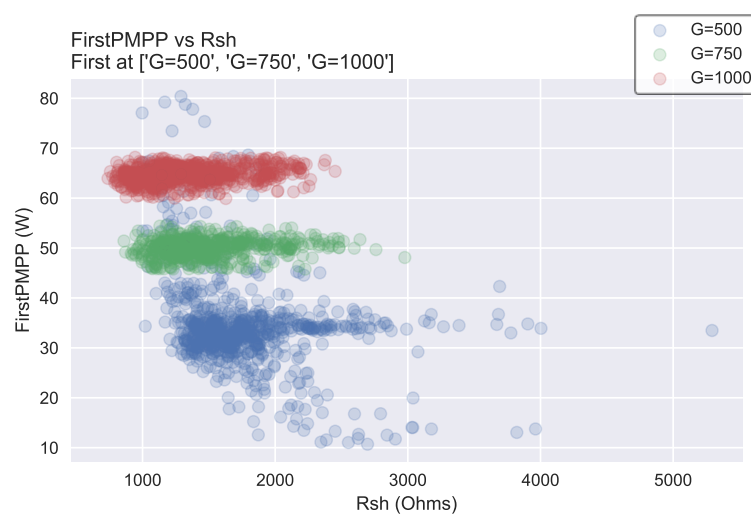


Figure 4.4.3 (c) Scattered plot to show the relationship between P_{MPP} and R_{SH} at three irradiance level

Figure 4.4.3 (c) shows that at each solar irradiance level, the P_{MPP} showed no relation to the increase of R_{SH} . Figure 4.4.3(d) below shows the correlation, 95% confidence and predication limits of the values at $1000W/m^2$.

4.4 First Solar – CdTe solar panel

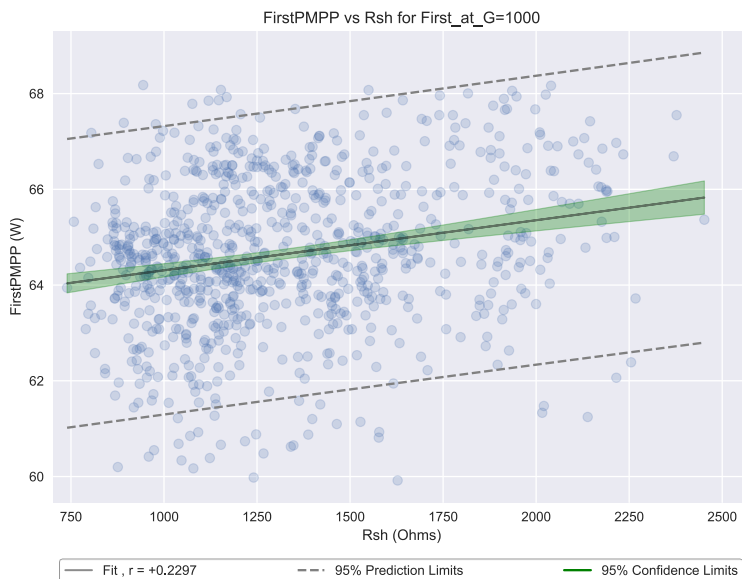


Figure 4.4.3 (d) Graph to show the correlation of P_{MPP} and R_{SH} at $1000W/m^2$

no impacts on the performance degradation in CdTe panel. However, the positive value of the correlation has proved the general trend of R_{SH} decreases, P_{MPP} decreases, which was covered in the literature in Chapter2, see Table 2.5.

The correlation of R_{SH} and P_{MPP} is $+0.2297$, which is very close to 0. Therefore, it is considered that R_{SH} and P_{MPP} are not linearly related. However, the value of the correlation of R_{SH} is bigger than R_s , which means in this case, R_{SH} has slightly more impact on P_{MPP} than R_s .

The change of R_{SH} has

P_{MPP} and n

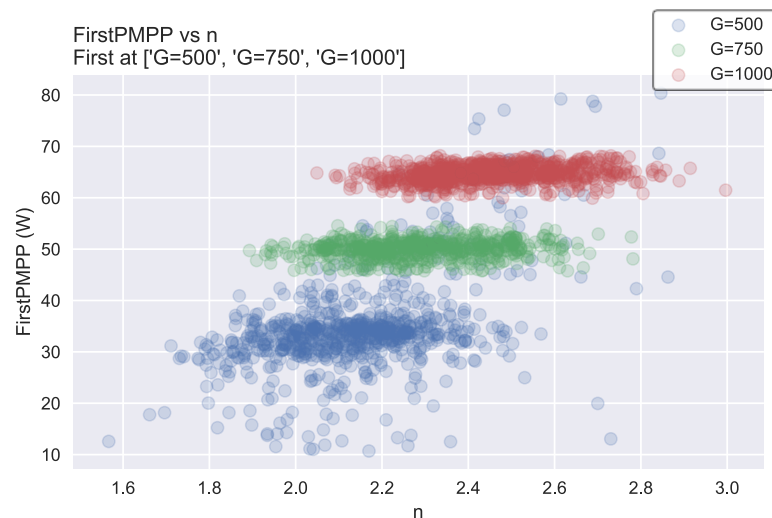


Figure 4.4.3 (e) Scattered plot to show the relationship between P_{MPP} and n at three irradiance level

ranged between 60W and 70W, with n ranged between 2.1 and 2.8. The change of P_{MPP} shows no relations to the growth of n.

Figure 4.4.3 (e) shows that at $500W/m^2$, P_{MPP} is ranged between 10W and 45W, with n ranged between 1.6 and 2.4. At $750W/m^2$, P_{MPP} is ranged between 45W and 55W, with n ranged between 2 and 2.6. At $1000W/m^2$, P_{MPP} is



Figure 4.4.3 (f) Graph to show the correlation of P_{MPP} and n at $1000W/m^2$

Figure 4.2.3 (f) shows the correlation, 95% confidence and predication limits of the values at $1000W/m^2$. The correlation of n and P_{MPP} is $+0.0548$, which is almost equal to 0. Therefore, it is considered that n and P_{MPP} are not linearly related.

The change of n has no impacts on the performance degradation

in CdTe panel. This finding has not been mentioned in any of the literature covered in Chapter2, see Table 2.5.

P_{MPP} and I_0

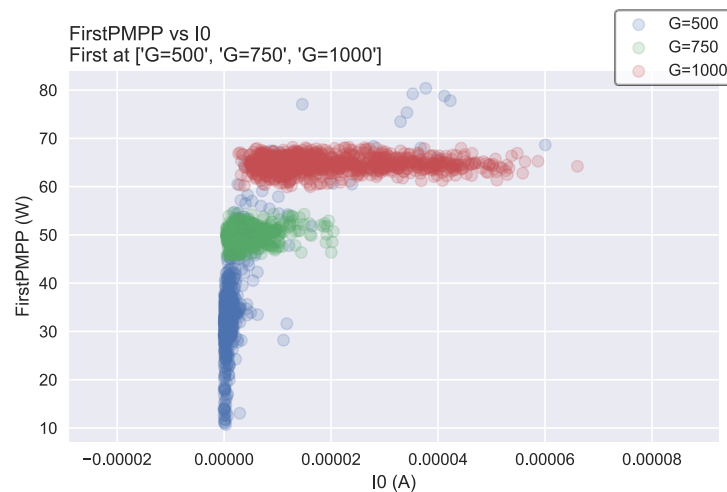


Figure 4.4.3 (g) Scattered plot to show the relationship between P_{MPP} and I_0 at three irradiance level

Figure 4.4.3 (g) shows that at $500W/m^2$, the values varied between 10W and 45W when I_0 is around 0A. At $750W/m^2$, P_{MPP} shows a converging trend from varying between 45W and 55W when I_0 increases. At $1000W/m^2$, P_{MPP} shows no relevant changes while I_0 increasing.

Therefore, it is reasonable to determine that **the relationship between P_{MPP} and I_0 varies depend on different solar irradiance in CdTe panel.** This finding has not been mentioned in any of the literature covered in Chapter2, see Table 2.5.

4.4 First Solar – CdTe solar panel

P_{MPP} and I_{PH}

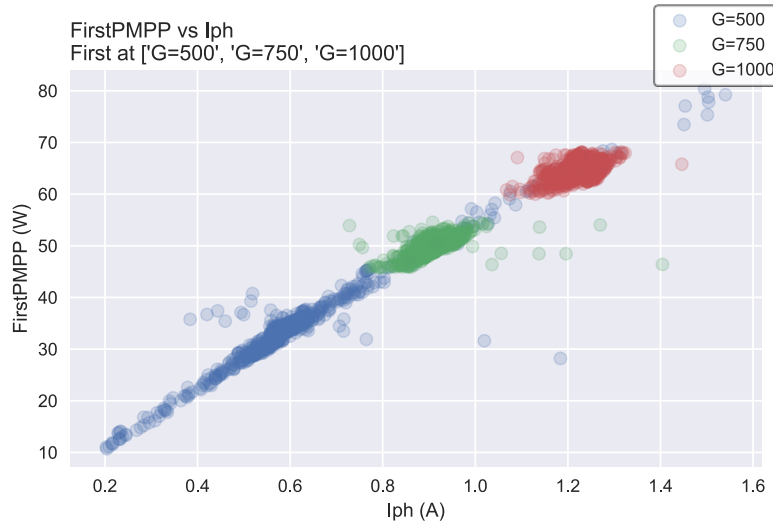


Figure 4.4.3 (h) Scattered plot to show the relationship between P_{MPP} and I_{PH} at three irradiance level

values at 1000W/m^2 .

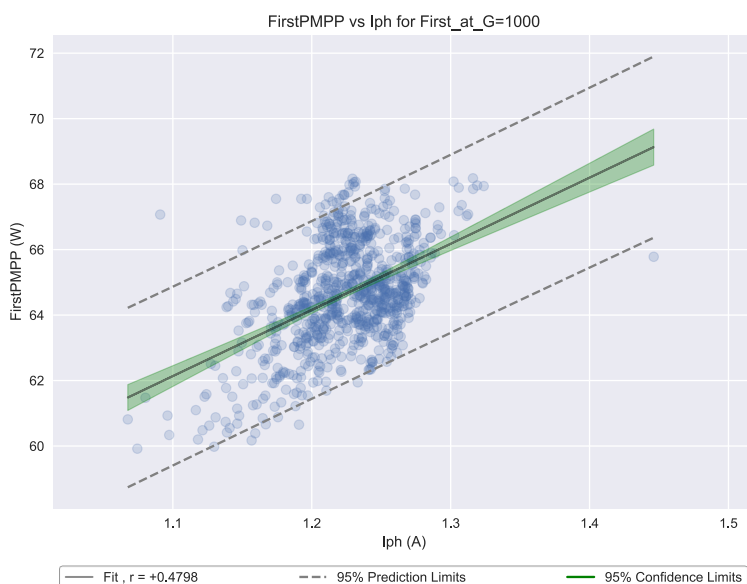


Figure 4.4.3 (i) Graph to show the correlation of P_{MPP} and I_{PH} at 1000W/m^2

Figure 4.4.3(h) clearly shows that when I_{PH} increases, P_{MPP} increases, it is can be observed that there is a linear relationship between the two variables. Figure 4.4.3 (i) below shows the correlation, 95% confidence and prediction limits of the

The correlation of I_{PH} and P_{MPP} is $+0.4798$, which is between 0 and 1. Therefore, it is sensible to conclude that **there is a positive linear relationship between I_{PH} and P_{MPP} in CdTe panel**, which is expected based on the literature covered in Chapter2 (Table2.5).

In summary, the correlation of R_s , R_{SH} , n and I_{PH} and P_{MPP} are $+0.0732$, $+0.2297$, $+0.0548$ and $+0.4798$ respectively. Therefore, the order of the impact strength on degradation of CdTe panel is: $I_{PH} > R_{SH} > R_s > n$, the last three almost have no obvious impact on PV performance in this case. Furthermore, the relationship between P_{MPP} and I_0 varies depends on different solar irradiance in this case.

4.5 Comparisons among CIS, mono-Si, μc-Si and CdTe panels

4.5.1 Level of degradation

In this section, the averaged I-V data of each solar panel of September 2009 and

September 2010 (Which is the first month and the last month) at 1000W/m² are presented in the tables and the level of degradation of each solar panel will be determined, in order to identify the most affected solar panel during this test.

Furthermore, the number of the days that hit 1000W/m² in both months have been included in the tables. (All numbers mentioned in discussion have been rounded up to 3 decimal places based on the values from the tables)

Table4.1 below shows the averaged I-V data of September 2009 and September 2010 for Würth-CIS panel. V_{OC} has increased by 0.618% and I_{SC} has increased by 1.994% during the test period, whereas P_{MPP} has decreased by 1.343%. Hence, the drop in P_{MPP} has shown a **degradation in PV performance of 1.343% in Würth-CIS panel** during the test period.

Würth CIS Panel							
Month	Solar Irradiance	number of days	V_{OC} (V)	I_{SC} (A)	P_{MPP} (W)		
Sep. 2009	G=1000W/m ²	17	44.47357	2.39	74.49		
Sep. 2010		12	44.74841	2.437659	73.48982		
Difference			0.274843	0.047659	-1.00018		
Percentage (%)			0.617992	1.994081	-1.34271		

Table4.1 Würth CIS panel averaged I-V data (Sep.2009 and Sep.2010) at 1000W/m²

Table4.2 below shows the averaged I-V data of September 2009 and September 2010 for Solar World mono-Si panel. V_{OC} has increased by 1.416% and I_{SC} has increased by 2.115% during the test period, P_{MPP} has increased by 4.239%. Therefore, the growth in P_{MPP} has shown an **improvement in PV performance of 4.239% in Solar World mono-Si panel** during the test period.

Solar World mono-Si Panel							
Month	Solar Irradiance	number of days	V_{OC} (V)	I_{SC} (A)	P_{MPP} (W)		
Sep. 2009	G=1000W/m ²	16	41.97207	5.062644	150.1137		
Sep. 2010		11	42.56644	5.169712	156.4764		
Difference			0.594369	0.107069	6.362733		
Percentage (%)			1.416107	2.114876	4.23861		

Table4.2 Solar World mono-Si panel averaged I-V data (Sep.2009 and Sep.2010) at 1000W/m²

4.5 Comparisons among CIS, mono-Si, μ c-Si and CdTe panels

Table4.3 below shows the averaged I-V data of September 2009 and September 2010 for Sharp μ c-Si panel. V_{OC} has increased by 0.699% and I_{SC} has increased by 1.069% during the test period, whereas P_{MPP} has decreased by 0.212%. Hence, the decrease in P_{MPP} has shown **a degradation in PV performance of 0.212% in Sharp μ c-Si panel** during the test period.

Sharp μ c-Si Panel						
Month	Solar Irradiance	number of days	Voc (V)	I_{SC} (A)	P_{MPP} (W)	
Sep. 2009	G=1000W/m ²	17	58.81413	2.208462	81.86462	
		11	59.22553	2.232079	81.69087	
Difference			0.411392	0.023617	-0.17375	
Percentage (%)			0.699478	1.069405	-0.21224	

Table4.3 Sharp μ c-Si panel averaged I-V data (Sep.2009 and Sep.2010) at 1000W/m²

Table4.4 below shows the averaged I-V data of September 2009 and September 2010 for First CdTe panel. V_{OC} has decreased by 0.093% and I_{SC} has increased by 1.303% during the test period, P_{MPP} has increased by 0.216%. Therefore, the increase in P_{MPP} has shown **an improvement in PV performance of 0.216% in First-CdTe panel** during the test period.

First CdTe Panel						
Month	Solar Irradiance	number of days	Voc (V)	I_{SC} (A)	P_{MPP} (W)	
Sep. 2009	G=1000W/m ²	17	87.47317	1.211089	66.25931	
		10	87.39203	1.22687	66.40261	
Difference			-0.08114	0.01578	0.143299	
Percentage (%)			-0.09276	1.302997	0.21627	

Table4.4 First CdTe panel averaged I-V data (Sep.2009 and Sep.2010) at 1000W/m²

In conclusion, the most affected solar panel is Würth - CIS panel with a degradation of 1.343%, then Sharp - μ c-Si panel with a degradation of 0.212%. The least affected solar panel is Solar World - mono-Si panel with an improvement of 4.239%, then First - CdTe panel with an improvement of 0.216%. Therefore, **the order of the degradation level is: Würth - CIS panel (-1.343%) > Sharp - μ c-Si panel (-0.212%) > First - CdTe panel (+0.216%) > Solar World - mono-Si panel (+4.239%)**

4.5.2 Change in key electrical characteristics

In this section, the averaged values of the key electrical characteristics of each solar panel in September 2009 and September 2010 at 1000W/m² are presented in the tables and the level of change in the key electrical characteristics of each solar panel will be determined, in order to identify the most affected key electrical characteristics for each panel during this test. (All numbers mentioned in discussion have been rounded up to 3 decimal places based on the values from the tables)

Table4.5 below shows the averaged values of key electrical characteristics in September 2009 and September 2010 for Würth-CIS panel. R_S has increased by 74.656%, R_{SH} has decreased by 35.843%, n has increased by 2.886%, I₀ has increased by 53.921% and I_{PH} has increased by 2.339% during the test period. It is reasonable to determine that **the increase in R_S, I₀ and decrease in R_{SH} are responsible for the degradation.**

Würth CIS Panel							
Month	Solar Irradiance	R _S (Ω)	R _{SH} (Ω)	n	I ₀ (A)	I _{PH} (A)	
Sep. 2009	G=1000W/m ²	0.53754	270.2025	1.511134	1E-06	2.397826	
		0.938845	173.3532	1.55474	1.54E-06	2.453922	
Difference		0.401305	-96.8493	0.043605	5.39E-07	0.056096	
Percentage (%)		74.6557	-35.8432	2.885614	53.92071	2.339457	

Table4.5 Würth CIS panel averaged values of key electrical characteristics (Sep.2009 and Sep.2010) at 1000W/m²

Table4.6 below shows the averaged values of key electrical characteristics in September 2009 and September 2010 for Solar World-mono-Si panel. R_S has increased by 8.099%, R_{SH} has increased by 12.796%, n has increased by 0.077%, I₀ has decreased by 26.356% and I_{PH} has increased by 2.251% during the test period. It is reasonable to determine that **the increase in R_{SH} and decrease in I₀ are responsible for the improvement.**

Solar World mono-Si Panel							
Month	Solar Irradiance	R _S (Ω)	R _{SH} (Ω)	n	I ₀ (A)	I _{PH} (A)	
Sep. 2009	G=1000W/m ²	0.144916	572.8903	1.526179	6.66E-06	5.058957	
		0.156653	646.1989	1.52735	4.9E-06	5.172815	
Difference		0.011737	73.3086	0.001171	-1.8E-06	0.113858	
Percentage (%)		8.099478	12.79627	0.076733	-26.3559	2.250613	

Table4.6 Solar World mono-Si panel averaged values of key electrical characteristics (Sep.2009 and Sep.2010) at 1000W/m²

Table4.7 below shows the averaged values of key electrical characteristics in September 2009 and September 2010 for Sharp-μc-Si panel. R_S has increased by 7.305%, R_{SH} has decreased by 8.889%, n has increased by 5.313%, I₀ has increased by 58.995% and I_{PH}

4.5 Comparisons among CIS, mono-Si, μ c-Si and CdTe panels has increased by 1.170% during the test period. It is reasonable to determine that **the increase in I_0 , R_S and the decrease in R_{SH} are responsible for the degradation.**

Sharp μ c-Si Panel						
Month	Solar Irradiance	R_S (Ω)	R_{SH} (Ω)	n	I_0 (A)	I_{PH} (A)
Sep. 2009	G=1000W/m ²	2.346116	252.7823	1.824238	8.59E-06	2.232468
		2.51749	230.3116	1.921153	1.36E-05	2.258578
Difference		0.171374	-22.4707	0.096915	5.06E-06	0.02611
Percentage (%)		7.304574	-8.88935	5.312603	58.99481	1.169558

Table4.7 Sharp μ c-Si panel averaged values of key electrical characteristics (Sep.2009 and Sep.2010) at 1000W/m²

Table4.8 below shows the averaged values of key electrical characteristics in September 2009 and September 2010 for First-CdTe panel. R_S has decreased by 6.797%, R_{SH} has decreased by 2.763%, n has increased by 0.106%, I_0 has decreased by 0.884% and I_{PH} has increased by 1.039% during the test period. It is reasonable to determine **that the drop in R_S are responsible for the improvement and the key electrical characteristics in this panel are relatively stable during the test period.**

First CdTe Panel						
Month	Solar Irradiance	R_S (V)	R_{SH} (A)	n	I_0 (A)	I_{PH} (A)
Sep. 2009	G=1000W/m ²	7.270711	1513.3	2.488163	1.76E-05	1.220703
		6.776493	1471.494	2.490796	1.77E-05	1.233385
Difference		-0.49422	-41.8068	0.002633	1.55E-07	0.012682
Percentage (%)		-6.79739	-2.76263	0.105813	0.883512	1.038941

Table4.8 First CdTe panel averaged values of key electrical characteristics (Sep.2009 and Sep.2010) at 1000W/m²

In conclusion, it is mainly the change in R_S , R_{SH} and I_0 responsible for both degradation and improvement among all four solar panels that involved in the test.

The order of the dominant level of key electrical characteristics that affect PV performance:

- **Würth-CIS panel: $R_S > I_0 > R_{SH}$**
- **Solar World-mono-Si panel: $I_0 > R_{SH}$**
- **Sharp- μ c-Si panel: $I_0 > R_{SH} > R_S$**
- **First-CdTe: R_S**

4.5.3 PV performance under STC and under real conditions

In Table4.9 below, values of η under STC are taken from Table1.1 from the Introduction section. Values of η under real conditions are the averaged values in September 2009 at 1000W/m^2 . The reason of using data from September 2009 at 1000W/m^2 is because 1000W/m^2 is one of the STC conditions, control one parameter allows valid comparison and September 2009 was when the test first started, which means all panels were new and there were no degradation affects the comparison. The difference between η under STC and real conditions are also stated in the table. (All numbers mentioned in discussion have been rounded up to 3 decimal places based on the values from the tables)

For CIS panel, the η difference between STC and real conditions is 2.205%. For mono-Si panel, the η difference between STC and real conditions is 6.596%. For $\mu\text{-Si}$ panel, no η under STC were found. For CdTe panel, the η difference between STC and real conditions is 5.865%. Hence, there is a gap of PV performance between manufacturer provided information (test under STC) and under real conditions.

η (%)	Würth-CIS	SolarWorld-mono-Si	Sharp- $\mu\text{-Si}$	First-CdTe
STC	12.9	18.45	/	15.5
real condition	10.6949093	11.85403607	8.12580949	9.6353067
Difference	2.20509071	6.59596393	/	5.8646933

Table4.9 Comparison of PV efficiency under STC and real coniditions

5.1 Key findings

5. Conclusion

5.1 Key findings

The research aim proposed in Chapter1 is: Investigating electrical characteristics and the performance of PV panels. Understand the significance of electrical characteristics regarding the performance degradation.

The aim has been reached by meeting the objectives listed below:

5. To understand PV panels' basic theories and electrical characteristics: Research on previous literature have been done, previous literature has stated that among all characteristics of solar PV, the 5 key electrical characteristics are related to the PV performance: Series resistance (R_s), Shunt resistance (R_{sh}), Ideality factor (n), Reverse saturation current (I_0) and photogenerated current (I_{ph}).
6. To identify which key electrical characteristics are significant in relation to PV performance: I-V curves and P-V curves were plotted to identify the existence of degradation for all 4 panels, use P_{MPP} as the indicator to determine which key electrical characteristics are significant in relation to PV performance. (Findings are listed in the tables below)
7. To understand the relationship between the key electrical characteristics and PV performance: Correlation between P_{MPP} and each key electrical characteristic for all 4 panels were calculated and showed on graph. (Findings are listed in the tables below)
8. To analyse the relationship between the key electrical characteristics and PV performance/degradation under real conditions: Data given for analysing were collected under real conditions. The relationship between each key electrical characteristic and the cell temperature, the ambient temperature, solar irradiance was identified. The relationship between P_{MPP} and each key electrical characteristic was also identified. Furthermore, comparisons were made among all 4 panels. (Findings are listed in the tables below)

The research hypothesis proposed in Chapter1 is: There is a strong correlation between key electrical characteristics and the PV performance.

This has been partly proved by all the findings listed in the tables below. All findings showed that for each different solar panel, there are correlation between key electrical

characteristics and the PV performance, however, some are weak, and some are strong, it depends on the type of the solar panel.

Würth -CIS				
Solar irradiance (G) - 1000W/m²				
Relationship between the key characteristics and environmental factors				
	Tamb	Tmod	Solar Irradiance	Note
RS	x	x	inversely proportional	x
RSH	x	x	inversely proportional	x
n	x	x	x	x
I₀	proportional	proportional	x	only at high G level
IPH	x	proportional	proportional	x

Table 5.1 Findings for Würth CIS panel

Solar World -mono-Si				
Solar irradiance (G) - 1000W/m²				
Relationship between the key characteristics and environmental factors				
	Tamb	Tmod	Solar Irradiance	Note
RS	proportional	proportional	inversely proportional	only at high G level
RSH	x	proportional	x	only at high G level
n	inversely proportional	inversely proportional	proportional	only at high G level
I₀	proportional	proportional	x	only at high G level
IPH	x	proportional	proportional	only at high G level

Table 5.2 Findings for Solar World-mono-Si panel

Sharp -μc-Si				
Solar irradiance (G) - 1000W/m²				
Relationship between the key characteristics and environmental factors				
	Tamb	Tmod	Solar Irradiance	Note
RS	inversely proportional	inversely proportional	inversely proportional	x
RSH	proportional	proportional	inversely proportional	only at high G level
n	x	x	x	x
I₀	proportional	proportional	x	only at high G level
IPH	proportional	proportional	proportional	x

Table 5.3 Findings for Sharp -μc-Si panel

First-CdTe				
Solar irradiance (G) - 1000W/m²				
Relationship between the key characteristics and environmental factors				
	Tamb	Tmod	Solar Irradiance	Note
RS	inversely proportional	inversely proportional	inversely proportional	x
RSH	x	x	inversely proportional	x
n	inversely proportional	inversely proportional	proportional	x
I₀	proportional	proportional	x	only at high G level
IPH	proportional	proportional	proportional	x

Table 5.4 Findings for First CdTe panel

5.1 Key findings

In Table 5.5, 5.6, 5.7 and 5.8, the change in % of the key electrical characteristics are in descending order.

Würth -CIS		
Solar irradiance (G) - 1000W/m ²		
Sep.2009 & Sep.2010 PV performance: Degradation 1.343%		
	Change in %	Correlation with PMPP
RS	74.656%	-0.1221
I_O	53.921%	see * at the bottom of the table
R_{SH}	-35.843%	0.184
n	2.886%	0.1181
I_{PH}	2.339%	0.5753

*PMPP converges from varying in a broader range to an averaged value of the range when I_O increases
impact strength on PMPP of CIS panel is: I_{PH} > R_{SH} > RS > n,

Table 5.5 Findings for Würth CIS panel

SolarWorld -mono-Si		
Solar irradiance (G) - 1000W/m ²		
Sep.2009 & Sep.2010 PV performance: Improvement 4.239%		
	Change in %	Correlation with PMPP
I_O	-26.356%	see * at the bottom of the table
R_{SH}	12.796%	0.2546
RS	8.099%	-0.4163
I_{PH}	2.251%	0.4816
n	0.077%	0.5016

*the relationship between PMPP and I_O varies depends on different solar irradiance in mono-Si panel
impact strength on PMPP of mono-Si panel is: n > I_{PH} > RS > R_{SH}

Table 5.6 Findings for Solar World-mono-Si panel

Sharp -μc-Si		
Solar irradiance (G) - 1000W/m ²		
Sep.2009 & Sep.2010 PV performance: Degradation 0.212%		
	Change in %	Correlation with PMPP
I_O	58.995%	see * at the bottom of the table
R_{SH}	-8.889%	0.2206
RS	7.305%	-0.2734
n	5.313%	0.0572
I_{PH}	1.170%	0.7045

*PMPP converges from varying in a broader range to an averaged value of the range when I_O increases
the impact strength on PMPP of μc-Si panel is: I_{PH} > RS > R_{SH} > n

Table 5.7 Findings for Sharp -μc-Si panel

First-CdTe		
Solar irradiance (G) - 1000W/m²		
Sep.2009 & Sep.2010 PV performance: Improvement 0.216%		
	Change in %	Correlation with PMPP
RS	-6.797%	0.0732
RSH	-2.763%	0.2297
IPH	1.039%	0.4798
n	0.106%	0.0548
I₀	0.884%	see * at the bottom of the table
*the relationship between PMPP and I₀ varies depend on different solar irradiance impact strength on PMPP of CdTe panel is: IPH > RSH > RS > n		

Table 5.8 Findings for First CdTe panel

5.2 Limitations

Originally, a similar experiment was scheduled on Heriot-Watt University Edinburgh Campus, as mentioned in Chapter3. The plan was to install two sets of solar panels: two identical mono-Si solar panels and two identical poly-Si solar panels, the procedure was to keep one panel of each type regularly cleaned and allow the rest expose to the outdoor conditions naturally without cleaning them. Hence, the factors causing PV degradation should be identified, the level of impacts on PV degradation should be determined and a study of soiling effect on PV degradation could be carried out. The exact same concept has been proposed and ready to carry out on Heriot-Watt University Dubai Campus at the same time, in order to reach the goal of making cross comparisons between two different climate conditions. However, at the beginning, the experiment was postponed due to the delay in site installation and delivery of key equipment (SMU, source measuring unit). Then instead of installing two sets of solar panels, four identical poly-Si solar panels were installed. Later when started to collect data, it was discovered that the SMU delivered is a faulty product. Till this point, the experiment was postponed again and due to the time limit of the dissertation, an alternative plan is needed.

Therefore, a data set of four different solar panels collected in Germany 10 years ago was given by the supervisor and the data were pre-sorted in a MATLAB programme and analysed in a Python programme. The data set given contains missing data from October 2009 to February 2010, as well as August 2010. The downside of obtaining second-handed data elsewhere is it takes time to get familiar with the data and limited information were known regard to the test site set up. Furthermore, the data was collected 10 years ago, both PV technology and climate were changed nowadays.

5.3 Recommendations for future study

5.3 Recommendations for future study

- Similar study can be repeated.

A similar study can be repeated easily with different data set. The bigger the data set, the accurate the analysis will be. Generally speaking, PV degradation appears gradually year by year. Therefore, data collected over more than a year would theoretically provide more information regard to the relationship between the key electrical characteristics and PV degradation.

- Possibilities of different experiments.

As previously mentioned in the limitation, many similar experiments can be carried out. If carrying out a study on soiling effect and PV degradation, then different types of solar panels should be installed in pairs, as mentioned in the limitation, one panel of each type should be maintained regularly to keep it clean, whereas the rest should be exposed to the outdoor environment without cleaning. If carrying out a study on understanding the key electrical characteristics' behaviour, then it is recommended to carry out two sets of experiments at the same time, one under real conditions, the other under STC to match the manufacturers' testing environment. With multiple types of solar panels, in depth results should be expected and it can possibly lead to the study of the gap between PV performance information provided by manufacturers and the actual PV performance under real conditions. The studies mentioned above could also be expanded by experimenting in a long period time in different climate zone, as it is well known that the factors cause degradation in PV performance are often complicated and highly related to the surrounding outdoor environment.

- Computer programmes.

Multiple computer programmes can be used for the convenience of sorting bigger size of data. Programming in MATLAB, Python and LATEX are all efficient programming tool for analysing data, do calculations and generating graphs.

6. References

IEA (International Energy Agency) (2017) *World Energy Outlook*. Available at: <https://www.iea.org/weo2017/> (Accessed 18 Oct 2018).

IEA (International Energy Agency) (2018) *World Energy Outlook*. Available at: <https://www.iea.org/weo/> (Accessed 29 Mar 2019).

IEA (International Energy Agency) (2018) *Solar Energy*. Available at: <https://www.iea.org/topics/renewables/solar/> (Accessed 18 Oct 2018).

IRENA (International Renewable Energy Agency) (2018) *Solar Energy*. Available at: <https://www.irena.org/solar> (Accessed 18 Oct 2018).

Cebr (Centre for Economics and Business Research) (2014) *Solar powered growth in the UK – The macroeconomic benefits for the UK of investment in solar PV*. Available at: <https://www.solar-trade.org.uk/wp-content/uploads/2015/03/CEBR-STA-report-Sep-2014-1.pdf> (Accessed 29 Mar 2019).

SEIA (Solar Energy Industries Association) (2019) *Solar Industry Research Data*. Available at: <https://www.seia.org/solar-industry-research-data> (Accessed 29 Mar 2019).

ISE (Fraunhofer Institute for Solar Energy Systems) (2019) *Photovoltaics Report*. Available at:

<https://www.ise.fraunhofer.de/content/dam/ise/de/documents/publications/studies/Photovoltaics-Report.pdf> (Accessed 29 Mar 2019).

Green Business Watch (no date) *UK Domestic Solar Panel Costs and Returns 2014-2017*. Available at: <https://greenbusinesswatch.co.uk/uk-domestic-solar-panel-costs-and-returns-2010-2017> (Accessed 29 Mar 2019).

Ofgem (2019) *Feed-In Tariff (FIT) rates*. Available at:

<https://www.ofgem.gov.uk/environmental-programmes/fit/fit-tariff-rates> (Accessed 29 Mar 2019).

5.3 Recommendations for future study

European Commission. (2017) *JRC Science for policy report- PV Status Report 2017.* Luxembourg: Publications Office of the European Union

European Commission. (2013) *Green Paper- A 2030 framework for climate and energy policies* (52013DC0169). Available at: <https://eur-lex.europa.eu/legal-content/EN/ALL/?uri=CELEX:52013DC0169> (Accessed 18 Oct 2018).

BEIS (Department for Business, Energy& Industrial Strategy) (2018) *Solar photovoltaics deployment.* Available at:
<https://www.gov.uk/government/statistics/solar-photovoltaics-deployment> (Accessed 18 Oct 2018). c

BEIS (Department for Business, Energy& Industrial Strategy) (2018) *Solar PV cost data.* Available at: <https://www.gov.uk/government/statistics/solar-pv-cost-data> (Accessed 18 Oct 2018). d

BEIS (Department for Business, Energy& Industrial Strategy) (2018) *Renewable electricity capacity and generation (ET6.1)* Available at:
<https://www.gov.uk/government/statistics/energy-trends-section-6-renewables> (Accessed 18 Oct 2018). e

Scottish Government (2017) *Scottish Energy Strategy: The future of energy in Scotland.* Available at: <https://www.gov.scot/publications/scottish-energy-strategy-future-energy-scotland/pages/5/> (Accessed 18 Oct 2018).

BRE (Building Research Establishment) (2016) *The Government's Standard Assessment Procedure (SAP) for Energy Rating of Dwellings.* Available at:
<https://www.bre.co.uk/filelibrary/SAP/2016/SAP-2016-10.00--July-2016--CONSULTATION-VERSION-14-07-2016.pdf> (Accessed 29 Mar 2019).

BRE (Building Research Establishment) (2015) *Planning guidance for the development of large scale ground mounted solar PV systems.* Available at: <https://www.solar-trade.org.uk/wp-content/uploads/2015/05/BRE-Planning-Guidance-for-Solar-Farms.pdf> (Accessed 29 Mar 2019).

Salas,V. (2016) ‘9- Stand-alone photovoltaic systems’, *The Performance of Photovoltaic (PV) Systems*. Edited by Pearsall.N. pp.251-296

Wu,L. et al. (2017) ‘A Single-Stage Three-Phase Grid-Connected Photovoltaic System With Modified MPPT Method and Reactive Power Compensation’, *IEEE Transactions on Energy Conversion*, 22(4), pp.881-886. doi: [10.1109/TEC.2007.895461](https://doi.org/10.1109/TEC.2007.895461)

Mahela,O. and Shaik,A. (2016) ‘ Comprehensive overview of grid interfaced solar photovoltaic systems’, *Renewable and Sustainable Energy Reviews*, 68(1), pp.316-332.

Wolfe,P.R. (2011) ‘Chapter IIE-2- Solar Parks and Solar Farms’, *Practical Handbook of Photovoltaics* 2nd edn. Edited by Augustin McEvoy, Tom Markvart and Luis Castañer. pp.943-962

FE Online. (2017) ‘Longyangxia Dam Solar Park: Know all about world’s largest solar farm built by China on Tibetan plateau; NASA releases images’, *Financial Express*, 17 March. Available at: <https://www.financialexpress.com/world-news/longyangxia-dam-solar-park-know-all-about-worlds-largest-solar-farm-built-by-china-on-tibetan-plateau-nasa-releases-images/591279/> (Accessed 1 Nov 2018).

Solar Guide (2018) Available at: <https://www.solarguide.co.uk/how-much-does-it-cost-to-install-solar-panels#/> (Accessed 1 Nov 2018).

BEIS (Department for Business, Energy& Industrial Strategy) (2018) *Consultation on the Feed-In Tariffs Scheme*. Available at:
<https://www.gov.uk/government/consultations/feed-in-tariffs-scheme> (Accessed 1 Nov 2018).

Fouad,M.M. et al. (2017) ‘An integrated review of factors influencing the performance of photovoltaic panels’, *Renewable and Sustainable Energy Reviews*, 80 (Dec), pp.1499-1511

Fonash, R.T. et.al. (no date) *Solar cell*. Available at:
<https://www.britannica.com/technology/solar-cell> (Accessed 5 Nov 2018).

5.3 Recommendations for future study

Bagher, A.M. et al. (2015) ‘Types of Solar Cells and Application’, *American Journal of Optics and Photonics*, 3(5), pp.94-113. doi: 10.11648/j.ajop.20150305.17

IEA (International Energy Agency) (2010) *Technology Roadmap Solar photovoltaic energy*. France: IEA publications.

Cheshire,D. (2012) *CIBSE Guide F: Energy efficiency in buildings*, 3rd edn. London: The Chartered Institution of Building Services Engineers.

Niclas. (2012) ‘Polycrystalline Silicon Cells: production and characteristics’, *Sino Voltaics*, 6 January. Available at: <https://sinovoltaics.com/learning-center/solar-cells/polycrystalline-silicon-cells-production-and-characteristics/> (Accessed 5 Nov 2018).

Richardson, L. (2018) ‘How are solar panels made? What parts are they made of? List of cell types and parts of a solar panel’, *energysage*, 16 October. Available at: <https://news.energysage.com/what-are-solar-panels-made-of-list-of-solar-pv-materials/> (Accessed 5 Nov 2018).

CIBSE. (no date) *TM25 Understanding building integrated photovoltaics*.

Rawlings,R. (no date) ‘Capturing solar energy’ *CIBSE Knowledge Series: KS15*.

Knier,G. (2008) *How do Photovoltaics Work?* Available at: <https://science.nasa.gov/science-news/science-at-nasa/2002/solarcells> (Accessed 21 Dec 2018).

Nocito,C. and Koncar,V. (2016) ‘ 18- Flexible photovoltaic cells embedded into textile structures’, *Smart Textiles and their Applications*. Edited by Koncar,V. pp.401-422

Rahman,M.Z. and Khan,S.I. (2012) ‘ Retraction: Modelling Electrical Characteristics of a pn- Junction Silicon Solar Cell Using PSpice’, *Smart Grid and Renewable Energy*, 3(2), pp.133-138. doi: 10.4236/sgre.2012.32019

Gul,M. *et al.* (2016) ‘Review on recent trend of solar photovoltaic technology’, *Energy Exploration & Exploitation*, 34(4), pp.485-526. doi:
<https://doi.org/10.1177%2F0144598716650552>

Dhar,M. (2017) *How Do Solar Panels Work?* Available at:
<https://www.livescience.com/41995-how-do-solar-panels-work.html> (Accessed 21 Dec 2018)

Qazi, S. (2016) *Standalone Photovoltaic (PV) Systems for Disaster Relief and Remote Areas*. Publisher: Joe Hayton

Ma,T. *et al.* (2014) ‘Solar photovoltaic system modelling and performance prediction’, *Renewable and Sustainable Energy Reviews*, 36(Aug), pp.304-315.

Georgia State University, Department of Physics and Astrology. (no date) *DC Circuits - DC Electric Power*. Available at: <http://hyperphysics.phy-astr.gsu.edu/hbase/electric/elepow.html#c1> (Accessed 21 Dec 2018)

Alternative Energy Tutorials (no date) *Solar Cell I-V Characteristics* Available at:
<http://www.alternative-energy-tutorials.com/energy-articles/solar-cell-i-v-characteristic.html> (Accessed 21 Dec 2018)

Horowitz,P. and Hill, W. (2015) *The Art of Electronics*. 3rd edn. New York: Cambridge University Press

Azli,N.A. *et al* (2008) ‘Effect of fill factor on the MPPT performance of a grid-connected inverter under Malaysian conditions’, *2008 IEEE 2nd International Power and Energy Conference*, Johor Bahru, Malaysia, 1-3 December. doi:
[10.1109/PECON.2008.4762509](https://doi.org/10.1109/PECON.2008.4762509)

National Instruments (2012) *Part II – Photovoltaic Cell I-V Characterization Theory and LabVIEW Analysis Code*. Available at: <http://www.ni.com/white-paper/7230/en/> (Accessed 21 Dec 2018)

5.3 Recommendations for future study

Ghani,F. *et al* (2013) ‘Numerical calculation of series and shunt resistance of a photovoltaic cell using the Lambert W-function: Experimental evaluation’, *Solar Energy*, 87(Jan), pp.246-253.

Ramalingam,K. and Idulkar,C. (2017) ‘Chapter3 – Solar Energy and Photovoltaic Technology’, in Gharehpétian,C.B. and Mohammad Mousavi Agah,S. (ed.) *Distributed Generation Systems-Design, Operation and Grid Integration*. Oxford: Butterworth-Heinemann, pp.69-147.

Ghani,F. *et al* (2013) ‘Numerical calculation of series and shunt resistance and diode quality of a photovoltaic cell using the Lambert W-function’, *Solar Energy*, 91(May), pp.422-431.

Meyer,E.L. and Ernest van Dyk,E. (2005) ‘The effect of reduced shunt resistance and shading on photovoltaic module performance’, *Thirty-first IEEE Photovoltaic Specialists Conference*, Lake Buena Vista, FL, USA, 2-7 January. doi: [10.1109/PVSC.2005.1488387](https://doi.org/10.1109/PVSC.2005.1488387)

Ernest van Dyk,E. and Meyer,E.L. (2004) ‘Analysis of the effect of parasitic resistances on the performance of photovoltaic modules’, *Renewable Energy*, 29(3), pp. 333-344.

Ghani,F. (2015) ‘On the influence of temperature on crystalline silicon solar cell characterisation parameters’, *Solar Energy*, 112(Feb), pp.437-445.

Boylestad,R. and Nashelsky,L. (1998) *Electronic Devices and Circuit Theory*. 7th edn. New Jersey and Ohio: Prentice Hall

Villalva,M.G. *et al* (2009) ‘Comprehensive Approach to Modeling and Simulation of Photovoltaic Arrays’, *IEEE Transactions on Power Electronics*, 24(5), pp.1198-1208.

Chenni,R. *et al* (2007) ‘A detailed modeling method for photovoltaic cells’, *Energy*, 32(9), pp. 1724-1730.

Sharma,V. *et al* (2013) ‘Performance assessment of different solar photovoltaic technologies under similar outdoor conditions’, *Energy*, 58(Sep), pp.511-518.

Balaska,A. *et al* (2017) ‘Performance assessment of five different photovoltaic module technologies under outdoor conditions in Algeria’, *Renewable Energy*, 107(Jul), pp.53-60.

Cañete,C. *et al* (2014) ‘Energy performance of different photovoltaic module technologies under outdoor conditions’, *Energy*, 65(Feb), pp.295-302.

Sera,D. *et al* (2007) ‘PV panel model based on datasheet values’, *2007 IEEE International Symposium on Industrial Electronics*, Vigo, Spain, 4-7 June. doi: [10.1109/ISIE.2007.4374981](https://doi.org/10.1109/ISIE.2007.4374981)

Zhang,Y., *et al* (2017) ‘Prediction of I-V characteristics for a PV panel by combining single diode model and explicit analytical model’, *Solar Energy*, 144(Mar), pp.349-355.

Singh,N.S., *et al* (2009) ‘Determination of the solar cell junction ideality factor using special trans function theory (STFT)’, *Solar Energy Materials and Solar Cells*, 93(8), pp.1423-1426.

Bayhan,H. and Bayhan,M. (2011) ‘A simple approach to determine the solar cell diode ideality factor under illumination’, *Solar Energy*, 85(5), pp.769-775.

Amaral da Luz,C.M. *et al* (2018) ‘Assessment of the ideality factor on the performance of photovoltaic modules’, *Energy Conversion and Management*, 167(Jul), pp.63-69.

Meteoblue (no date) Climate Obing Available at:

https://www.meteoblue.com/en/weather/forecast/modelclimate/obing_germany_2858424 (Accessed: 26 February 2019)

Wirth,H. (2018) *Recent Facts about Photovoltaics in Germany*, Fraunhofer ISE.

Available at: <https://www.ise.fraunhofer.de/en/publications/studies/recent-facts-about-pv-in-germany.html> (Accessed: 26 February 2019)

5.3 Recommendations for future study

Li,C. *et al.* (2017) ‘Understanding individual defects in CdTe thin-film solar cells via STEM: From atomic structure to electrical activity’, *Materials Science in Semiconductor Processing*, 65(Jul), pp.64-76.

Green,M.A. *et al.*(2017) ‘Solar cell efficiency tables (version 51)’, *Progress in Photovoltaics: Research and Applications*, 26(1). doi: <https://doi.org/10.1002/pip.2978>

Hsiang,H. *et al.* (2016) ‘Leaching and re-synthesis of CIGS nanocrystallites from spent CIGS targets’, *Advanced Powder Technology*, 27(3), pp. 914-920.

Ghani,F. *et al.* (2014) ‘The numerical calculation of single-diode solar-cell modelling parameters’, *Renewable Energy*, 72(Dec), pp.105-112.

Fernández,F. *et al.* (2013) ‘Calculation of cell temperature in a HCPV module using V_{oc} ’, *2013 Spanish Conference on Electron Devices*, Valladolid, Spain, 12-14 February. doi: <https://doi.org/10.1109/CDE.2013.6481406>

Ghosal,K. *et al.* (2015) ‘Ultra high efficiency HCPV modules’, *2015 IEEE 42nd Photovoltaic Specialist Conference (PVSC)*, New Orleans, LA, USA, 14-19 June. doi: <https://doi.org/10.1109/PVSC.2015.7356412>

Cuevas,A. *et al.* (1982) ‘ 50 percent more output power from an albedo-collecting flat panel using bifacial solar cells’, *Solar Energy*, 29(5), pp.419-420.

Guerrero-Lemus. *et al.* (2016) ‘Bifacial solar photovoltaics – A technology review’, *Renewable and Sustainable Energy Reviews*, 60(Jul), pp. 1533-1549.

Kabir,E. *et al.* (2018) ‘Solar energy: Potential and future prospects’, *Renewable and Sustainable Energy Reviews*, 82 Part1 (Feb), pp.894-900.

Ueda,Y. *et al.* (2013) ‘Five years operation results of different crystalline-Si PV systems and analysis of the degradation rate in the field’, *2013 IEEE 39th Photovoltaic Specialists Conference (PVSC)*, Tampa, FL, USA, 16-21 June. doi: <https://doi.org/10.1109/PVSC.2013.6745148>

Alshushan,M.A.S. and Saleh,I.M. (2013) 'Power degradation and performance evaluation if PV modules after 31 years of work', *2013 IEEE 39th Photovoltaic Specialists Conference (PVSC)*, Tampa, Fl, USA, 16-21 June. doi: <https://doi.org/10.1109/PVSC.2013.6745088>

Cassini,D.A. *et al.* (2017) 'Experimental Evaluation of the Performance of Crystalline Si PV Module Degradation After 15-Years of Field Exposure', *2017 IEEE 44th Photovoltaic Specialist Conference (PVSC)*, Washington, DC, USA, 25-30 June. doi: <https://doi.org/10.1109/PVSC.2017.8366114>

Thongpao,K. *et al.* (2010) 'Outdoor performance of polycrystalline and amorphous silicon solar cells based on the influence of irradiance and module temperature in Thailand', *The 2010 ECTI International Conference on Electrical Engineering/Electronics. Computer, Telecommunications and Information Technology*, Chiang Mai, Thailand, 19-21 May.

Ibrahim,H. and Anani,N. (2017) 'Variations of PV module parameters with irradiance and temperature', *Energy Procedia*, 134(Oct), pp.276-285.

Maftah,A. and Maaroufi,M. (2019) 'Experimental evaluation of temperature effect of two different PV Systems Performances under arid climate', *Energy Procedia*, 157(Jan),pp.701-708.

Dhoke,A. and Mengede,A. (2017) 'Degradation analysis of PV modules operating in Australian environment', *2017 Australasian Universities Power Engineering Conference (AUPEC)*, Melbourne, VIC, Australia.
doi:<https://doi.org/10.1109/AUPEC.2017.8282420>

Ramli,M.Z. and Salam,Z. (2019) 'Performance Evaluation of DC Power Optimizer (DCPO) for Photovoltaic (PV) System During Partial Shading', *Renewable Energy*. doi: <https://doi.org/10.1016/j.renene.2019.02.072>

5.3 Recommendations for future study

Sundareswaran,K. *et al.* (2015) ‘Application of a combined particle swarm optimization and perturb and observe method for MPPT in PV systems under partial shading conditions’, *Renewable Energy*, 75(Mar), pp.308-317.

Maghami M.R. *et al.* (2016) ‘Power loss due to soiling on solar panel: A review’, *Renewable and Sustainable Energy Reviews*, 59(Jun), pp.1307-1316.

Mekhilef,S. *et al.* (2012) ‘Effect of dust, humidity and air velocity on efficiency of photovoltaic cells’, *Renewable and Sustainable Energy Reviews*, 16(5), pp.2920-2925.

Schill,C. *et al.* (2015) ‘Impact of soiling on IV-curves and efficiency of PV-modules’, *Solar Energy*, 112(Feb), pp.259-262.

Kalogirou,S.A. *et al.* (2013) ‘On-site PV characterization and the effect of soiling on their performance’, *Energy*, 51(Jan), pp.439-446.

Revesz,M. *et al.*(2018) ‘Potential increase of solar irradiation and its influence on PV facades inside an urban canyon by increasing the ground-albedo’, *Solar Energy*, 174(Nov), pp.7-15.

SUNPOWER

https://www.sunpowercorp.co.uk/sites/multilingual/files/sunpower_maxeon_3_390w_370w_com_uk.pdf (Accessed:12 March 2019)

Trinasolar

http://static.trinasolar.com/sites/default/files/Tallmax%20PD14%20Feb2017_A.pdf
(Accessed: 12 March 2019)

Amerisolar <http://www.weamerisolar.com/english/product/pro3/423.html> (Accessed: 12 March 2019)

Polysolar <http://www.weamerisolar.com/english/product/pro3/423.html> (Accessed: 12 March 2019)

First Solar <http://www.firstsolar.com/Modules/Series-6> (Accessed: 12 March 2019)

Flisom https://flisom.com/wpcontent/uploads/2019/01/Datasheet_eFlex_1.6m_rev.pdf
(Accessed: 12 March 2019)

bsq solar <https://www.bsqsolar.com/product/hcpv-module/> (Accessed: 12 March 2019)

YINGLI SOLAR <http://www.yinglisolar.com/en/products/56> (Accessed: 12 March 2019)

GeneCIS solar module 80W

WSG0036E080

FEATURES

- GeneCIS solar module for connection in series
- Optimum energy yield through outstanding temperature and low-light behaviour
- A homogenous black surface provides an attractive appearance
- Glass-glass construction provides a high level of protection against environmental influences
- Black anodised aluminium frame
- 20-year power output guarantee
- Made in Germany (Würth Solar)



TECHNICAL DATA

Electrical data in STC

Nominal output according to STC	80 W
MPP voltage (Umpp)	35 V
Current at max. capacity (Impp)	2.29 A
Open circuit voltage (Uoc)	44 V
Short circuit current (Isc)	2.5 A

Electrical data at NOCT

NOCT	47 (+/- 3) °C
------	---------------

Systems

Maximum Voltage systems	1,000 V
Performance tolerance	-2 / +5 %
Reverse current stability	3 x Isc
SysUoc, open circuit voltage (Uoc) at -10 °C	48.5 V
MPP voltage (Umpp) at 70 °C	29.5 V
Temperature coefficient (Pmpp)	-0.36 % / °C
Temperature coefficient (Voc)	-0.29 % / °C
Temperature coefficient (Isc)	0.05 % / °C
Cell material	CIS
Cell technology	CIS
Mechanical assembly	Glass-glass module with black anodised aluminium frame
Frame height	35 mm
Max. distortion	1.2 °
Max. surface pressure	2,400 N/m ²
DC connection	MC4 plug connector
Ambient operating temperature	-40 ... +85 °C
Weight	12.71 kg
Dimensions (W x L x D)	605 x 1,205 x 35 mm

Electrical data under standard test conditions (STC): I=1,000 W/m², AM 1.5, Tu=25°C

Cell operating temperature (NOCT): I=800 W/m², Tu=20°C, Vw =1 m/s

We reserve the right to make technical and product changes.
Illustrations may differ from actual product.

Würth Solar GmbH & Co. KG

Alfred-Leikam-Straße 25 · D-74523 Schwäbisch Hall
Tel. +49 (0) 791 946 00-0 · Fax +49 (0) 791 946 00-119
wuerth-solar@we-online.de · www.wuerth-solar.com



SolarWorld Module SW 165/175/185 mono



The Sunmodule® SW 165/175/185 mono by SolarWorld offers an innovative module concept. The unique, fully automated production process ensures the highest level of precision and consistently high production quality. The machine finishing produces a highly homogeneous design.

The monocrystalline 5" cells lie behind a 3 mm hardened-glass glazing and are embedded in transparent EVA (ethylene-vinyl-acetate). The back of the module is sealed with a very high quality Tedlar film. The module stability is the result of the deep inset of the glass in the frame and its continuous bond between the two.

The flat and compact connecting socket is mounted on the back of the module using a unique, patented process. The connecting socket has no hollow cavities, is watertight, resistant to UV radiation and microbes, as well as very temperature resistant. This flat and compact top-quality product represents the ideal solution for every application.

Module

Length:	1610 mm
Width:	810 mm
Height:	34 mm
Frame:	Aluminium
Weight:	15 kg

Edition: April 2006



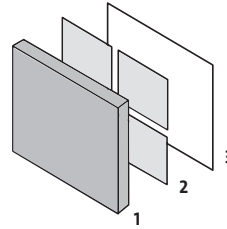
SolarWorld AG
Kurt-Schumacher-Straße 12-14
53113 Bonn/Germany

Tel.: +49-228-55920-0
E-Mail: service@solarworld.de
www.solarworld.de



SolarWorld Module SW 165/175/185 mono

Design



- 1] Front: tempered glass
- 2] 72 monocrystalline solar cells
125 mm x 125 mm
embedded in EVA
(ethylene-vinyl-acetate)
- 3] Rear: Tedlar foil

Performance under standard test conditions (STC)

	165 Wp	175 Wp	185 Wp
Peak power (Pmax)	165 Wp	175 Wp	185 Wp
Maximum power point voltage (Vmpp)	35.3 V	35.7 V	36.0 V
Maximum power point current (Impp)	4.7 A	4.9 A	5.1 A
Open circuit voltage (Voc)	44.1 V	44.4 V	44.5 V
Short circuit current (Isc)	5.2 A	5.4 A	5.5 A

Performance at 800 W/m², NOCT, AM 1.5

	125 Wp	131 Wp	138 Wp
Peak power (Pmax)	125 Wp	131 Wp	138 Wp
Maximum power point voltage (Vmpp)	32.7 V	33.1 V	33.4 V
Maximum power point current (Impp)	3.8 A	4.0 A	4.1 A
Open circuit voltage (Voc)	40.9 V	41.1 V	41.2 V
Short circuit current (Isc)	4.2 A	4.4 A	4.5 A

Minor reduction in efficiency under partial load conditions at 25°C:

at 200 W/m², 95 % (+/- 3 %) of the STC efficiency (1000 W/m³) is achieved.

Component materials

Cells per module	72
Solar cells	monocrystalline silicon
Cell dimensions	125 x 125 mm

Thermal characteristics

NOCT	46°C
TK Isc	0.06 %/K
TK Voc	-0.35 %/K

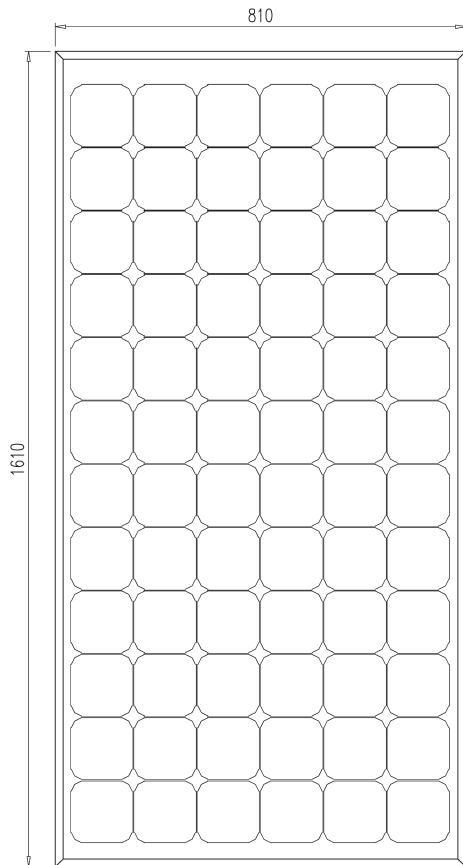
System design characteristics

Maximum system voltage	715 V
Reverse current load	Do not apply external voltages in excess of Voc to the module.

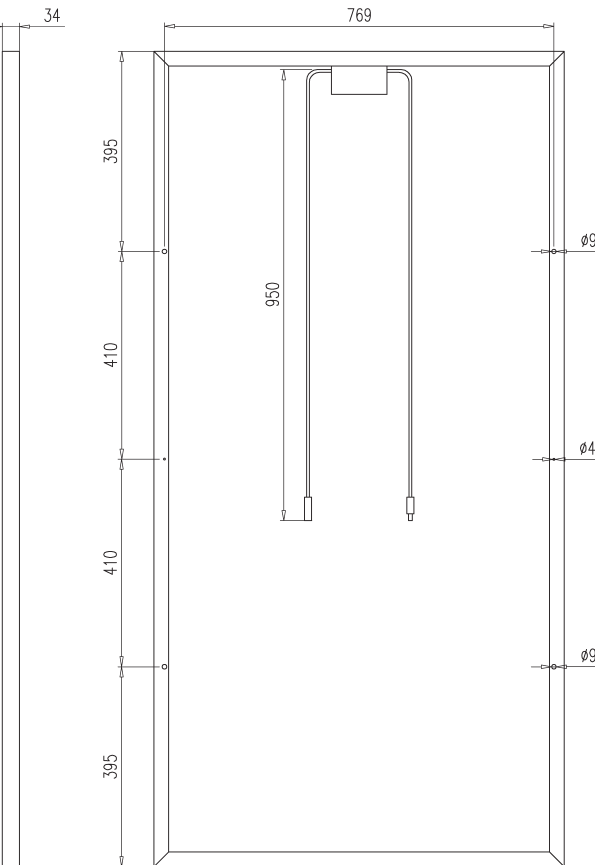
Rated power and maximum tolerance

Rated power	165/175/185 Wp +/- 3 %
Connecting socket	IP 65
Plug	MC type 4

front view



rear view



Modules certified according to:



SolarWorld AG reserves the right to make specification changes.

This data sheet complies with the requirements of EN 50380.

This data sheet is also available in german language.

<http://www.wholesalesolar.com/products.folder/module-folder/SolarWorld/SolarWorld175.html>

JETZT MIT ENDKUNDENREGISTRIERUNG



MIKROAMORPHES TANDEM-SILIZIUM DÜNNSCHICHT-PHOTOVOLTAIKMODUL

Die Photovoltaikmodule der NA-Serie bestehen aus einer amorphen und einer mikrokristallinen Siliziumschicht. Diese mikroamorphe Tandemstruktur absorbiert nicht nur die sichtbaren, sondern auch die nicht sichtbaren Anteile des Sonnenspektrums. Dies führt zu einer besonders effektiven Nutzung der Sonnenenergie.



Eigenschaften

- Tandemstruktur aus einer amorphen und einer mikrokristallinen Siliziumschicht mit einem stabilisierten Modulwirkungsgrad von bis zu 8,5 %.
- Die schwarze Moduloptik schafft ein harmonisches Erscheinungsbild.
- Höhere Energieerträge pro Watt sowohl bei hohen Temperaturen als auch bei diffusem Licht.
- Verwendung von vergütetem Weißglas, EVA-Kunststoff und Witterungsschutzfolie sowie eines schwarz eloxierten Aluminiumrahmens für den Langzeiteinsatz im Außenbereich.
- Ausgang: Anschlusskabel mit spritzwassergeschütztem Steckanschluss.
- Der Qualitätsanspruch von Sharp Solar setzt Maßstäbe. Ständige Kontrollen garantieren eine gleichbleibend hohe Qualität. Jedes Modul wird optisch, mechanisch und elektrisch geprüft. Sie erkennen es am Original Sharp Label, der Seriennummer und der Sharp Garantie.
- Zur Gewährung der Produkt- und Leistungsgarantie müssen die Module durch den Endkunden bei Sharp registriert werden. Die Registrierungsunterlagen werden vom Installateur oder direkt von Sharp ausgehändigt.

Technische Daten NA-Serie

Zelle	Tandemzelle aus amorphem (α -Si) und mikrokristallinem (μ c-Si) Silizium
Maximale Systemspannung	600 V DC
Abmessungen	1.129 x 934 x 46 mm
Gewicht	18 kg
Anschlussyp	Kabel mit Steckanschluss
Bypassdioden	1

Umgebungsbedingungen

Parameter	Nennwert	Einheit
Betriebstemperatur	-40 bis +90	°C
Lagerungstemperatur	-40 bis +90	°C
Lagerungsluftfeuchtigkeit (rel.)	bis 90	%

Temperatur-Koeffizienten

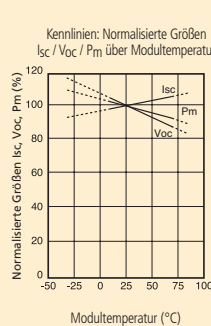
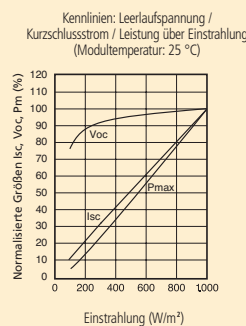
$\alpha_{V_{OC}}$	-0,24 % / °C
$\alpha_{I_{SC}}$	+0,07 % / °C
$\alpha_{P_{M}}$	-0,30 % / °C

Elektrische Daten

Parameter	Symbol	NA-801WP	Anfangswerte			Nominal Werte			Einheit
			NA-851WP	NA-901WP	NA-801WP	NA-851WP	NA-901WP	NA-801WP	
Leerlaufspannung	V_{OC}	64,5	65,0	66,6	63,3	63,8	65,2	V	
Spannung bei maximaler Leistung	V_{PM}	50,5	52,0	53,5	47,6	49,0	49,3	V	
Kurzschlussstrom	I_{SC}	2,16	2,20	2,20	2,08	2,11	2,11	A	
Strom bei maximaler Leistung	I_{PM}	1,86	1,92	1,98	1,68	1,74	1,83	A	
Nennleistung	P_m	94,0	100,0	105,9	80,0	85,0	90,0	W	
Wirkungsgrad Modul	η_m	—	—	—	7,6	8,0	8,5	%	

Die elektrischen Daten gelten bei Standard-Testbedingungen (STC): Einstrahlung 1.000 W/m² mit Spektrum AM 1.5 bei einer Zellentemperatur von 25 °C.
Die Spannungsangaben unterliegen einer Fertigungstoleranz von $\pm 5\%$, die Leistungsangaben von $\pm 10\%$.

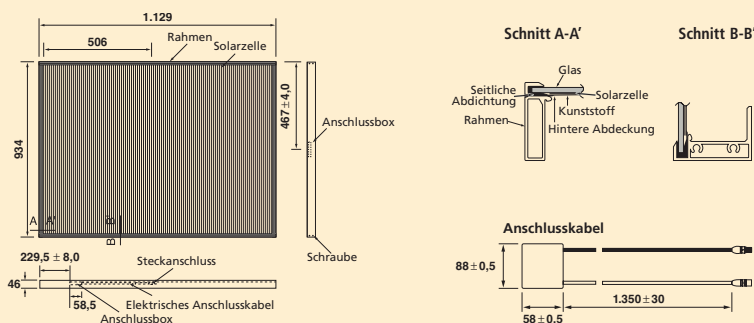
Kennlinien



Einsatzmöglichkeiten

- Netzgekoppelte Wohnhausanlagen
- Bürogebäude
- Solarkraftwerke
- Solardörfer
- Villen, Berghütten
- Beleuchtungseinrichtungen
- Telekommunikationssysteme

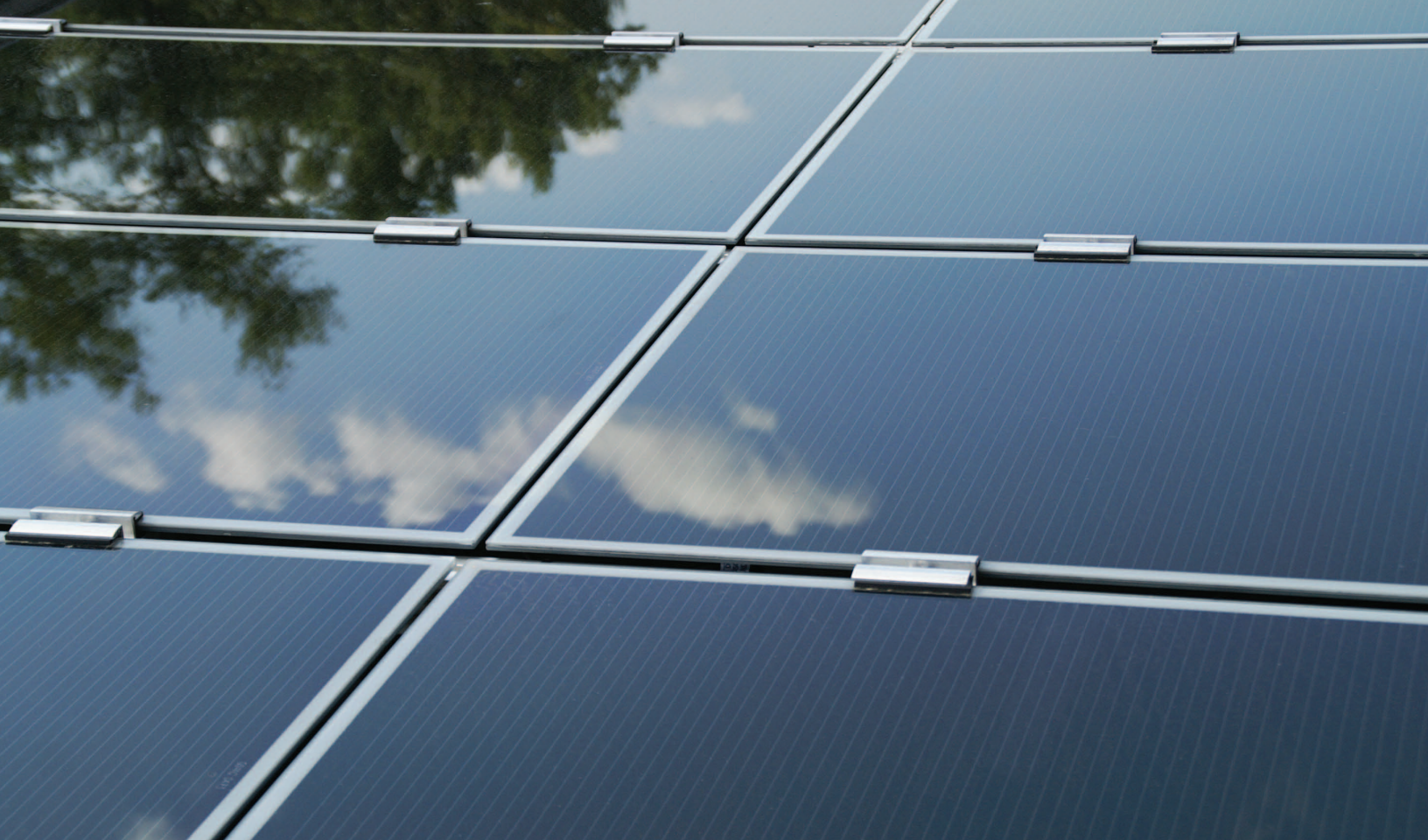
Außenabmessungen



SHARP

Sharp Electronics (Europe) GmbH
Sonnenstraße 3 • 20097 Hamburg
Tel.: 0 40/23 76-0 • Fax: 0 40/23 76-21 93
www.sharp.de/solar

Zuständigkeit Österreich: München Office
Landsberger Straße 398 • 81241 München
Tel.: 0 89/54 68 42-25 • Fax: 0 89/54 68 42-60
www.sharp.at/solar



First Solar®

First Solar (US)
Tel: 877 850 3757
info@firstsolar.com

First Solar (Europe)
Tel: +800 3757 3757
info@firstsolar.de

www.firstsolar.com

First Solar FS Series 2 PV Module

Thin film solutions for high performance PV systems

First Solar® FS Series 2™ PV Modules are IEC 61646 and IEC 61730 certified for use in systems up to 1000 VDC, UL Listed (600VDC), and meet the requirements of Safety Class II. First Solar provides cost effective thin film module solutions to leading solar project developers and system integrators for large scale, grid-connected solar power plants. First Solar application engineers provide technical support and comprehensive product documentation to support the design, installation, and long term operations of high performance PV systems.



WARRANTY

- Material and workmanship warranty for five (5) years and a power output warranty of 90% of the nominal output power rating ($P_{MPP} \pm 5\%$) during the first ten (10) years and 80% during twenty-five (25) years subject to the warranty terms and conditions.
- Modules are life cycle managed with a collection and recycling program, providing module owners with no cost, pre-funded, end-of-life take back, and recycling of the modules.

All specifications and warranties apply only to products sold and installed in North America. For applications outside of North America, please refer to the Global Datasheet (PD-5-401-02).

ELECTRICAL SPECIFICATIONS

MODEL NUMBERS AND RATINGS AT STC^{1*}

Nominal Values		FS-270	FS-272	FS-275	FS-277	FS-280
Nominal Power(+/-5%)	P _{MPP} (W)	70	72.5	75	77.5	80
Voltage at P _{MAX}	V _{MPP} (V)	65.5	66.6	68.2	69.9	71.2
Current at P _{MAX}	I _{MPP} (A)	1.07	1.09	1.10	1.11	1.12
Open Circuit Voltage	V _{OC} (V)	88.0	88.7	89.6	90.5	91.5
Short Circuit Current	I _{SC} (A)	1.23	1.23	1.23	1.22	1.22
Maximum System Voltage	V _{SYS} (V)	1000 (600 UL ²)				
Temperature Coefficient of P _{MPP}	T _K (P _{MPP})	-0.25%/°C				
Temperature Coefficient of V _{OC} , high temp (>25°C)	T _K (V _{OC} , high temp)	-0.25%/°C				
Temperature Coefficient of V _{OC} , low temp (-40°C to + 25°C)	T _K (V _{OC} , low temp)	-0.20%/°C				
Temperature Coefficient of I _{SC}	T _K (I _{SC})	+0.04%/°C				
Limiting Reverse Current	I _R (A)	2				
Maximum Series Fuse	I _{CF} (A)	2				

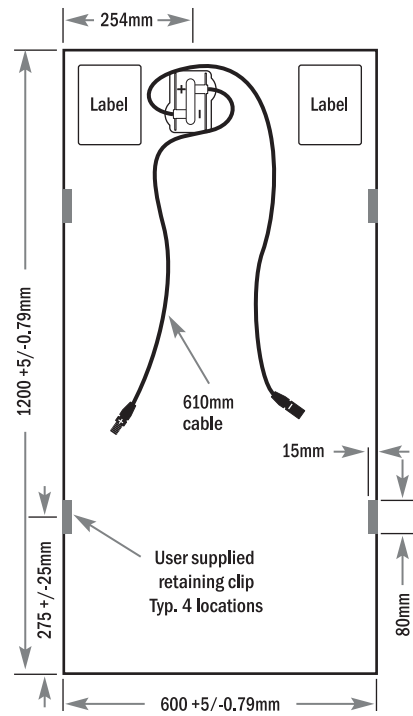
MODEL NUMBERS AND RATINGS AT 800W/m², NOCT³ 45°C, AM 1.5*

Nominal Values		FS-270	FS-272	FS-275	FS-277	FS-280
Nominal Power(+/-5%)	P _{MPP} (W)	52.5	54.4	56.3	58.1	60.0
Voltage at P _{MAX}	V _{MPP} (V)	61.4	62.4	63.9	65.5	66.8
Current at P _{MAX}	I _{MPP} (A)	0.86	0.87	0.88	0.89	0.90
Open Circuit Voltage	V _{OC} (V)	81.8	82.5	83.3	84.2	85.1
Short Circuit Current	I _{SC} (A)	1.01	1.01	1.01	1.00	1.00

MECHANICAL DESCRIPTION

Length	1200mm	Thickness	6.8mm
Width	600mm	Area	0.72m ²
Weight	12kg	Leadwire	4.0mm ² , 610mm
Connectors	Solarline 1 type connector		
Bypass Diode	None		
Cell Type	CdS/CdTe semiconductor, 116 active cells		
Frame Material	None		
Cover Type	3.2mm heat strengthened front glass laminated to 3.2mm tempered back glass		
Encapsulation	Laminate material with edge seal		

MECHANICAL DRAWING



* All ratings +/-10%, unless specified otherwise.
Specifications are subject to change.

¹ Standard Test Conditions (STC) 1000W/m², AM 1.5, 25°C

² Required to maintain UL compliance

³ Nominal Operating Cell Temperature: Module operation temperature at 800W/m² irradiance, 20°C air temperature, 1m/s wind speed.

High Performance PV System Solutions

Key Features:

- Produces high energy output across a wide range of climatic conditions with excellent temperature response coefficient
- Proven to perform as predicted with a high Performance Ratio (PR)
- Frameless laminate is robust, cost-effective and recyclable, and does not require module grounding
- Manufactured in highly automated, state-of-the-art facilities certified to ISO 9001:2008 and ISO 14001:2004 quality and environmental management standards
- Tested by leading international institutes and certified for reliability and safety:

- Certified to IEC 61646
- Certified to IEC 61730
- CE Marking
- Safety Class II @ 1000 V
- UL 1703 and ULC 1703 Listed (Class C Fire Rating)
- Eligible CSI PV Module
- FSEC Certified



www.firstsolar.com

Appendix

GitHub Repo Link:

<https://github.com/danielbee/RowenaSolarAnalysis>